

Water and Wind: The Fluvial and Eolian Forces Behind the  
Pennsylvanian-Permian Halgaito Formation, Utah

By

Dawn E. Tobey

Submitted in partial fulfillment of the requirements  
for the degree of Masters of Science

at

Dalhousie University  
Halifax, Nova Scotia  
September 2020

© Copyright by Dawn E. Tobey, 2020

## Table Of Contents

<b>List of Tables</b> .....	<b>v</b>
<b>List of Figures</b> .....	<b>vi</b>
<b>Abstract</b> .....	<b>vii</b>
<b>List of Abbreviations Used</b> .....	<b>viii</b>
<b>Acknowledgements</b> .....	<b>ix</b>
<b>Chapter 1: Introduction</b> .....	<b>1</b>
1.1 Statement of Problem.....	1
1.2 Objectives .....	6
1.3 Contributions of the Author .....	6
<b>Chapter 2: Fine-grained Dryland Rivers Reworking Loess in the Paradox Basin of Western Pangea: Halgaito Formation, Pennsylvanian-Permian of Utah</b> .....	<b>10</b>
2.1 Abstract .....	10
2.2 Introduction .....	11
2.3 Geological Overview .....	14
2.4 Methods.....	17
2.5 Stratigraphic Sections, Facies, and Fossils .....	19
2.5.1 <i>Stratigraphic Sections</i> .....	19
2.5.2 <i>Facies</i> .....	20
2.5.3 <i>Fossils</i> .....	31
2.5.4 <i>Grain size comparison of eolian and fluvial siltstones</i> .....	32

2.5.5 Root Traces.....	36
2.6 Channel Bodies at Study Sites.....	37
2.6.1 Rooster - Setting Hen.....	37
2.6.2 Seven Sailors.....	42
2.6.3 Fossil Site.....	44
2.6.4 Lime Ridge.....	46
2.7 Facies Associations.....	50
2.7.1 Fluvial Ribbons (FR).....	51
2.7.2 Broad Fluvial Sheets (BFS).....	51
2.7.3 Confined to Unconfined Sheets (CUS).....	55
2.7.4 Floodplain Siltstone (FS).....	56
2.7.5 Loess-Paleosol Blankets (LPB).....	56
2.7.6 Lacustrine Fines (LF).....	57
2.7.7 Fluvial Paleoflow Patterns.....	57
2.8 Discussion.....	58
2.8.1 Fluvial-Eolian Interaction on the Halgaito Plains.....	58
2.8.2 Comparison of Fluvial Architectural Styles with Facies Models.....	61
2.8.3 Contribution of Vegetation to the Halgaito Landscape.....	68
2.8.4 Evolution of Fluvial and Eolian Processes during Halgaito Deposition.....	70
2.8.5 Rivers Flowing North into the Paradox Basin.....	75
2.9 Conclusions.....	78
<b>Chapter 3: Discussion.....</b>	<b>80</b>

3.1 Synthesis .....	80
3.1.1 Purpose of the Research.....	80
3.1.2 Modern implications.....	82
3.2 Analogues .....	83
3.2.1 Namibia.....	83
3.2.2 Loess Plateau.....	83
3.2.3 Volcanic ash.....	84
3.3 Further Work.....	84
3.3.1 Paleoflow.....	84
3.3.2 Grain Size.....	85
3.3.3 Biostratigraphy.....	85
3.3.4 Diagenesis.....	85
<b>References .....</b>	<b>87</b>

## List of Tables

Table 1: Facies in the Halgaito Formation in Valley of the Gods and Lime Ridge.....	21
Table 2: Grain-size analysis of eolian and fluvial siltstones.....	32
Table 3: Measured data regarding root depth, width .....	37
Table 4: Facies associations in the Halgaito Formation.....	53
Table 5: Architecture of some dryland-river deposits in the geological record.....	64

## List of Figures

Figure 1 Schematic diagram of the Paradox Basin to show main bounding uplifts .....	2
Figure 2 Map Study sites in southeast Utah.....	3
Figure 3 Geological map of the region.....	4
Figure 4: Terrain in the Valley of the Gods.....	5
Figure 5: Stratigraphic sections for the Halgaito Formation.....	8
Figure 6: Sedimentary features and fossils.....	24
Figure 7: Sedimentary features and fossils from Lime Ridge.....	24
Figure 8: SEM images of representative samples.....	26
Figure 9: Fossils.....	28
Figure 10: Grain-size frequency curves, normalized to percentages.....	34
Figure 11: Two examples of Fluvial Ribbons.....	38
Figure 12: Architecture of Channel-Bodies A and B.....	40
Figure 13: Architectural details for Channel-Body A and C.....	42
Figure 14: Architecture of channel bodies at Seven Sailors.....	44
Figure 15: Series of images of Lime Ridge.....	48
Figure 16: Channel geometries of the Halgaito Formation.....	49
Figure 17: An idealized view of the Upper, Middle, and Lower Halgaito.....	71
Figure 18: Evolution of the three main environments.....	73
Figure 19: The paleogeographic positions of the Uncompahgre Highlands.....	75

## Abstract

The study of dryland fluvial systems has yielded a broad and well established body of work. As rivers in semi-arid and arid environments cover nearly 50% of the present land surface, there are many modern examples to turn to as reference; Australia, India, Africa, and mid-west USA all have examples of dryland fluvial environments that are intermittently active. Many modern examples, as well as those documented in the rock record, are typically associated with sudden high-energy floods that carry fine sand to gravel sized particles. Few examples of dryland river systems have a majority of the sediment in the medium silt to very fine sand range.

The Halgaito Formation of Southeastern Utah is a magnificently exposed section of rock which records the transition from Late Pennsylvanian to Early Permian as seen on the western margin of Pangea. This study documents an interaction between windblown silt, forming loess deposits, and a discontinuous fluvial system that carved into the landscape. The Halgaito Formation is herein subdivided informally into lower, middle, and upper divisions based on the relationship between these two distinct yet interacting environments. An overall upward increase of channel width, depth, and complexity is apparent from the lower to middle divisions, whereas the upper division is marked by overland sheet floods that scoured the landscape, forming small localized depressions and reworking the topmost layer of loess that covered the region. This transition overall records a deepening of the water table, decrease in clusters of vegetation, and an increase of plants with deeply penetrating roots that stem from thin paleosol layers that cap the sheet flood deposits below subsequent loess beds.

Previous to this study, various research teams working within Southeast Utah have published papers for their respective specialties; however, no broader study of the general paleo-landscape and paleo-environment framed these specialized papers. The following research endeavors to do so.

## List of Abbreviations Used

SEM	Scanning Electron Microscope	<u>Architectural elements</u>
<u>Minerals</u>		SB Silty Bedforms
Ba	Barite	LS Laminated Sheets
Bi	biotite	DA Downstream accreted elements
Dol	Dolomite	LA Laterally accreted elements
He	Hematite	<u>Facies associations</u>
Illm	Illmenite	FR Fluvial Ribbons
Ksp	Potassium Feldspar	BFS Broad Fluvial Sheets
Mu	Muscovite	CUS Confined to Unconfined Sheets
Pb	Lead	FS Floodplain Siltstone
Pl	Plagioclase	LPB Loess-Paleosol Blankets
Ru	Rutile	LF Lacustrine Fines
Qz	Quartz	<u>Informal divisions</u>
<u>Grain size</u>		UD Upper Division
VF	Very Fine sand	MD Middle Division
FS	Fine sand	LD Lower Division
MS	Medium sand	<u>Sample Numbers (XX-YY)</u>
CS	Coarse sand	XX Year collected (2015/2017)
VC	Very coarse sand	YY Order in which sample was gathered
<u>Facies codes</u>		
Sr	Ripple cross-laminated siltstone	
St	Trough cross-stratified siltstone	
Sh	Laminated siltstone	
Gm	Introformational Conglomerate	
Sm	Structureless siltstone	
Sp	MS- VC may be pebbly in planar crossbeds	
Ss	FS- CS may be pebbly in cross stratification	
Fl	sand, silt or mud in fine laminations	
Fsc	Silty Mudstone	
Ca	Limestone/Calcite	



## Acknowledgements

I would like to thank my supervisors Martin Gibling and Isabelle Coutand for their continued guidance and support throughout my MSc. I am indebted to my supervisor Martin Gibling for all of his patience and mentorship as I dealt with life's trials. I would also like to thank Martin for the opportunity to work in such an amazing location as southeast Utah. My geological education started in Utah and it was a fitting bookend to return in order to put my education to use. I would also like to thank Martin for the chance to present my research at national and international conferences both in Calgary and Baltimore. A large thank you to my committee members Anne-Marie Ryan and John Calder for their thoughtful comments and discussions during our committee meetings and for the time they took to review my thesis.

I would like to thank the very welcoming group of scientists that converged in Utah in 2015, all of whom added their own specialty to this body of work. Bill DiMichelle, Dan Chaney, Scott Elrick, John Nelson, Amy Henrici, David Berman, Tyler Schlotterbeck, and Adam Huttenlocker helped me with this research and without their assistance; this would have been a much harder endeavor. The incalculable assistance of Grant Shortreed as my field assistant during my second field season was an unexpected blessing. I would also like to thank Randolph Corney, and Xiang Yang at SMU for their help with point counting, SEM work, and petrographic image collection.

A big thank you to the Earth Science Department and fellow graduate students for their support and comradeship, especially Carla Skinner and Shelby Sanders for the long phone calls, and discerning eyes cast over the many stages of the manuscript. Finally, I thank my family and friends, both near and far; without their unconditional love and support, I would not be who I am today.

# Chapter 1: Introduction

## 1.1 Statement of Problem

The study of ancient dryland fluvial systems, which border and interact with windblown sediments, focus strongly on sand- to gravel-dominated systems. This research examines the Pennsylvanian to Permian Halgaito Formation which is predominantly medium silt, ranging from fine silt to very fine sand, with minor lenses of pebble conglomerate. The Halgaito Formation was deposited in western equatorial Pangea, which is now in the San Juan River area of the Paradox Basin, SE Utah, in a region known as the Valley of the Gods. The Paradox Basin was an oval catchment basin in the central Colorado Plateau (Condon 1997). During formation, the basin was bounded to the northeast by the Uncompahgre Highlands, an upland of Precambrian rock with a fault zone on the basinward side (Fig 1) (Condon 1997; Barbeau 2003; Thomas 2008). Along the remaining three sides of the basin were a series of small highlands, monoclines and upwarps, which were uplifted at various stages in the basin history and later deformation. Repeated transgressions and regressions of the Panthalassa Ocean to the south of the Paradox Basin deposited limestone beds at irregular intervals within the late Pennsylvanian Rico Formation, which are notably rare in the overlying Halgaito Formation (Sears 1956; Condon 1997). Denudation of the highlands created thick alluvial-fan deposits in the basin, known in proximal areas of the basin as the Cutler Group undivided. This undifferentiated unit transitions to the southwest into mappable units and a much thinner succession of sediments (Baker and Reeside 1929; Condon 1997) (Fig 2B, 3). The conformable succession of Permian rocks in the

Valley of the Gods has been eroded into towering buttes, mesas, and plateaus (Fig. 4). This notable location has been the site of many geological, paleobotanical, and paleontological studies undertaken by a variety of universities and research institutes.

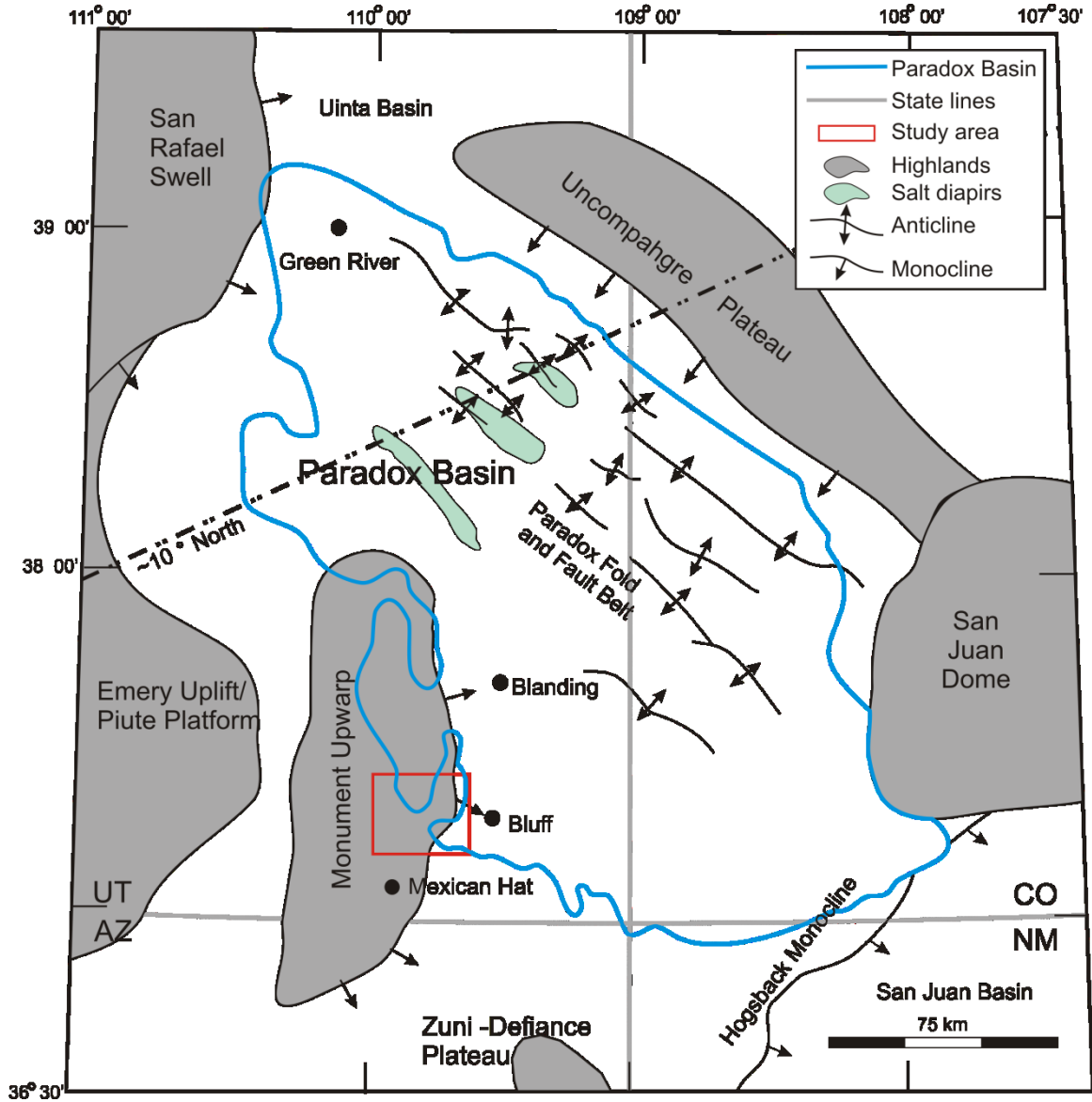


Figure 1 Schematic diagram of the Paradox Basin to show main bounding uplifts and some broad facies relationships. Modified from Condon 1997; Venus et al. 2015; Lawton et al. 2015.

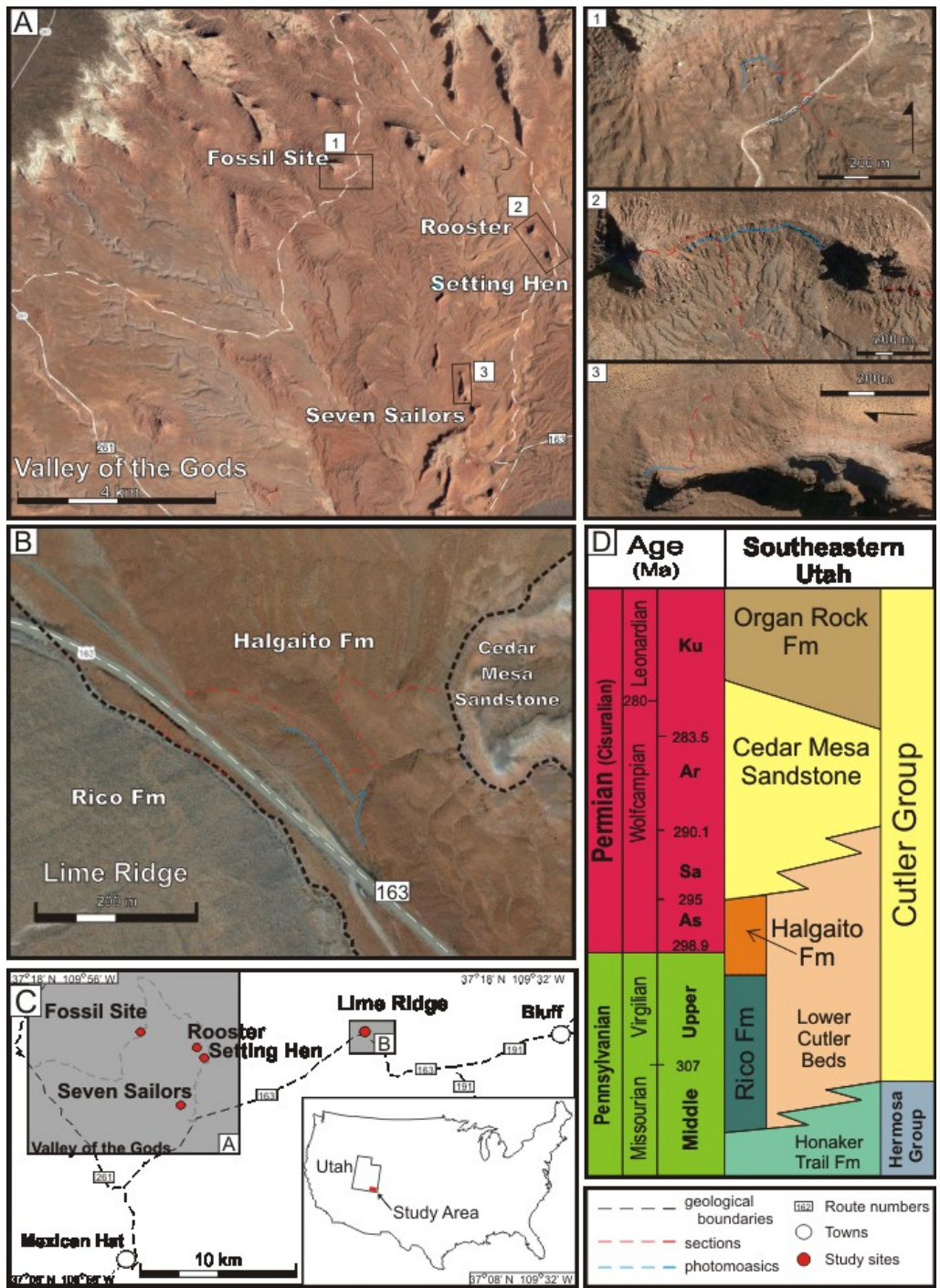
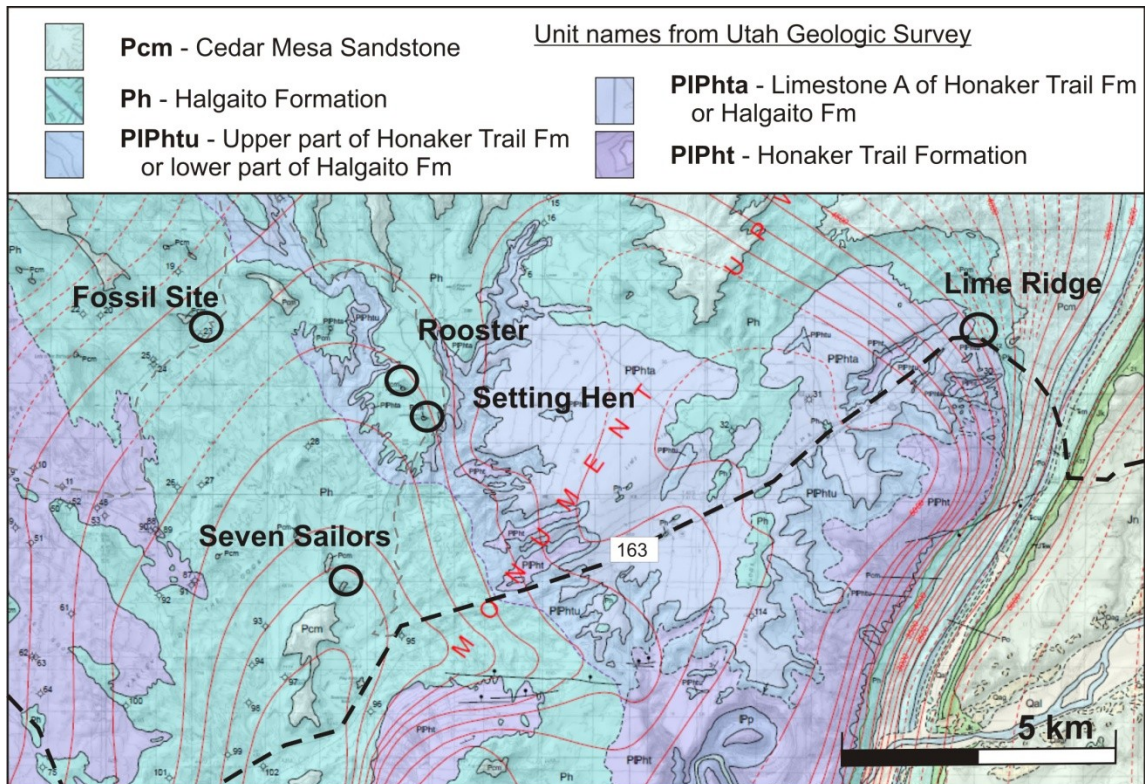
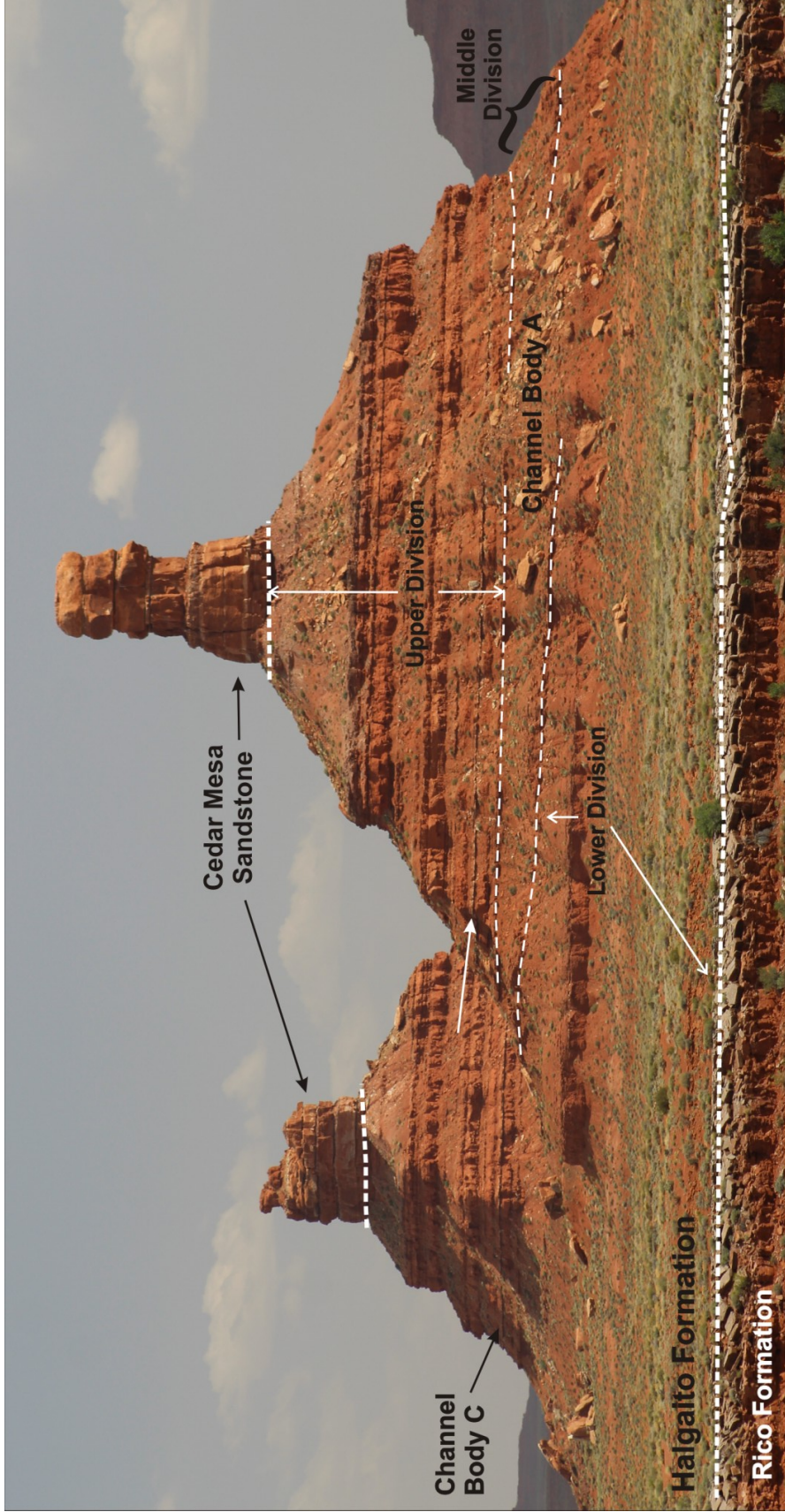


Figure 2 Map Study sites in southeast Utah. A) Valley of the Gods showing 1: Fossil site, 2: Rooster (left) and Setting Hen (right), 3: Seven Sailors. The Rico and Halgaito formations form the lower ground and the Cedar Mesa Sandstone forms higher buttes and mesas. B) Lime Ridge with the Rico Formation, Halgaito Formation, and Cedar Mesa Sandstone distinguished through colour differences. C) Map of southeast Utah with field sites. D) Stratigraphic column for southeast Utah (modified from DiMichele et al. 2014).



**Figure 3 Geological map of the region. Note boundaries of units are not always certain and depend on location. Modified from Utah Geological Survey)**

Early oil and gas exploration in the region established the names for the succession of rocks in this area, including the Halgaito Formation (Baker and Reeside 1929). A substantive amount of geological study has focused on the loess deposits found in the Halgaito Formation, the source of eolian sediments, and the mapping of regional units (Stanescio and Campbell 1989; Soreghan et al. 2002a; Soreghan et al. 2002b; Soreghan et al. 2009; among others). Paleobotanists from the Smithsonian Institution, Washington, DC have several well documented plant fossil sites in the Valley of the Gods (Chaney et al. 2013; DiMichele et al. 2014), and important vertebrate localities are present (Vaughn 1962; Huttenlocker et al. 2018).



**Figure 4: Terrain in the Valley of the Gods to show the outcrop belts of the Rico and Halgalto formations and the Cedar Mesa Sandstone. For the purposes of the present study, the Halgalto is divided into informal lower, middle and upper divisions.**

(Photograph by D. Tobey, 16/06/17)

## **1.2 Objectives**

The objective of this research is to describe the early Permian landscape through the interaction between fluvial and eolian systems, the observed fossilized plant life (including root depletion halos), and the limited bioturbation and fossilized tetrapod records of the region. This landscape integration has the following objectives:

- I. Describe a fine-grained fluvial system influenced by eolian sedimentation in varying degrees by applying the established classifications of fluvial bedforms for a silt-dominated system.
- II. Establish the importance of using fossilized vegetation in inferring fluvial style and environmental changes within this fine-grained system.
- III. Further the scientific body of knowledge regarding the topography and paleogeography at the time of deposition, specifically in regard to the Monument Upwarp.
- IV. Create a depositional framework to guide specialists who undertake work in this region by describing the landscape in terms of fluvial style, eolian interactions, vegetation, and climate.

## **1.3 Contributions of the Author**

The research necessary for this thesis was conducted during two separate field seasons, in 2015, and 2017, both of which were approximately 28 days in length. In 2015 the author, with Martin Gibling supervising and advising, measured and recorded bed-by-bed sections of Lime Ridge, Rooster, Setting Hen, and Fossil Site. Lateral sections that traced channel beds were first photographed and then formed into photomosaics in order to record bedforms and paleoflow, among other important features, at Lime Ridge and between the Rooster and Setting Hen buttes. These locations were chosen due to the previous work conducted at these locations

by two paleobotanists from the Smithsonian Institution, Bill DiMichele and Dan Chaney, who were on site during the 2015 season conducting their own research. With their assistance the locations of fossil plants were noted, as well as several trackways attributed to *Diplichnites cuithensis*. The Fossil Site was included, and so named, because of an excavation underway at this site, the findings of which were published in Huttenlocker et al. (2018). Work at the Fossil site was a collaboration between paleontologists Amy Henrici, David Berman, and Tyler Schlotterbeck from the Carnegie Museum in Pittsburgh, PA; John Nelson and Scott Elrick of the Illinois state Geological Survey, IL; and Adam Huttenlocker on behalf of the University of Southern California, CA. John Nelson and Scott Elrick traced key beds and measured other sections in the study area; their logs and stratigraphic attributions provided valuable regional correlation. The bed-by-bed measurements by the present author were recorded as vertical logs accompanied by descriptions which were the basis for the logs found in Figure 5.

In 2017 the author, with Grant Shortreed as field assistant, revisited the previous sites to obtain further samples, reconfirm measurements, and to look for any features not seen in 2015. Logs and lateral photomosaics were measured at Seven Sailors location, and the lateral tracing at the Fossil Site was done during this field season. The second season reinforced many of the findings from 2015 and was able to fill in minor data gaps, notably the measurements of root depletion halos. Petrographic analysis was conducted by the author at St. Mary's University, with the assistance of Randolph Corney (point counting) and Xiang Yang (SEM). All image drafting, facies analysis and preparation of the manuscript were the product of the author with guidance and editing provided by Martin Gibling, co-supervisor Isabelle Coutand, supervisory committee members John Calder and Anne-Marie Ryan. Chapter 2 is intended for submission to Journal of Sedimentary Research, coauthored by Dawn Tobey and Martin Gibling.



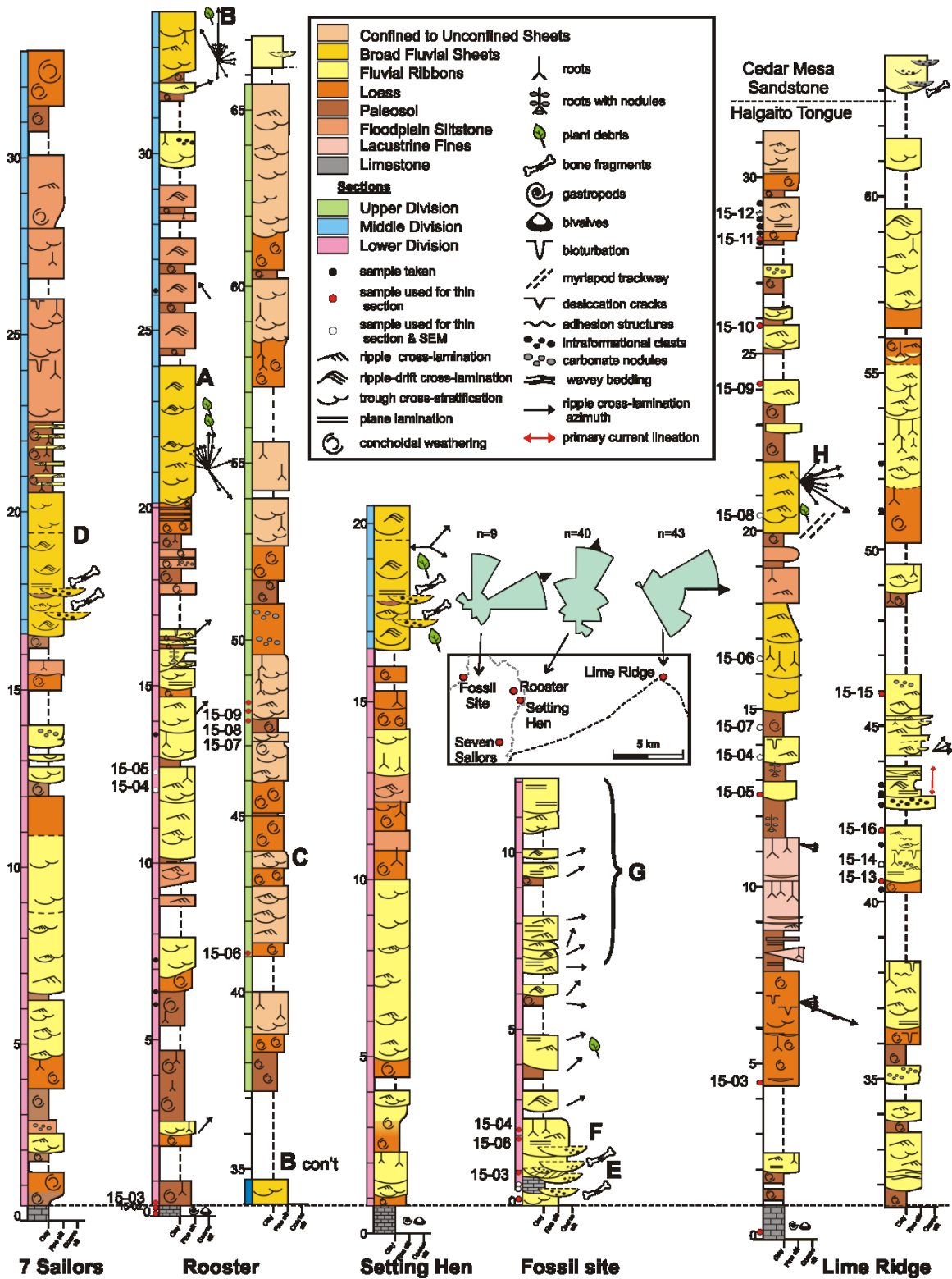


Figure 5: Stratigraphic sections for the Halgaito Formation in the study areas in southeast Utah. The base of each section is the uppermost carbonate bed of the Rico Formation, which is the "A" limestone in this area. The "A" limestone is not present at the Fossil Site, but a

correlative position for the limestone is taken from Huttenlocker et al. (2018). Two sections reach the overlying Cedar Mesa Sandstone. Composite rose diagrams for ripple cross-lamination are shown for the three main study areas. A-H represents significant beds which will be the focus of later discussion.

## **Chapter 2: Fine-grained Dryland Rivers Reworking Loess in the Paradox Basin of Western Pangea: Halgaito Formation, Pennsylvanian-Permian of Utah**

### **2.1 Abstract**

The Halgaito Formation, an approximately 65 m thick unit in the Valley of the Gods and Lime Ridge, is an unusual example of fine grained fluvial systems interacting with aggrading loess under seasonal conditions at the distal margin of the Paradox Basin. The channel sediments have a coarse silt modal class with a few samples in the very fine sand range, closely comparable to the modal class of the associated loess beds. This indicates that the fluvial sediments are predominantly reworked loess. Grain-size comparison of Halgaito loess with Quaternary loess suggests eolian transport in suspension clouds over tens of kilometers, with a predominant source from exposed coastal sand flats to the west.

In an informal lower division of the formation, ribbon channel bodies 1 – 5 m thick and up to 17 m wide cut into floodplain deposits of eolian and fluvially-derived siltstone. In the middle division, sheet-like, multilateral channel bodies up to 5 m thick and more than 500 m wide contain suites of scour fills where systematic channel migration widened the channel belt, cutting into loess and locally choked by loess accumulations. Subcritical bedforms predominate, with local critical to supercritical bedforms. This style of architecture is typical of many dryland rivers with strongly fluctuating discharge. The larger scale of channels may reflect more water on the landscape or the migration of a larger system into the area. In the upper division, loess-paleosol blankets indicate progressive aridification, and the loess was reworked into very broad siltstone sheets that represent largely unconfined flows, thickening locally into channel forms.

The channel bodies contain a mixture of dryland and wetland plant taxa, with the latter suggesting local availability of water rather than prevailing humid conditions. Deep and tightly-spaced root systems testify to the periodic presence of vegetation across the landscape, assisting in stabilizing the loess. Faunal elements in the channel bodies include tetrapods and a range of invertebrate tracemakers.

Northward and eastward paleoflow measurements indicate the rivers were not sourced from the Uncompahgre Uplift to the north but had their headwaters in the Monument Upwarp at the southern basin margin, where reworked loess provided the bulk of the sediment. It is not known whether the Halgaito rivers joined the northern drainages or died out in the basin.

#### *Keywords*

Uncompahgre Uplift; Monument Upwarp; fluvial ribbons and sheets; scours; unconfined flows; vegetation; root systems

## **2.2 Introduction**

Rivers in hyperarid, arid, semi-arid and dry sub-humid settings with seasonal climates (herein termed “dryland rivers”) cover some 50% of the current global land surface (Tooth 2000) and exhibit great variability in discharge and sediment transport, with extensive floods and periods of minimal or no flow. The rivers exhibit a wide facies spectrum, a range of planforms, and sedimentation styles that include lateral and downstream accretion, oblique accretion, and vertical aggradation in channels that range from narrow fixed channels to broad washes and continental-scale rivers (Abdullatif 1989; Nanson and Knighton 1996; Gibling et al. 1998; Fielding et al. 1999; Page et al. 2003; Sambrook Smith et al. 2016; Carling and Leclair 2019). Subject to prolonged dry periods, the rivers commonly exhibit dynamic interaction between flow and vegetation growing on the banks and within the channels (Tooth 2000, 2005; Jansen and Nanson 2010). Recent research (Fielding et al. 2009; Allen et al. 2014; Fielding et al. 2018) has emphasized the importance of seasonal flow and peak discharge variability in governing fluvial facies assemblages and architecture, yielding new insight for classifying the alluvial rock record beyond planform-based categories.

Studies of ancient dryland river systems have tended to focus on channels with sand and gravel but only modest amounts of mud (e.g., Tunbridge 1984; Stear 1985; Olsen 1989; Bhiry and Occhietti 2004; Cain and Mountney 2009; Wilson et al. 2014). Dryland systems dominated by silt and clay have received less attention, despite their local importance (Mack et al. 2003; Ghosh et al. 2006; Wright and Marriott 2007; Simon and Gibling 2017a, b; Simon et al. 2018).

A distinctive subset of Quaternary, fine-grained terrestrial systems is present where extensive loess sheets blanket the landscape. Such loess tracts cover as much as 10% of the Earth's land surface (Muhs and Bettis 2003) across Eurasia, North America and South America, with an especially prominent accumulation in the Chinese Loess Plateau (Smalley 1995; Porter 2001; Muhs and Bettis 2003; Antoine et al. 2009). The silt-sized loess is attributed largely to glacial grinding during ice advances, with additions from eolian abrasion, fluvial comminution, salt weathering in playa systems, and erosion of silt-rich bedrock (Whalley et al. 1982; Pye and Sperling 1993; Muhs and Bettis 2003; Bullard et al. 2007; Soreghan et al. 2008). Rivers transport glacially derived sediment to the plains and, along with playa lakes, provide a dust source for eolian transport. Many of the world's large rivers transport and erode loess (Smalley et al. 2009; Stevens et al. 2013; Licht et al. 2016; Sambrook Smith et al. 2016), and grain-size analysis of loess successions yields evidence for fluvial reworking (Vandenberghe 2013; Vandenberghe et al. 2018). However, studies of fluvial-eolian interaction in modern settings and the rock record have largely focused on dune fields (Langford and Chan 1989; Herries 1993; Jones and Blakey 1997; Bullard and McTainsh 2003; Krapf et al. 2003; Williams 2015), and fluvial architecture in ancient loess-rich terrains has received little attention.

From the latest Devonian through the Permian, western equatorial Pangea accumulated the thickest dust deposits yet documented on Earth, with as much as 1 km of loess in places and

a peak of accumulation in the latest Pennsylvanian and Early Permian (Kessler et al. 2001; Soreghan et al. 2008; Sur et al. 2010; Soreghan et al. 2014). Soreghan et al. (2008) attributed the unusual abundance of silt to the Late Paleozoic Ice Age, during which periodic glacial and cold-weathering processes generated abundant silt even at low latitudes. This setting was accentuated by the growth of the Appalachian and Ouachita-Marathon orogens and local uplifts of the Ancestral Rocky Mountains, which were glaciated locally (Soreghan et al. 2009; Brezinski et al. 2010; Sweet and Soreghan 2010). Monsoonal circulation fostered strong, seasonal winds, with progressive aridification of western Pangea (Tabor and Poulsen 2008).

The Paradox Basin of Utah and Colorado includes thick accumulations of dune sand and loess. In what is now southeast Utah, eolian and fluvial systems interacted to form the loess-rich Pennsylvanian to Permian Halgaito Formation, which passes upwards and laterally into eolian dunes of the Cedar Mesa Formation (Fig. 2D). Previous studies of the Halgaito Formation have focused on loess composition (Murphy 1987; Soreghan et al. 2002a; Soreghan et al. 2002b; Soreghan et al. 2009), paleobotany (DiMichele et al. 2014), vertebrate paleontology (Vaughn 1962; Huttenlocker et al. 2018), and paleosols (Soreghan et al. 2002; Golab et al. 2018). This research contributes and expands the body of knowledge with an account of the formation's dryland fluvial systems to 1) document the architecture of these fine-grained, ephemeral river deposits, 2) compare the grain size and composition of the fluvial and eolian deposits, 3) investigate the interaction of rivers with aggrading loess, and 4) evaluate the influence of vegetation on the river systems in this relatively arid setting.

## 2.3 Geological Overview

During the Virgilian and Wolfcampian, the Paradox Basin lay on the western margin of Pangea close to the equator (Fig. 1; Torsvik and Cocks 2004). The depocenter is a large intraforeland flexural basin that developed along the southwest margin of the Uncompahgre Uplift, a fault-bounded cratonic structure (Fig. 1; Hoyt and Ridgway 2002; Barbeau 2003; Thomas 2007). The Uncompahgre and other uplifts in the region form part of the Ancestral Rocky Mountains, variously considered a response to tectonic activity in the Ouachita-Marathon Orogen or to subduction along southwestern North America (Kluth et al. 1998; Moore et al. 2008; Soreghan et al. 2012; Blakey 2019). Barriers along the distal basin margin, represented by the Zuni-Defiance and Emery-Piute uplifts, restricted access to the Panthalassa Ocean to the south and west, and thick evaporites and rhythmic successions of the Pennsylvanian Paradox Formation and coeval rock units were laid down in the basin (Goldhammer et al. 1991; Dyer and Maloof 2015). Much of the region was overprinted by Laramide deformation during the Cretaceous and early Cenozoic, contributing to the Monument Upwarp along the southern basin margin (Bump and Davis 2003).

During the Pennsylvanian and Permian, some 5,000 m of strata accumulated in the basin proximal to the Uncompahgre Uplift (Ritter et al. 2002). Exhumation linked to thrust faults along the southern margin of the uplift led to southwest-flowing river systems that formed coalesced alluvial fans and megafans of the undivided Cutler Group. Basinward progradation of the Cutler Group drove growth of salt walls up to 4,500 m high from the underlying evaporites, separated by minibasins (Fig. 1; Dubiel et al. 1996; Barbeau 2003; Trudgill 2011; Venus et al. 2015). The salt walls formed effective topographic barriers that diverted paleoflow to the west and northwest (Lawton et al. 2015), but salt-weld formation allowed clastic sediments to

overtop the salt walls and reach the distal basin, aided by bypass zones along transfer faults (Lawton et al. 2015).

Proximal coarse-grained alluvium of the Cutler Group passed distally southwest into finer grained fluvial, eolian, and lacustrine red beds, subdivided by Baker and Reeside (1929) into the Rico Formation and overlying Cutler Formation, the latter containing the Halgaito tongue and the Cedar Mesa sandstone member. Subsequent researchers noted regional facies variations and applied different ranks to the subdivisions (Gregory 1938). Individual limestones of the Rico Formation die out laterally and intertongue with Halgaito strata, with the McKim Limestone or the higher "A" limestone forming the topmost bed locally (Sears 1956; O'Sullivan 1965; Golab et al. 2018). The Halgaito has variously been mapped as a tongue or member of the Cutler Formation (Fig. 3) (Sears, 1956; Lewis and Campbell 1965; O'Sullivan 1965; Stanesco and Campbell 1989) or as a formation of the Cutler Group (Wengerd and Matheny 1958; Baars 1962; Dubiel et al. 1996). Loope et al. (1990) and Condon (1997) grouped the broadly similar Rico and Halgaito redbeds as the informal "lower Cutler beds", and Golab et al. (2018) included Rico strata in the Halgaito Formation, within the underlying Hermosa Group.

This research follows Soreghan et al. (2002), DiMichele et al. (2014) and Nelson and Elrick (2015) in recognizing the Rico Formation, Halgaito Formation, and Cedar Mesa Sandstone of the Cutler Group as mappable units within the study area of the Valley of the Gods and Lime Ridge (Fig. 2D, 3, & 4). The base of the Halgaito Formation is diachronous and time transgressive, marked by the locally highest fossiliferous Rico limestone, and the formation grades northwards and eastwards into the Cedar Mesa Sandstone (Condon 1997; Scott 2013).

The Rico Formation in the study area is about 120 m thick (Sears 1956) and comprises mudstone, siltstone, quartzose sandstone, minor conglomerate, and marine limestone with a



variety of shallow-marine fossils (Lewis and Campbell 1965), periodically connected to an open ocean to the west and south (Condon 1997). The Halgaito Formation is approximately 70-120 m thick and comprises reddish brown to pale gray siltstone and silty sandstone, with thin beds of intraformational limestone conglomerate and paleosols (Condon 1997; DiMichele et al. 2014). Fine-grained redbeds in both formations were identified as loess, locally reworked into fluvial deposit (Murphy 1987 and Soreghan et al. 2002). The precise age range of the formation is uncertain, but fossil assemblages at the Birthday Bonebed between the McKim Limestone and the "A" limestone suggest a topmost Pennsylvanian age, with higher Halgaito strata probably of earliest Permian age (Fig. 2D; Huttenlocker et al. 2018).

The Cedar Mesa Sandstone is 300-400 m thick and comprises stacked erg sequences of fine- to coarse-grained sandstone with fluvial-channel and interdune deposits (Loope 1984; Langford and Chan 1989; Soreghan et al. 2002; Mountney 2006; Langford et al. 2008; Lawton et al. 2015). Near the Valley of the Gods, gypsum and limestone associated with the eolian dunes suggests a playa setting (Stanescu and Campbell, 1989).

Western Pangean climate models and field evidence from Carboniferous and Permian strata indicate progressive aridification linked to the waning of Gondwanan glaciation and rising atmospheric CO<sub>2</sub> levels (Parrish 1993; Peyser and Poulsen 2008; Tabor and Poulsen 2008; Soreghan et al. 2009; Montañez et al. 2016). The Paradox Basin has been considered hot and arid during this interval, with humid periods and loess-paleosol rhythms and rhythmic facies successions that probably reflect global glacial and interglacial rhythms (Soreghan et al. 2002; Jordan and Mountney 2012; Soreghan et al. 2014). However, evidence from the Cutler Group indicates a relatively arid proglacial-periglacial system with low-latitude upland glaciers, supporting glacial grinding for much of the silt-sized loess (Soreghan et al. 2008; Soreghan et al.

2009; Sweet and Soreghan 2010). Soreghan et al. (2002) inferred semi-arid conditions for the Rico Formation and more humid conditions with fluvial influence for the Halgaito Formation, with increased loess and more arid conditions below the Cedar Mesa Sandstone.

Provenance analysis using detrital zircons from Paradox Basin loess suggest northeasterly winds for the later Pennsylvanian, with a shift to monsoonal circulation and northwesterly winds by the earliest Permian (Wolfcampian)(Soreghan et al. 2002). Eolian dune sands in the Cedar Mesa Sandstone show a southeasterly paleowind direction (Loope 1984; Peterson, 1988; Parrish and Peterson, 1988; Mountney 2006; Langford et al. 2008).

## **2.4 Methods**

The study area has numerous mesas and buttes separated by low-lying desert, with partially exposed slopes underlain by the Rico Formation and lower strata of the Halgaito Formation and cliffs and pinnacles underlain by higher Halgaito strata and the Cedar Mesa Sandstone (Fig. 4). During 2015 and 2017 field seasons, five sections were measured in detail (Figs. 2A-C, 5) to define the range of facies and studied well exposed channel bodies in order to characterize fluvial composition and geometry. Photomosaics were annotated in the field for facies, channel margins, paleoflow, and fossils. Facies and architectural elements were categorized using systems in Miall (1996). Many facies are relatively fine grained, which prevented field classification of the sediments further than “silt”. Samples were collected for further study and detailed classification. For general description of the silt, we use the standard Udden-Wentworth system of very fine (4-8  $\mu$ ), fine (8-16  $\mu$ ), medium (16-31  $\mu$ ), and coarse (31-63  $\mu$ ) silt.

Known fossil plant localities were studied in relation to fluvial channels and bedforms, with observations of the size of the fragments. New specimens were identified in the field by W.A. DiMichele and D. Chaney of the Smithsonian Institution. Fossilized root traces were used as a partial proxy for floral abundance. Measurements were gathered of the depth of penetration of the roots below former vegetated levels; the width of the main root axis as recorded by drab mottles (wider than the original root); the width of the main axis and zones of rootlets that branch from it; the width of clustered large roots; the spacing of major root traces in outcrop faces; and the frequency of evidence for downward branching

Paleoflow was measured for 92 occurrences of ripple cross-lamination on exposed bed surfaces, with measurements considered accurate to within 5°. Primary current lineation trends were also recorded. Although dune cross-strata are present, none were sufficiently well exposed for reliable directional measurement. Paleoflow vector means were calculated to indicate regional flow directions for sections and to constrain the geometry of individual channel bodies. The aspect ratio (width:thickness) of channel bodies was used to define very broad sheets (>1,000:1), broad sheets (100-1000:1), narrow sheets (15-100:1), broad ribbons (5-15:1), and narrow ribbons (<5:1)(Gibling 2006). Krynine (1948) defined “blankets” as equidimensional sediment bodies with a width:thickness ratio of >1,000:1.

Thin sections and polished thin sections for representative rock samples were studied for grain type, size, roundness, cementation, and fabrics. Point counts to establish the composition of 400-500 grains were carried out using a PETROG automated stepping stage and PetrogLit software mounted on a Nikon Eclipse E400 Pol petrographic microscope with a Pixe-Link digital camera and point-counting software at St. Mary’s University, Halifax. To estimate the grain size for 7 eolian and 17 fluvial siltstones (stratal positions shown on Fig. 5), the maximum

apparent diameter was measured for 350-450 selected quartz grains and a small number of feldspar grains, selected randomly by the stepping stage.

The minimum size of grain measured was 0.013 mm, restricting analysis to medium and coarse silt. To correct for the reduction of grain diameter measured in random 2D cuts through samples, the method of Johnson (1994, p. 996) was used to estimate the true maximum diameter, multiplying the mean long-axis measurement for each sample by 1.3 for mm values, for an estimate within 6%. Johnson (1994) noted that standard deviations are difficult to correct for thin-section measurements but can be used to compare samples.

Fifteen samples were selected for high-resolution imaging using a TESCAN MIRA 3 LMU Variable Pressure Schottky Field Emission Scanning Electron Microscope (SEM) at St. Mary's University. The Energy Dispersive X-ray Spectroscopy associated with the SEM was used for mineralogical identification of grains and cements.

## **2.5 Stratigraphic Sections, Facies, and Fossils**

### **2.5.1 Stratigraphic Sections**

Sections were recorded at Seven Sailors, Rooster, Setting Hen, Fossil Site (including the Birthday Bonebed of Huttenlocker et al. 2018), and Lime Ridge, covering an east-west distance of about 15 km (Fig. 2A-C). Lime Ridge and Rooster provided complete sections of the Halgaito Formation of 63.0 m and 66.0 m, respectively, and the other three Valley of the Gods sections ranged from 14.0 m at the Fossil Site to 20.5 m at Setting Hen and 33 m at Seven Sailors, starting above or close to the "A" limestone (Fig. 5).

For descriptive purposes, the formation was divided into informal lower (15-20 m thick), middle (~15 m), and upper (>30 m) divisions (Fig 4). The boundary between the lower and middle division is taken at the base of the first large channel body at all sites. The boundary between the middle and upper division is based on the onset of widespread, discrete loess beds with paleosols and thin water-reworked units; this is less clear at Lime Ridge than elsewhere.

### **2.5.2 Facies**

Six siliciclastic and one carbonate facies were identified (Table 1; Figs. 5, 6, & 7). Ripple cross-laminated siltstone (Sr) is the predominant facies (Fig. 6D), commonly laid down by climbing ripples and locally bioturbated. Trough cross-stratified siltstone (St) is also common and locally features high-angle cross-strata in sets up to 25 cm thick laid down by subaqueous dunes, although cosets of low-angle and structureless troughs are also present (Fig. 6B, C). The facies locally contains disarticulated plant material and trace fossils. Laminated siltstone (Sh) with parting lineation and locally abundant disarticulated plant material is present locally (Fig. 6A, I), and was laid down as plane beds under critical to supercritical flow, in deeper channels or in topmost channel fills under shallow-water conditions. Desiccation cracks and adhesion structures (Fig. 7G) in some facies indicate periods of subaerial exposure.

These facies conform to the standard bedform suite for unidirectional flow, but petrographic analysis confirmed a predominance of coarse silt with minor very fine sand -- finer than is typical for dunes (Southard and Boguchwal 1990). In a study of the silt-dominated Bermejo River of Argentina, Sambrook Smith et al. (2016) noted that, with a fine sand and silt mixture, no clay, and a high suspended-sediment load, low-angle migrating dunes may develop

**Table 1: Facies in the Halgaito Formation in Valley of the Gods and Lime Ridge. Codes and names are based on Miall (1996), adjusted for the fine-grained nature of the strata. BI = bioturbation intensity. See Soreghan et al. (2002) and Golab et al. (2018) for a detailed description of paleosols, represented by facies Fsc in this study.**

<b>Facies</b>	<b>Lithofacies</b>	<b>Contacts</b>	<b>Fossils</b>	<b>Interpretation</b>
<b>Gm</b> <b>Intra-</b> <b>formational</b> <b>conglomerate</b>	Red to purple/red with 2 to 10 mm rounded fragments of reworked carbonate; in broad scours and trough cross-sections	Erosional base and locally steep margins; Sh and Sm interbeds	Tetrapod bone fragments; roots and rhizoconcretions	Erosive events and channel lags, where intraformational fragments and fossils were concentrated
<b>St</b> (Fig. 6B & C) <b>Trough cross-</b> <b>stratified</b> <b>siltstone</b>	Coarse red siltstone, calcite-cemented with minor dolomite and barite; trough cross-sets 5-30 cm thick and 50-70 cm wide with gently dipping laminae filling scours; some structureless scour-based fills weather as low mounds; rare adhesion structures and carbonate nodules	Gradational with Sr and Sm, rare scours into Sm; abrupt with Fsc, Ca and Gm	Calamites, Walchia Annularia, Diplichnites paleophycus; BI 2; root traces	Downflow migration of dunes in fluvial channels; a few occurrences may be small eolian dunes
<b>Sr</b> (Fig. 6D) <b>Ripple cross-</b> <b>laminated</b> <b>siltstone</b>	Coarse red siltstone, calcite-cemented with minor dolomite, ripple and ripple-drift cross-lamination; rare desiccation cracks and adhesion structures	Gradational with St and Sm; abrupt with Fsc, Ca, and Gm	Diffuse bioturbation, burrows <1 cm in diameter with or without spreite; BI 4; root traces	Downflow migration of ripples in fluvial channels; common at the top of waning-flow successions

<b>Facies</b>	<b>Lithofacies</b>	<b>Contacts</b>	<b>Fossils</b>	<b>Interpretation</b>
<b>Sh</b> (Fig. 6A) <b>Laminated siltstone</b>	Coarse red siltstone, calcite-cemented with minor dolomite; parallel to low-angle lamination, primary current lineation	Gradational with Sr, St, Sm, rare scoured contacts; abrupt base with Fsc	<i>Calamites</i> ; discrete layers of disarticulated plant debris	Critical to supercritical flow in channels and overbank areas
<b>Sm</b> (Fig. 6E) <b>Structureless siltstone</b>	Coarse red siltstone, calcite-cemented with minor dolomite, barite, and celestite; rarely weakly stratified; commonly conchoidally weathered; stacked planar sheets (thickness range?) and lenses in scour-based and stratified units	Gradational with Sr and St; abrupt base with Fsc	Root traces, locally penetrating to 2 m depth	Loess deposited as thin sheets by eolian processes or reworked in fluvial channels and standing-water bodies
<b>Fsc</b> (Fig. 6H & J) <b>Silty mudstone</b>	Coarse red to purple-red siltstone and claystone, weakly stratified and calcite-cemented, with common carbonate nodules; outcrops are friable and conchoidally weathered, with fractures and <10 cm mounds on bed surfaces; rare desiccation cracks.	Abrupt and commonly erosional under Sr, St, Sh, and Sm	Root traces with drab haloes, locally radiating on bed surfaces; sediment-filled root cavities, rhizoconcretions	Root traces, carbonate nodules, and clay content indicate an origin as paleosols
<b>Ca</b> <b>Limestone</b>	Two types: i) Red or blue/grey with >50% calcite, weakly stratified with rare internal scours; ii) Blue/grey crystalline calcite with fossils	Top contact abrupt but not erosional with all other facies	Gastropods, bivalves, echinoid spines, crinoid ossicles, oncolites	Carbonate units in topmost Rico Formation; i): Carbonate-cemented siliciclastic sediment; ii) Marine deposit, open-marine to brackish water

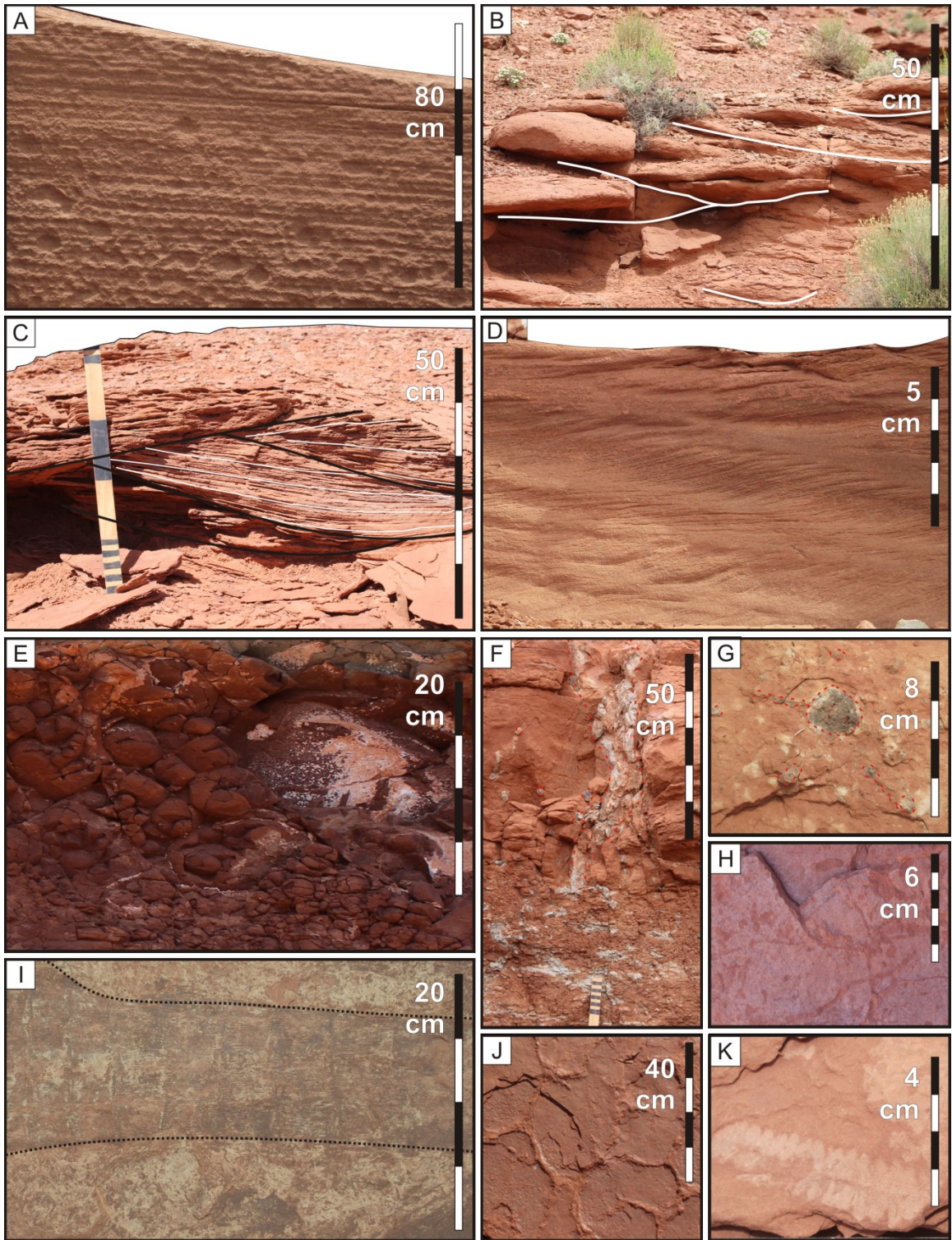
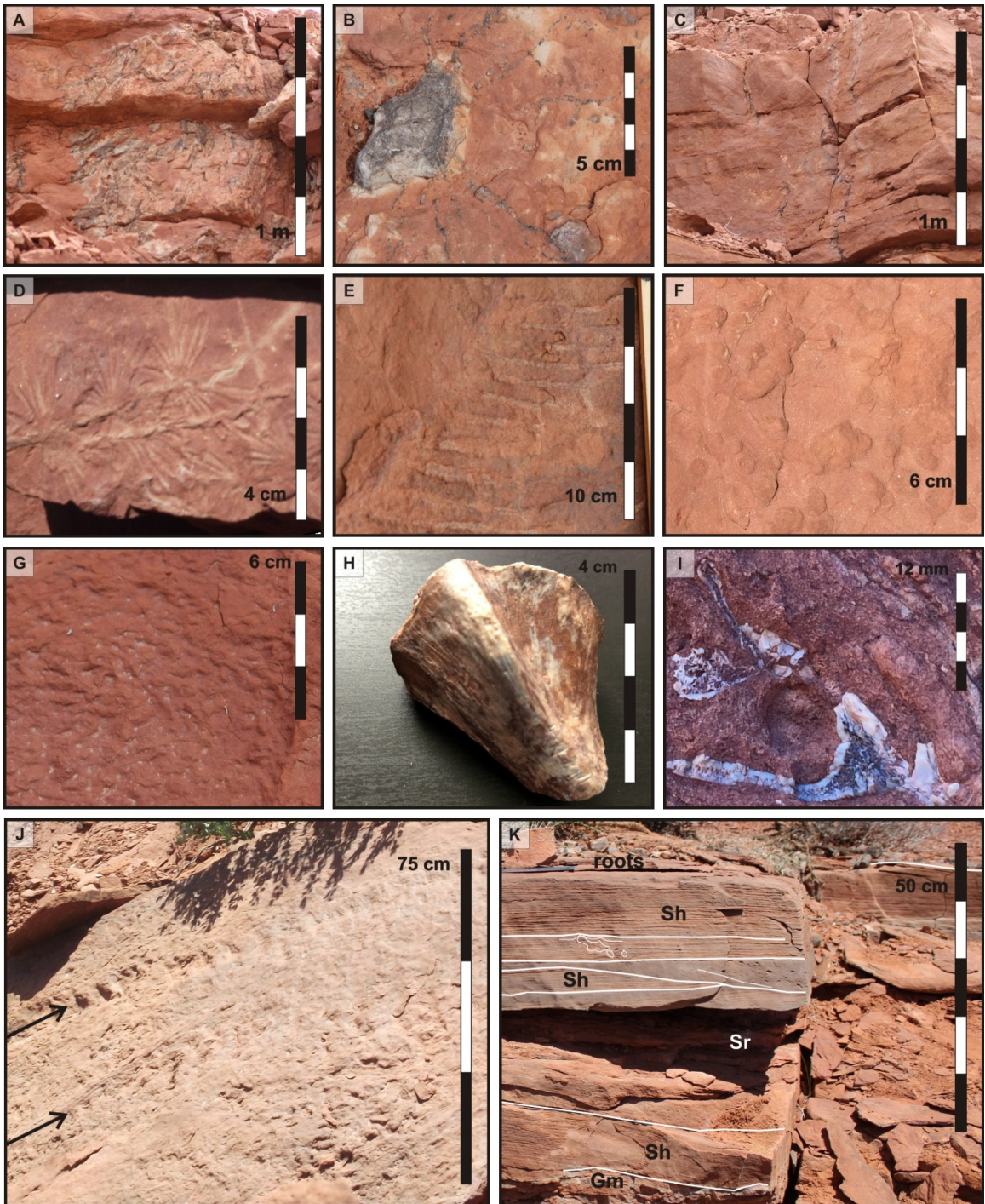




**Figure 6: Sedimentary features and fossils from the Rooster and Setting Hen locations. Locations of some photos are shown on Figures 8-10. Facies codes are in Table 1. A) Laminated siltstone (Sh). B) Trough cross-stratified siltstone (St) with poorly defined, weathered trough forms and sets 10-20 cm thick. C) Trough cross-sets (St) 20 cm thick with gently dipping lamination. D) Ripple cross-laminated siltstone (Sr), with sets climbing steeply to the left and fully preserved ripple crests. (E) Structureless siltstone (Sm) with conchoidal weathering, interpreted as loess. F) Root cluster preserved as drab areas in facies Sm, with a central portion outlined with red dashes and a zone of drab mottles below. G) Cross section of cement-filled root on bedding surface of facies Sm with smaller root traces extending out (red dashes). H) Silty mudstone (Fsc), micaceous, with *Palaeophycus* burrows 3-5 mm in diameter on bedding surface. I) Calamitalean axis ~10 cm in diameter (outlined in dotted lines) and comminuted plant debris on a bedding surface of facies Sh. J) Desiccation cracks in facies Fsc. K) *Pecopteris***

with a small proportion of sand. Mack et al. (2003) noted the presence of trough cross-beds in the Permian Abo Formation of New Mexico, a silt-dominated unit. Under the SEM, 17 fluvial samples from facies St, Sr and Sh consist predominantly of quartz and feldspar grains with minor muscovite, biotite, zircon, rutile, ilmenite, hematite, and apatite (Fig. 8A, from a St sample). Assemblages of calcite crystals of varied size and with irregular boundaries (Fig. 8A<sub>i</sub>) indicate the presence of reworked calcite grains, although they are difficult to differentiate from the cement. Grains are moderately well sorted and are sub-angular to sub-rounded, with a scatter of smaller grains but no discrete population of finer grains that would indicate a well-defined matrix.

**Figure 7: Sedimentary features and fossils from Lime Ridge (A-G, J, K), Seven Sailors (I) and Fossil Site (H), with meterage corresponding to sections in Figure 5. A) Root mass in cliff face (12 m level). B) Cross-section of cement-filled root on bedding surface, linked to root mass in A). C) Narrow, branching root traces seen as a purple-tinged zone, with minor holes in the rock representing the positions of near-horizontal branches (11 m level). D) *Annularia* (21 m level). E) *Walchia* (12.1 m level). F) Bioturbated bedding surface with burrows 0.5-1 cm in diameter, grain sorted *Palaeophycus*. G) Adhesion structures on bedding surface (43 m level). H) Tetrapod fossil fragment in bone-bearing bed at Fossil Site (3 m level). I) Bone fragments at Seven Sailors (17 m level). J) Myriapod trackway seen as two semi-parallel traces (arrowed) approximately 30 cm apart on fallen block (20 m level). K) Facies succession from conglomerate (Gm) to laminated siltstone (Sh) and ripple-drift cross-lamination (Sr). Top portion is laminated siltstone (Sh) with primary current lineation and a few 2-5 cm diameter pebbles, below few a rooted top (Loose block at 44.5 m level).**



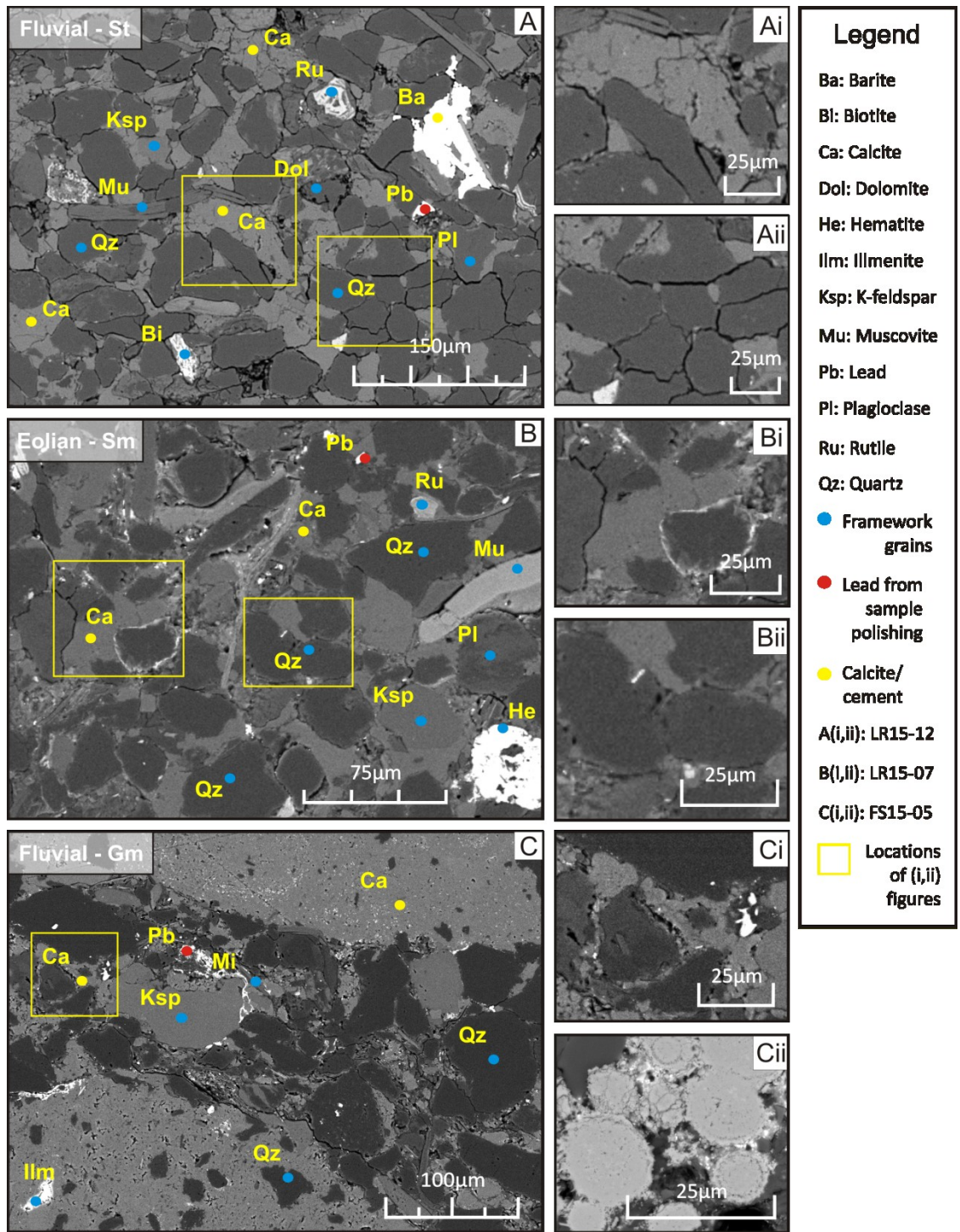


Figure 8: SEM images of representative samples of fluvial and eolian facies. A) Fluvial siltstone sample LR15-12 (St) at 29.5 m level at Lime Ridge (Fig. 5), with calcite and minor barite cement. Ai) Detrital calcite grains (pale grey areas). Aii) Long contacts of siliciclastic grains in an area with little calcite cement. B) Eolian siltstone sample LR15-07 (Sm) at 15 m level at Lime Ridge, with calcite cement and similar grain types but slightly better sorting than fluvial sample in A). Bi) Poikilotopic calcite cement. Bii) Rounded silt grains with point contacts. C) Fluvial siltstone sample FS15-05 (Gm) at 15 m level at Lime Ridge, with calcite cement and similar grain types but slightly better sorting than fluvial sample in A). Ci) Detrital calcite grains (pale grey areas). Cii) Long contacts of siliciclastic grains in an area with little calcite cement.

**Intraformational conglomerate FS15-05 (Gm) at 3.25 m level at Fossil Site. Two large clasts of crystalline calcite shown at top right and bottom left, containing scattered quartz and minor feldspar grains. Matrix is a poorly sorted siltstone similar to samples in A) and B). Ci) Rounded detrital calcite grains (top left) and cement (lower right). Cii) Hematite grains, with overgrowths of the same material (in another part of sample C). Murphy (1987) also noted the presence of detrital carbonate grains loess, including micrite peloids, micritized fossil fragments, and dolomite, and suggested that they originated from coeval regressive-marine flats exposed to the wind.**

Calcite cement comprises crystals a few tens of microns to about 75  $\mu\text{m}$  in diameter, with zones of poikilotopic cement. Barite (Fig. 8), celestite and dolomite are present as small, irregular cement patches in a few samples. Grains mainly show point and long contacts, with areas of closer packing with little cement (Fig. 8A<sub>ii</sub>). These fabrics suggest relatively early cementation in places by calcite and other minor cements, with the persistence of uncemented areas where compaction continued to improve grain packing.

Intraformational conglomerate (Gm) is composed of reworked carbonate and minor bone fragments, locally present on erosional surfaces, and forms part of waning-flow successions (Fig. 7K). As viewed under the SEM (Fig. 8C), the conglomerate has a framework of rounded granules of finely crystalline calcite enclosing a small proportion of quartz and other grains (Fig. 9E, F), probably reworked from paleosols. Some grains have siltstone fragments as a nucleus whereas others formed as rhizoconcretions, with the root positions visible as circular to elongate former cavities filled with detrital grains and calcite cement. The interstices between the larger clasts are filled with angular to subangular, poorly sorted grains of sand- and silt-sized quartz, feldspar, and other grains. Hematite aggregates with rims of hematite are present in one sample (Fig 8C<sub>ii</sub>). One coated carbonate grain or oncoid, 3 mm in diameter, comprises a siltstone nucleus and a cortex of alternate laminae of microspar up to  $\sim 100 \mu$  wide and micrite a few microns wide (Fig. 9F). Similar oncoids in ancient fluvial channels have been attributed to

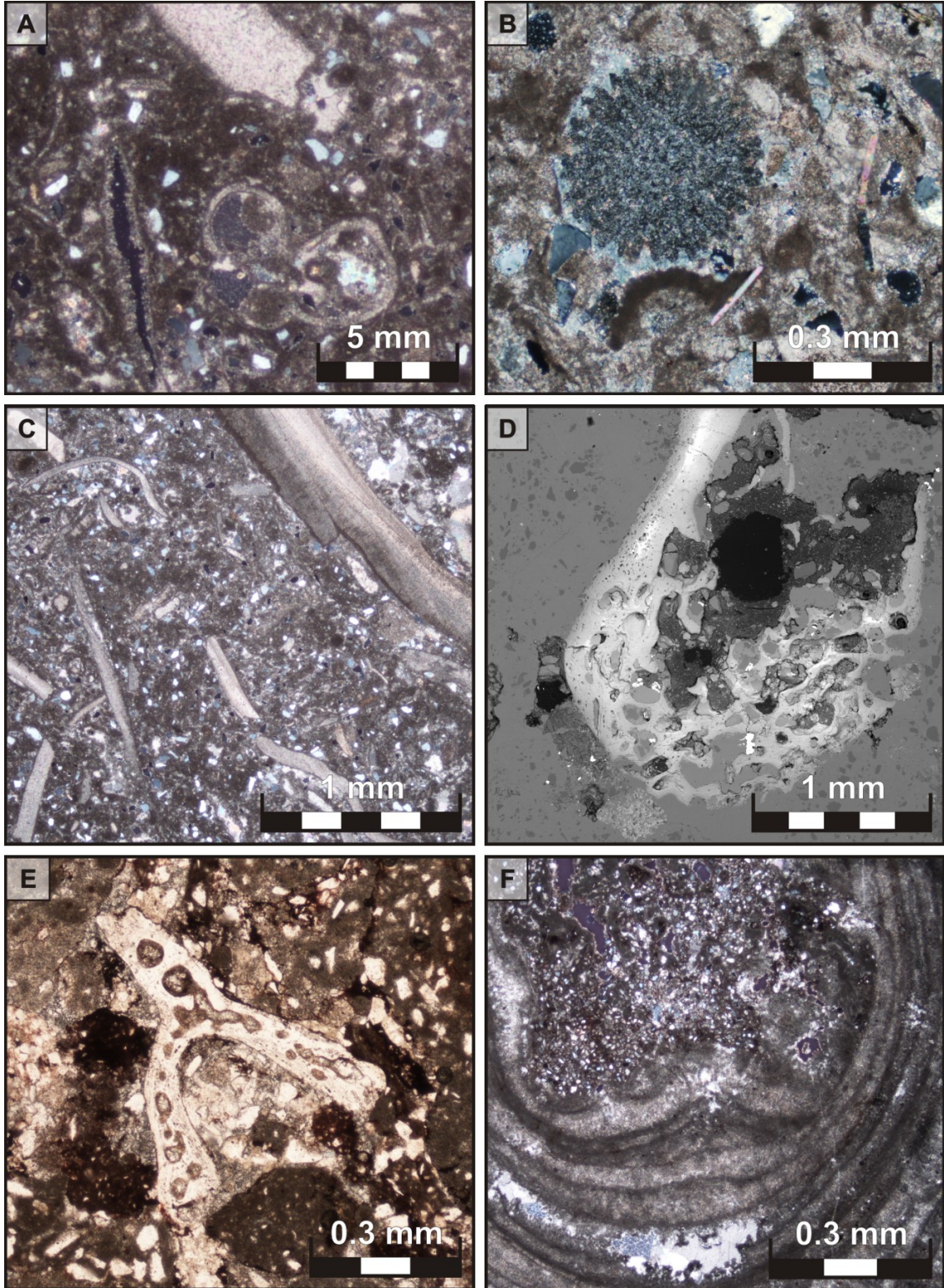


Figure 9: Fossils in the Rico Formation (A-C) and Halgaito Formation (D-F). A) Shell fragments (center top), gastropod shell (lower right), crinoid fragment (top center), peloids and scattered siliciclastic grains. Cross-polarized light, sample RS15-02, 0.5 m level at Rooster. B) Cross

**section of an echinoid spine with syntaxial cement, with shell fragments, peloids and scattered siliciclastic grains. Cross-polarized light, sample LR15-01, 0.5 m at Lime Ridge. C) Disarticulated bivalve fragments. Ordinary light. Same sample as in A). D) Bone material in SEM image, sample SH15-05, 18 m level at Setting Hen. E) Bone material. Plain-polarized light, sample FS15-05, 3 m level at Fossil Site. F) Oncolite (accretionary grain) with concentric growth of layered calcite around siltstone nucleus. Cross-polarized light, 17 m level at Setting Hen.**

reworking of grains formed in floodplain ponds, shallow lakes, or in the channels themselves, either in standing-water zones or disconnected ponds at low discharge (Zammareño et al. 1997; Dasgupta and Ghosh 2018).

Structureless siltstone (Sm) is orange to red and is prominent in all the sections. The facies forms layers and lenses in the lower and middle divisions and is especially prominent as stacked sheets with conchoidal weathering and deep root traces in the upper division (Fig. 6E). Seven eolian samples examined under the SEM consist predominantly of quartz and feldspar grains with minor rutile, hematite, muscovite and biotite, zircon, apatite (Fig. 8B), with fewer reworked calcite grains than in the fluvial samples. Grains are well to very well sorted and are mainly rounded to well rounded, with no fine-grained matrix. Calcite cement typically forms poikilotopic crystals (Fig. 8B<sub>i</sub>, B<sub>ii</sub>) within which the detrital grains show point and long contacts, suggesting relatively early cementation prior too much consolidation.

This study follows Murphy (1987) and Soreghan et al. (2002), who studied the Halgaito beds in the Mexican Hat area, in interpreting structureless siltstone as loess on the basis of the predominance of coarse, well sorted silt with minimal clay. Criteria for defining loess with its varied composition and post-depositional history have been widely debated (Pye, 1987, 1995; Tsoar and Pye 1987; Pecsí 1990; Kemp 2001; Stuut et al. 2009; Lehmkuhl et al. 2016). Muhs and Bettis (2003) defined loess in non-restrictive terms as terrestrial, wind-deposited sediment dominated by silt-sized particles, of sufficient thickness to be recognizable as a sedimentary

body in the field. Loess, including micrite peloids, micritized fossil fragments, and dolomite suggested that they originated from coeval regressive-marine flats exposed to the wind.

Silty mudstone (Fsc) is notable for the presence of root systems, carbonate nodules, rhizoconcretions, bioturbation (Fig. 6H), and higher amounts of clay. The facies is interpreted as paleosols developed on loess, with which it is commonly interbedded. Two studies have characterized Rico and Halgaito paleosols in detail. Soreghan et al. (2002) identified Protosols, Argillisols and Calcisols using the Mack et al. (1993) classification, variously characterized by root traces with clay linings and drab haloes, rhizoliths, illuvial clay accumulations in argillic B horizons, and coalescing carbonate nodules. They noted the addition of eolian dust to the paleosol profiles. Calcisols are prominent in the Rico Formation and Argillisols more prominent in the Halgaito Formation, suggesting an upward transition from semi-arid to seasonally wet conditions. In strata equivalent to the Halgaito Formation of the present study, Golab et al. (2018) identified mottled Inceptisols and fine-grained Entisols, the latter indicating incipient pedogenesis with deeply penetrating rhizoconcretions, pervasive bioturbation, and carbonate cementation. They noted little pedogenesis and few ichnofossils in the topmost 40 m of the formation and inferred a generally deepening water table based on the presence of deeply penetrating rhizohaloes.

Limestone (Ca) represents the topmost limestone of the Rico Formation immediately below the Halgaito Formation and includes a range of shallow-marine biota (Fig. 9A-C). Some units described as limestones in the literature may represent cemented siliciclastic beds. Previous studies of Rico biota have variously interpreted the depositional setting as open-marine to brackish (Lewis and Campbell 1965; O'Sullivan 1965). Thin sections from this study yielded gastropod, bivalve, and echinoid fragments with minor quartz and feldspar grains and a

sparry calcite cement (Fig 9A-D), and outcrops contained sub-spherical and platy oncolites up to 1.5 cm in maximum dimension.

### 2.5.3 Fossils

DiMichele et al. (2014) documented numerous plant taxa that included a fragmentary record of small trees from localities about 20-25 m above the base of the Halgaito Formation in the study area. The plants include large branches of walchian conifers, calamitaleans and cordaitaleans, the marattialean tree fern *Caulopteris*, the tree-fern foliage *Pecopteris*, a single medullosan pteridosperm, and fragments of the lycopsid *Sigillaria*. Plant fossils identified during the present study include fragments of *Annularia*, *Walchia*, and calamitalean axes (Fig. 6I, K; Fig. 7D, E), but no in situ stems were observed, although DiMichele et al. (2014) noted traces that are probably small upright stems.

Root traces locally penetrate deeply into the strata (Fig. 6F) and one large root mass was observed at Lime Ridge (Fig. 7A-C). A large myriapod track (*Diplichnites cuithensis*) is present in a channel body at Lime Ridge (Chaney et al. 2013; Fig. 7J), and *Planolites*, *Palaeophycus*, and indeterminate spreiten-filled burrows were identified in numerous beds.

Bone fragments were observed in a few beds (Fig. 7H, I), principally in facies Gm as noted by Vaughn (1962). The “Birthday Bonebed” (Huttenlocker et al. 2018) has yielded a range of aquatic and semi-terrestrial vertebrate fossils that include xenacanth chondrichthyans, actinopterygians, sagenodontid lungfish, and *Eryops*, as well as a riparian fauna of synapsids and araeoscelidan reptiles, variously articulated and disarticulated (Huttenlocker et al. 2018; see Vaughn 1962 for vertebrates collected from the Halgaito Formation near Mexican Hat).



#### 2.5.4 Grain size comparison of eolian and fluvial siltstones

Table 2 summarizes the sample mean, modal class, range of grain size, and standard deviation for 7 samples of eolian siltstone (facies Sm) and 17 samples of fluvial siltstone (8 St, 9 Sr, and 1 Sh) determined using thin-section measurements. Corrected mean size uses the 1.3 correction factor of Johnson (1994). Frequency curves are shown in Figure 10. Grain resolution and imaging restricts the method to medium and coarse silt. However, although the sample modes and means are probably slightly less than reported here, visual inspection suggests that fine and very fine silt is only a minor component.

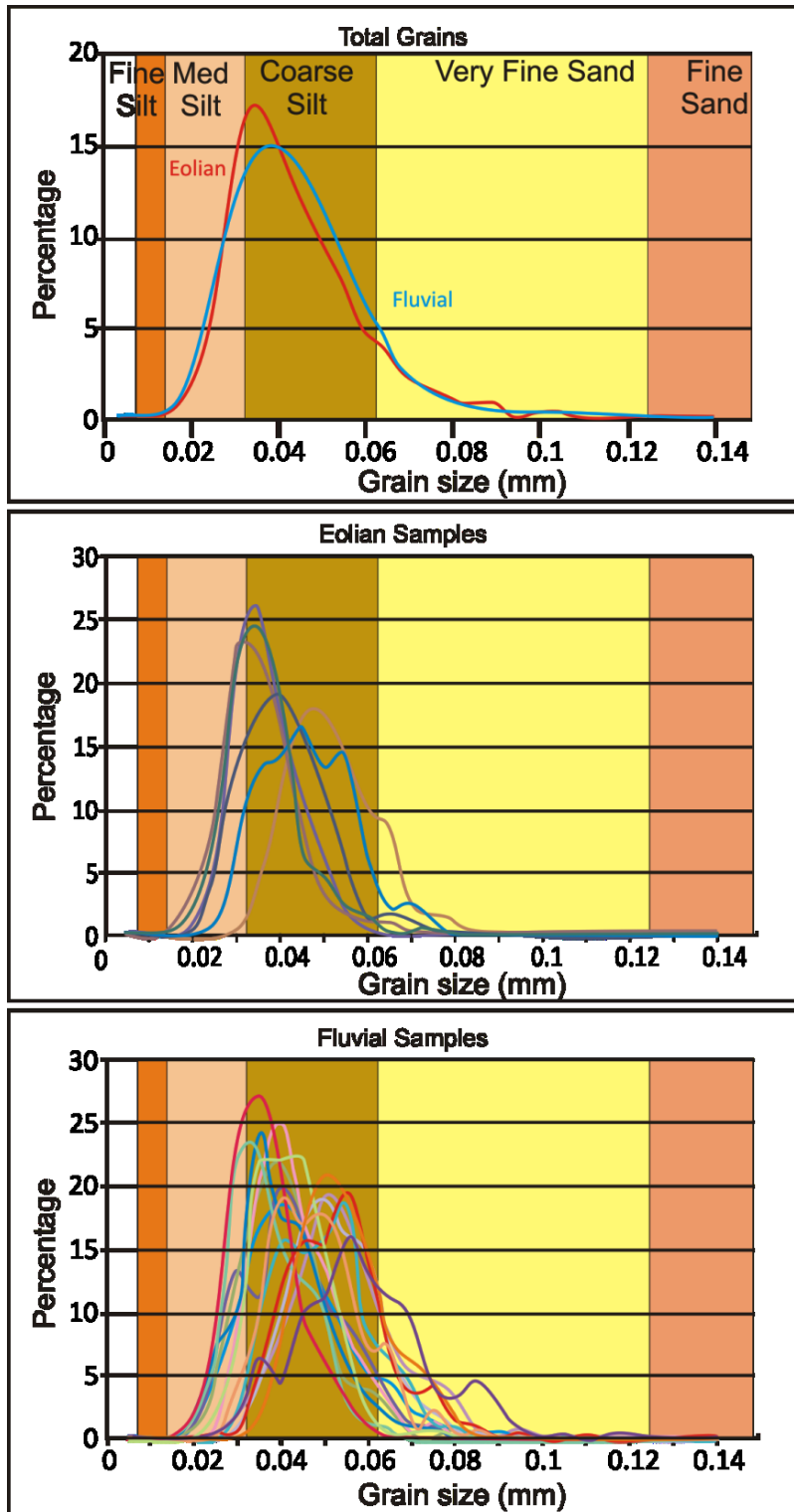
The measured grains in the eolian samples range from 13-144  $\mu$  in apparent maximum diameter, and the samples have modal classes in the coarse silt range, with one in the medium silt range. Mean sizes for samples range from 33-66  $\mu$ , with tails of very fine and fine sand but with few grains more than 80  $\mu$  in apparent maximum diameter. The average mean of all samples is  $43 \pm 11 \mu$ . Corrected mean grain size for each sample ranges from 43-85  $\mu$ , in the coarse silt to very fine sand range, and the average for the corrected sample means is 56  $\mu$ .

The measured grains in the fluvial samples range from 13-135  $\mu$ . All the fluvial samples have modal classes in the coarse silt range with mean sizes from 27-57  $\mu$  and tails of very fine and fine sand, with few grains more than 100  $\mu$  in apparent maximum diameter. The average mean of all samples is  $42 \pm 10 \mu$ .

**Table 2: Grain-size analysis of eolian and fluvial siltstones from Lime Ridge (LR), Rooster-Setting Hen (RS), and Fossil Site (FS), based on measurement in thin sections. Sample locations are shown on the columns of Figure 5. The corrected mean value for the samples, allowing conversion from 2D measurements to 3D grain diameter, is based on multiplying the mean long-axis measurement by 1.3 (Johnson 1994). See Table 1 for facies codes.**

Fluvial Samples										
Sample Name	Facies Code	# of points	M above base	Mean (mm)	Max (mm)	Mode (mm)	St. dev (mm)	Corrected mean (mm)	Division	Facies assoc.
LR15-03	St	350	5.25	0.052	0.030	0.081	0.045-0.0499	0.068	L	
LR15-04	Sr	350	14.25	0.038	0.019	0.072	0.030-0.0349	0.049	L	FR
LR15-06	Sr	350	17.00	0.046	0.025	0.085	0.035-0.0399	0.060	L	
LR15-08	St	350	21.25	0.027	0.014	0.048	0.025-0.0299	0.035	M	BFS
LR15-09	Sr	356	24.75	0.034	0.015	0.057	0.030-0.0349	0.044	M	FR
LR15-10	Sr	350	26.50	0.039	0.018	0.070	0.040-0.0449	0.051	M	FR/BFS
LR15-12	St	900	29.50	0.042	0.017	0.136	0.035-0.0399	0.055	M	CUS
LR15-14	Sr	350	42.00	0.039	0.017	0.079	0.035-0.0399	0.051	M	FR/BFS
LR15-15	St	395	46.75	0.057	0.020	0.116	0.055-0.0599	0.074	M	FR/BFS
LR15-16	Sr	350	43.00	0.035	0.016	0.064	0.030-0.0349	0.046	M	FR/BFS
RS15-04	St	450	12.25	0.041	0.018	0.104	0.035-0.0399	0.053	L	FR
RS15-05	Sr	352	12.50	0.051	0.024	0.107	0.050-0.0549	0.066	L	FR
RS15-08	St	350	48.25	0.050	0.028	0.092	0.045-0.0499	0.065	U	CUS
RS15-09	Sr	350	48.50	0.048	0.026	0.101	0.050-0.0549	0.062	U	CUS
FS15-03	St	350	2.25	0.052	0.022	0.095	0.045-0.0499	0.068	L	FR
FS15-04	Sh	351	3.75	0.041	0.024	0.074	0.035-0.0399	0.053	L	FR
FS15-06	St	352	2.75	0.027	0.014	0.049	0.025-0.0299	0.035	L	FR
<b>Average</b>				<b>0.042</b>			<b>0.010</b>	<b>0.055</b>		
Eolian Samples										
LR15-05	Sm	350	13.25	0.044	0.021	0.077	0.040-0.0449	0.011	L	FS
LR15-07	Sm	350	15.25	0.039	0.019	0.076	0.035-0.0399	0.010	L	FS
LR15-11	Sm	350	29.25	0.034	0.018	0.057	0.030-0.0349	0.007	M	LPB
LR15-13	Sm	352	41.50	0.033	0.013	0.070	0.025-0.0299	0.009	M/U	LPB
RS15-03	Sm	350	0.50	0.066	0.027	0.144	0.050-0.0549	0.021	L	FS
RS15-06	Sm	350	41.25	0.034	0.016	0.073	0.030-0.0349	0.008	U	LPB
RS15-07	Sm	350	48.00	0.050	0.030	0.087	0.045-0.0499	0.010	U	LPB
<b>Average</b>				<b>0.043</b>			<b>0.011</b>	<b>0.056</b>		

Figure 10: Grain-size frequency curves, normalized to percentages, to compare fluvial and eolian siltstone (Tab 2). A) Composite curves for all grains in 17 fluvial and 7 eolian samples, with both sample suites showing a coarse silt mode and fluvial samples slightly coarser overall. B) Eolian siltstones, showing coarse-silt sample modes and good central tendency, with bimodal tendencies in a few samples. C) Fluvial siltstones, showing coarse-silt sample modes, bimodal tendencies in several samples, and less good sorting than the eolian siltstones



Corrected mean grain size for each sample ranges from 35-74  $\mu$ , in the coarse silt to very fine sand range, and the average corrected sample means is 55  $\mu$ .

The modal populations reflect transport winds of different strength. In the Loess Plateau, Type 1b was laid down from short-term, near-surface to low suspension clouds during colder climatic periods, with a transport distance of tens of kilometers to 100 km from sources in alluvial plains, fluvio-glacial areas, and playa lakes (Stevens et al. 2013; Licht et al. 2016). Quaternary loess of modest thickness and extent in Israel (Crouvi et al. 2008; Amit et al. 2011) yields 50-60  $\mu$  and 3-8  $\mu$  modes and was attributed to deposition in suspension clouds from the Nile erg during periods of lowered sea-level, with the silt probably derived from abrasion of sand grains (see Whalley et al. 1982; Bullard et al. 2004, 2007). European loess with a similar size range was termed "large dust" by Stuut et al. (2009) and identified as an in-continent deposit with relatively short transport distances.

With its very different setting, western Pangea cannot be compared directly with the Loess Plateau or Near East. However, facies Sm accords well with Loess Plateau Type 1b and Negev loess in view of the predominant medium- to coarse-silt range with sample modes that match the 35-40  $\mu$  and 51-60  $\mu$  populations (Fig. 8B). The Halgaito eolian samples differ from Loess Plateau Type 1a, which was described as coarse silt and very fine to fine sand typically with a 75  $\mu$  mode, derived from local sources such as river terraces and wind-blown dunes with transport distances of hundreds of meters to a few kilometers.

Although analysis of the finest silt was beyond the imaging range of the present study, the finer limb of the Halgaito samples accords with Type 1c with modal sizes of 16-22  $\mu$  and 4  $\mu$ , transported by high suspension clouds active through the year. Stuut et al. (2009) attributed such European "small dust" to sources in the Sahara and Sahel. Finer silt and clay may also

originate in the samples during diagenesis of framework grains (Smalley and Markovic 2014; Sprafke and Obreht 2016). Secondary loess reworked by fluvial processes in the Loess Plateau is typically bimodal and coarser than primary samples, with an admixture of finer material and overall poorer sorting. The Halgaito fluvial samples similarly show a greater spread of sizes than eolian samples, with bimodal or multimodal distributions (Fig. 10C). These features support an origin of fluvial silt from reworking of loess.

### **2.5.5 Root Traces**

Fossil plant localities are present throughout the region (DiMichele et al. 2014) but are not frequent enough in any single section to assess floral abundance and facies occurrences. As a partial proxy, preserved root traces were measured for several parameters (Table 3). In the lower division, root traces with zones of drab mottles a few centimeters wide penetrate on average <30 cm, appearing both branched and unbranched and locally forming narrow clusters up to 20 cm in width. An exception is the topmost level of the 7 m unit at Lime Ridge, where roots penetrate 2 m and include root masses up to 1 m wide (Fig. 7A & C). In the upper division, root traces penetrate more deeply, averaging 50-90 cm (up to 2 m) at individual sites. The traces typically feature a main axis surrounded by a network of fine rootlets with an average width of 40-60 cm. The root systems in the lower divisions were typically spaced 48 cm apart. Too few data from the middle and upper divisions were observed and recorded for an assessment.

**Table 3: Measured data regarding root depth, width, cluster width, branching, and spacing of clusters used as a proxy for living plants during deposition in place of fossilized plant remains.**

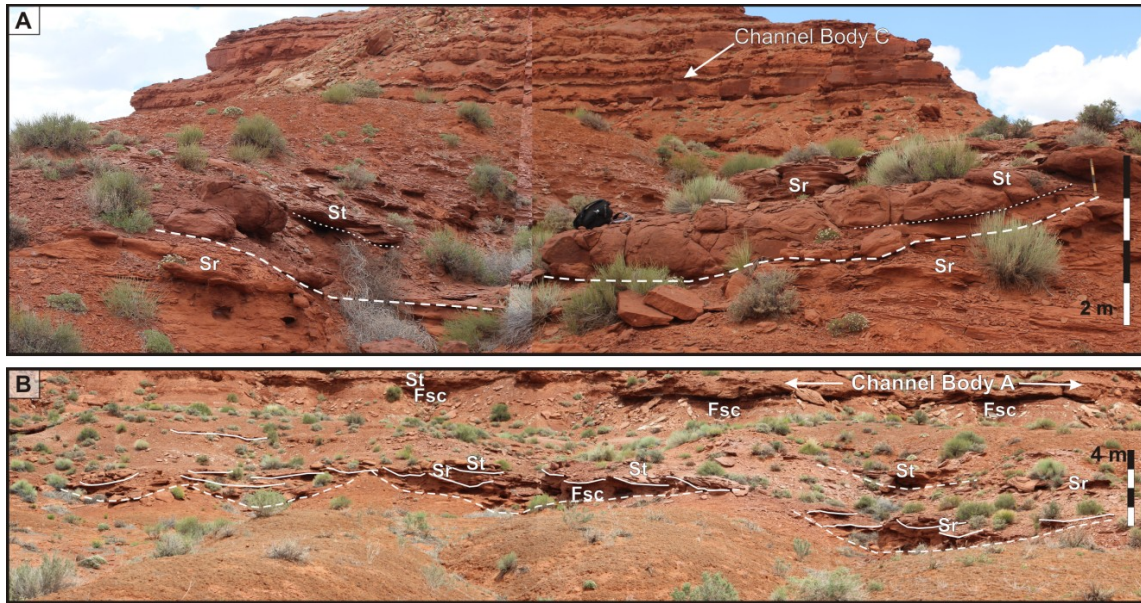
Location	Ave depth (cm)	n	Width (cm)	n	Cluster width (cm)	n	Branching	n	Spacing (cm)	n
<b>Upper Division</b>										
Rooster	87.5	4	2.6	23	57.5	4	100%	4	--	
Lime Ridge	53.4	14	4.9	14	40.7	6	100%	14	--	
<b>Middle Division</b>										
Rooster	--		2.9	15	--		--		--	
7 Sailors	8.9	5	1.7	41	--		--		--	
<b>Lower Division</b>										
Rooster	27.3	20	2.9	19	20.4	14	36%	19	48.6	10
Lime Ridge	29.7	14	0.3	14	12.9	8	71%	14	--	
7 Sailors	--		4.0	26	16	4	--		--	

## 2.6 Channel Bodies at Study Sites

### 2.6.1 Rooster - Setting Hen

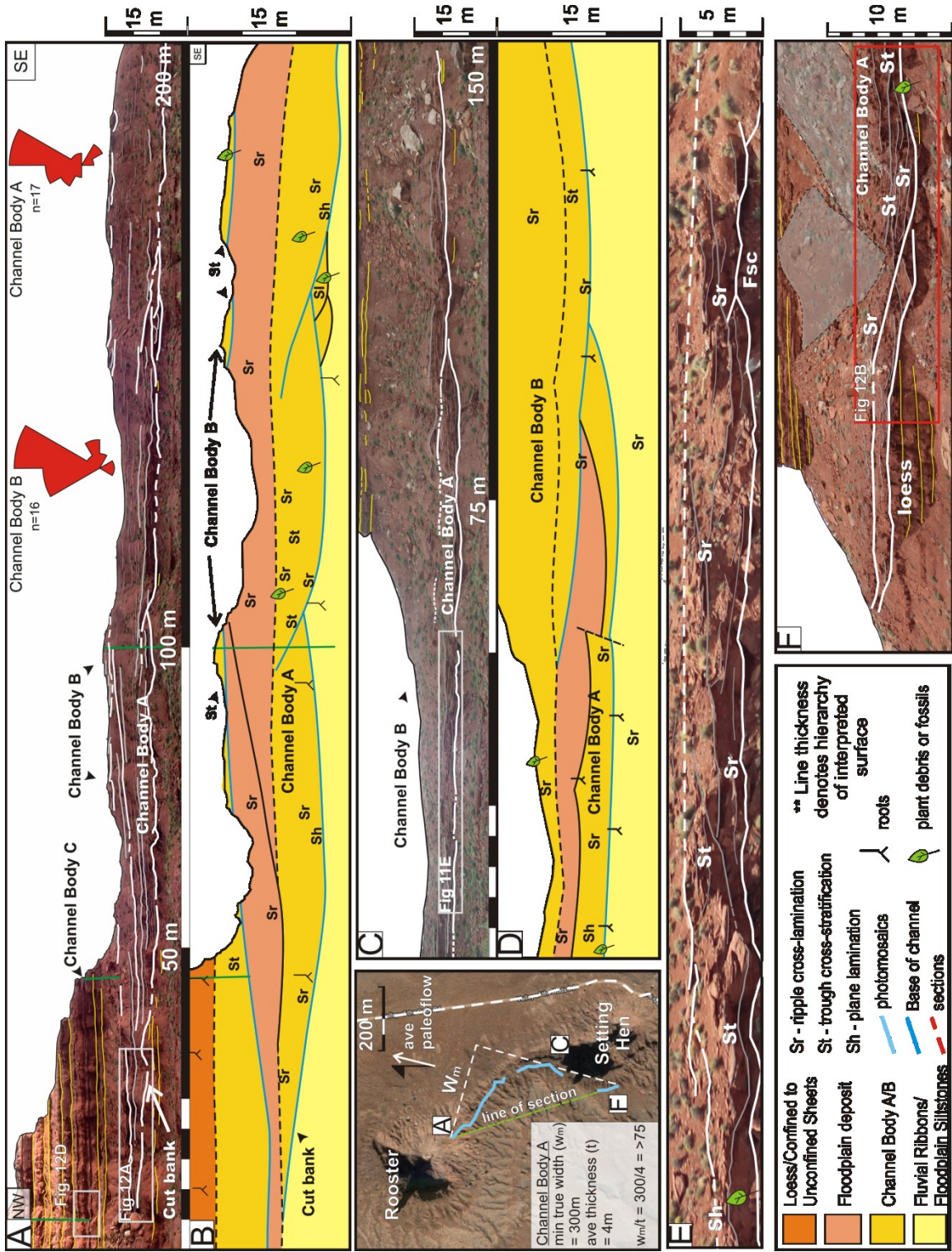
The study site includes the buttes of Rooster and Setting Hen, approximately 500 m apart and connected by a low ridge (Fig. 2A), with a plant-fossil locality (DiMichele et al. 2014). The “A” limestone of the Rico Formation is 300 m southwest of the base of the ridge, from where a full section to the base of the Cedar Mesa Formation was measured at Rooster. A shorter section was measured at Setting Hen (Fig. 5).

The lower division at Rooster and Setting Hen contains suites of small, narrow channel bodies. Seven measured channel bodies are 3-5 m thick and 10-17 m wide measured approximately normal to the paleoflow, with width:thickness ratios <5 (narrow ribbons). The channel bodies contain concentric fills that flatten upwards and locally extend across the adjacent floodplain deposits (Fig 11). Facies St and Sr predominate, with a higher proportion of Sr in the topmost channel fills.



**Figure 11: Two examples of Fluvial Ribbons from Rooster. A) is on the large end of the possible solitary fluvial ribbons found with minor scouring within the channel. B) Small but multistoried ribbons which are found throughout the lower portion of all Valley of the Gods sections and within Lime ridge. The top of B shows the base of Channel Body A.**

Two channel bodies are well exposed in the middle division in the ridge between Rooster and Setting Hen (Figs. 12, 13). Channel-Body A spans the two buttes and has a relatively planar basal surface with a prominent northwestern cutbank below Rooster, extending beyond the outcrop below Setting Hen. The channel body has a mean paleoflow of 14°NE, a minimum true width of 300 m, an average thickness of 4 m, and width:thickness ratio >75 (probably broad sheets). The channel body is multilateral, and the channel base is marked by at least seven concave-up erosional surfaces with low-angle margins of 10-20°, cutting down in places for 1-2 m below the broadly planar base of the channel body. The erosional surfaces have a vertical relief of 2-5 m and a width of 50-100 m and are highlighted in the vertically exaggerated panels of Figures 12B and D. They show a cross-cutting pattern from older to younger surfaces and fills from northwest to southwest along the outcrop belt, indicating that the position of active channel flow migrated systematically across the plain.

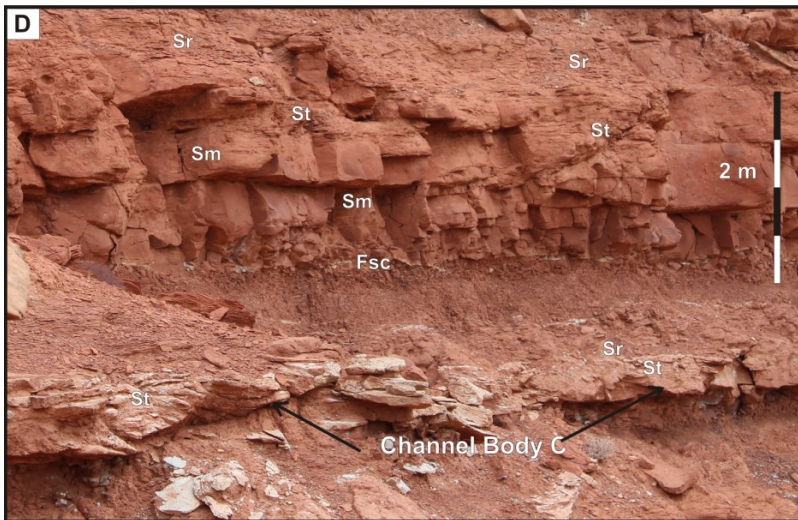
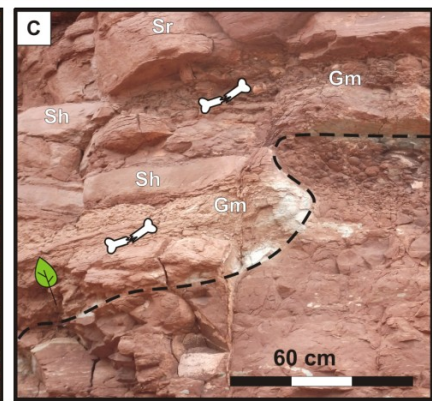
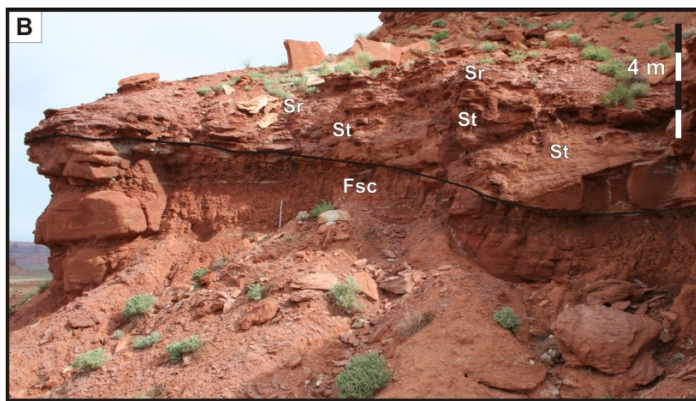






**Figure 12: Architecture of Channel-Bodies A and B at Rooster and Setting Hen (Fig. 2). A) and C) are annotated panoramas of Channel-Body A, showing the northwest (A) and southwest(C) parts of the outcrop, with paleoflow rose diagrams for Channel-Bodies A and B. B) and D) are interpreted diagrams of A) and C) with a 2X vertical exaggeration. Note that the base of Channel-Body B is exposed at the top of the ridge, with poor exposure under Rooster to the northwest. E) is an enlarged portion of C) from a different perspective to illustrate internal scours. F) from the southern end of Setting Hen shows the base of Channel-Body A cutting through 4 m of structureless siltstone (Sm). Inset shows paleoflow vector mean and geometric reconstruction of Channel-Body A. The topmost 20 m of the Halgaito Formation (upper division) in the buttes below the Cedar Mesa Sandstone comprise interbedded sheets of loess (Sm) and thin beds of silty mudstone (Fsc), with prominent root traces that stem from Fsc units. The division contains nine planar units 0.5-3.5 m thick (average 1.5 m) that comprise St passing up into Sr. The units rest on loess with abrupt to gradational contacts and thicken locally into deeper channel forms.**

The strata that fill the channel forms are flat-lying and comprise Sr and St, with beds of ripple-drift cross-lamination up to 75 cm thick (Figs. 6B, C). A prominent Sh bedset 0.5 m thick in the central part of the channel body (Fig. 6A) contains calamitalean fragments up to 1 m long and 30 cm wide (Fig. 6I), as well as comminuted plant debris from a few millimeters to 5 – 10 cm in length. There is little indication of an upward succession of bedforms within the channel fill.

Channel-Body A rests on and cuts into facies Fsc and Sm for much of its extent. The cutbank below Rooster is gently dipping (17°) and cut into 4 m of facies Sm (Fig. 13A). Flat-lying, aggrading Sr beds onlap the margin with slight depositional dips but no indication of inclined, systematically migrating bar surfaces. In the outcrop below Setting Hen, the basal surface is cut into 4 m of Sm with a locally vertical to overhanging margin with 60 cm of relief (Figs. 13B, C). Flat-lying to gently dipping beds of Gm, Sh, and Sr abut the incision. The oncolid of Figure 9F was a clast in facies Gm at this site. Overlying Channel-Body A is a poorly exposed 5 m succession of ripple-drift cross-lamination in planar beds that extend along the ridge, interpreted as a floodplain succession.



Sr	Ripple cross-lamination
Sm	Structureless siltstone
St	Trough cross-stratification
Sh	Plane lamination
Gm	Intraformational conglomerate
Fsc	Silty mudstone
	plant debris
	bone fragments

**Figure 13: Architectural details for Channel-Body A and C at Rooster (A and D) and Setting Hen (B and C). A) Cut bank under Rooster Butte showing the incision angle with loess under the bank. B) Basal part of Channel-Body A cutting into 4 m of structureless siltstone (loess) at left. C) Close-up of the contact between Channel Body A and the loess under Setting Hen, note overhanging scour. D) Channel Body C in foreground with an example of a Confined to Unconfined Sheet deposit in rear. Note the upward change from Structureless siltstone, to trough cross stratification and finally into ripple cross stratification on the top**

These strata are overlain by Channel-Body B, which is discontinuously exposed but is up to 6 m thick and at least 500 m in true width between the buttes, without exposed margins but cutting down and thickening under Rooster. Where exposed, the strata comprise a basal bed of Gm overlain by St and lesser amounts of Sr with climbing ripples prominent. Calamitalean axes up to 1.5 m long and 40 cm wide are present in facies St, as well as *Annularia*. Branching root traces cut the strata (Fig. 6C). It is important to note the especially prominent Channel-Body C which occurs in the Upper Division, it is a white siltstone with a planar base and an average thickness of 0.5 m, composed of St with minor Sr at the top (Fig. 13D). The channel body was traced between buttes in the Valley of the Gods for at least 5 km in the area surrounding Setting Hen to Fossil Site. Although the strata are not accessible for paleoflow measurements, the channel bodies probably form broad to very broad sheets.

## **2.6.2 Seven Sailors**

The outcrop lies west of the Valley of the Gods road at the northern point of the butte (Fig. 2). The "A" limestone of the Rico Formation lies 200 m east of the butte base, overlain by poorly exposed strata of the lower division that broadly resemble those at other sites.

A prominent, planar-based channel body (Channel-Body D) marks the base of the middle division. The channel body is traceable for 200 m on each side of the butte nose (Figs. 2A, 2A3, 14A).

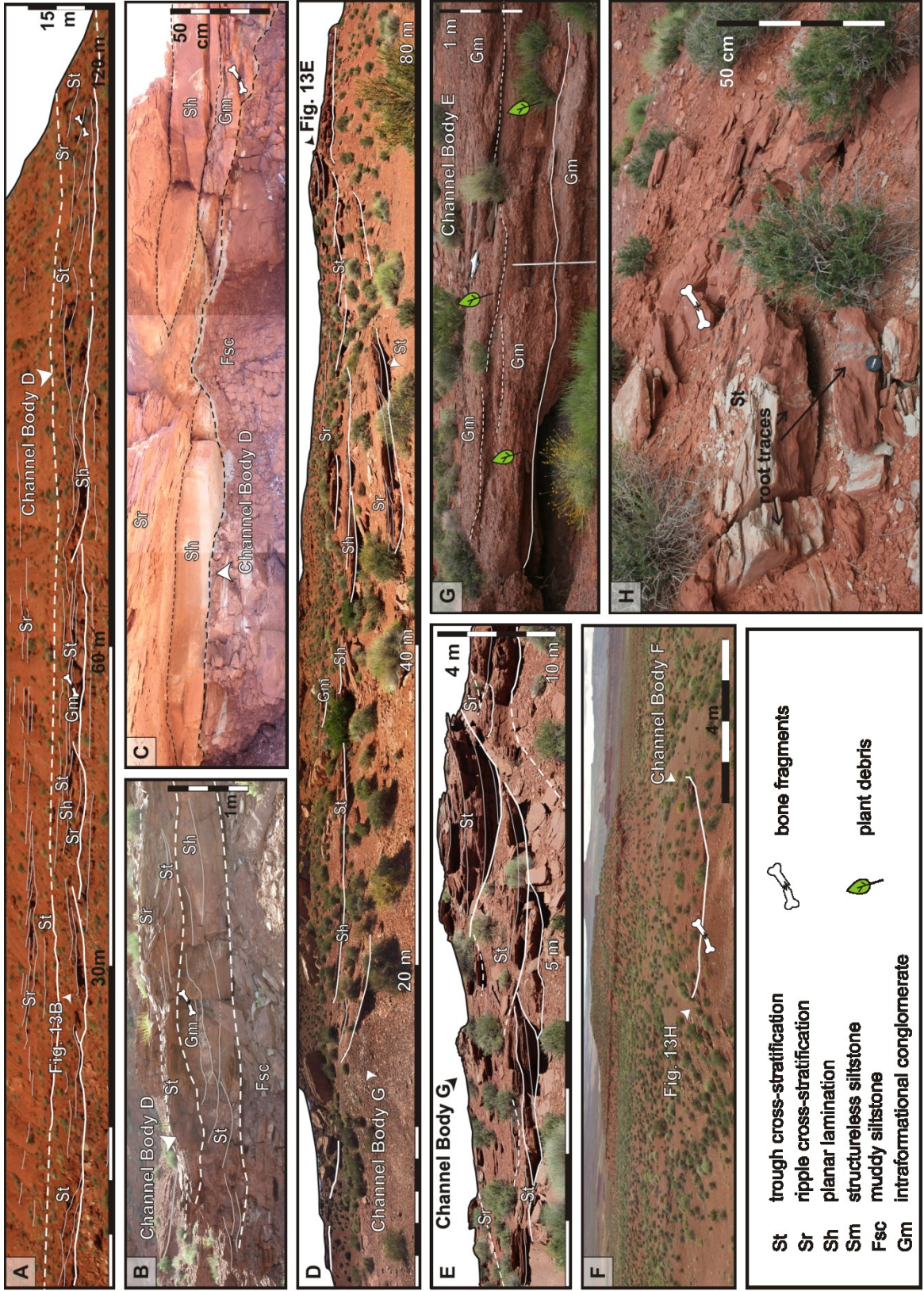


**Figure 14: Architecture of channel bodies at Seven Sailors (A, B, and C), and Fossil Site (D, E, and F). A) Photomosaic of channel body at Seven Sailors, with bedforms outlined, facies labeled and location of bone fragments. B) Close-up of a localized scour within the Seven Sailors channel body, location indicated with label on (A). C) Channel body seen from the north side of Seven Sailors, behind outcrop belt shown in (A), showing erosive based grouping of the complex relationship between and facies Gm and Sh. D) Panoramic view of a gullied area at Fossil Site, showing a composite channel body with numerous small channel bodies containing facies Gm, St, Sr and Sh. E) Close-up of the right hand side of (D) showing relatively deep incision of component small channel bodies. F) Landscape showing location of the bone bed in Channel Body F (for relative location to (E) see logs of Fig.5). G) Channel Body E which is largest single deposit of Gm of all locations. At one meter thick, this is an anomaly, but contained abundant fossilized roots and plant fragments too small to identify. H) Side view of unexcavated bone bed showing root traces and broken nature of the outcrop.**

Channel-body margins were not observed and insufficient paleoflow data were available to determine the channel-body geometry. The channel body is 4-5 m thick and multilateral, with cross-cutting, concave-up erosional surfaces that have a vertical relief of 1-3 m (Figs 13B, C). Facies St and Sr predominate with minor Sh, and Gm is more common than at other locations. Convolute lamination (soft-sediment deformation) was noted only in this channel body, where it is present as small isolated occurrences. Systematic upward sequences of bedforms are not apparent, and the flat-lying beds lack lateral- or downstream-accretion surfaces. Bone fragments are present in the Gm beds (Fig. 6I) and, less commonly, in St. Root traces are common and penetrate 1-2 m below formerly vegetated surfaces (Fig 7B & C). Migration directions of the scour-based fills are locally systematic, but the directions of migration vary within the channel body. The overlying, poorly exposed 5 m of strata are ripple cross-laminated, and the steep bluff above is composed largely of facies Sm, attributed to the middle division.

### **2.6.3 Fossil Site**

The section spans a road in the western part of the Valley of the Gods (Fig. 2), and forms part of the lower division. Huttenlocker et al. (2018) presented a detailed section in the vicinity

of the bonebed, commencing at the McKim Limestone and noting the absence of the “A” limestone in this area but the presence of other thin limestones. This study uses the description from Huttenlocker et al. (2018) of two vertebrate-bearing channel bodies low in the section, supplemented by our own observations and facies codes.

On the north side of the road is large, relatively narrow channel body (E) 7 m thick and up to 45 m wide (width:thickness ratio of 6.4) that cuts down to a resistant calcareous sandstone. The basal 2 m of channel fill is Gm composed of carbonate nodules, rhizoliths, siltstone clasts, and rare bone fragments, overlain by very fine-grained sandstone with Sr, Sh and St (Fig. 14G).

The bonebed channel body (F) is 78 cm thick and represents a minor channel 30 m to the south of Channel-Body E (Fig. 14F, H). A basal Gm unit 22 cm thick contains bone and teeth fragments. The overlying 26 cm comprises thin beds of reddish-gray mudstone and pebbly fine sandstone (Gm and Sm) with desiccation cracks, partial skeletons, bone fragments, and woody plant debris that includes calamitalean material. The topmost 30 cm is an orange massive siltstone (Sm) with a few bone fragments, probably redeposited loess. Huttenlocker et al. (2018) interpreted Channel-Body F as a small tributary to Channel-Body E that experienced slackwater flooding from the main channel.

At a higher level in the section, a set of relatively planar, resistant beds are partially exposed, composed largely of ripple cross-laminated siltstone with climbing ripples prominent. At a similar stratigraphic level and exposed around a modern gully 150 m away at the base of the nearby butte, a composite suite of incised channel fills (Channel-Body G) is exposed, with individual fills up to 5 m thick (Figs. 14D, E), cut into facies Sm. One of these selected for study is 5 m thick (Fig. 14E) with exposed channel margins that dip at up to 45° (Fig 14E); the true width

is uncertain. Cross-cutting scour fills 1-2 m thick and 10-15 m wide contain facies Sh, Sr with prominent climbing ripples, St and Gm. Waning-flow successions are prominent, and facies Sh and Gm constitute a greater proportion of the scour fills than at other locations.

#### **2.6.4 Lime Ridge**

The "A" limestone of the Rico Formation crops out on the south side of highway 163, and a road cut exposes the lowermost beds of the Halgaito Formation. The overlying strata form a series of benches that are stepped back on the north side of the highway up to the Cedar Mesa Sandstone (Fig. 2, 15C).

In the lower division, interbeds of Fsc, Sm, and rare Sr and St (Fig. 15C) form a distinctive, well stratified unit 7 m thick that is exposed for 125 m in the road cut, commencing approximately 5 m above the topmost Rico limestone. Units of facies Fsc comprise siltstone and claystone beds 5-50 cm thick, locally forming thin lenses in Sm beds; they differ from other occurrences in their stratified nature and prominence of trace fossils. Facies Sm forms abruptly based, structureless units up to 2 m thick, with mounded tops. Some of the units fill gentle scours cut into facies Fsc, and one 50 cm unit at the 9 m level pinches out northward within an Fsc unit (Fig. 15C). Basal siltstone surfaces show branching networks of *Palaeophycus* with grain sorting demarcating the burrows (Fig. 6H, 7F), as well as desiccation cracks and adhesion structures (Fig. 7G). Beds of facies Sm thicken upwards in the unit and beds of facies Fsc become less prominent.

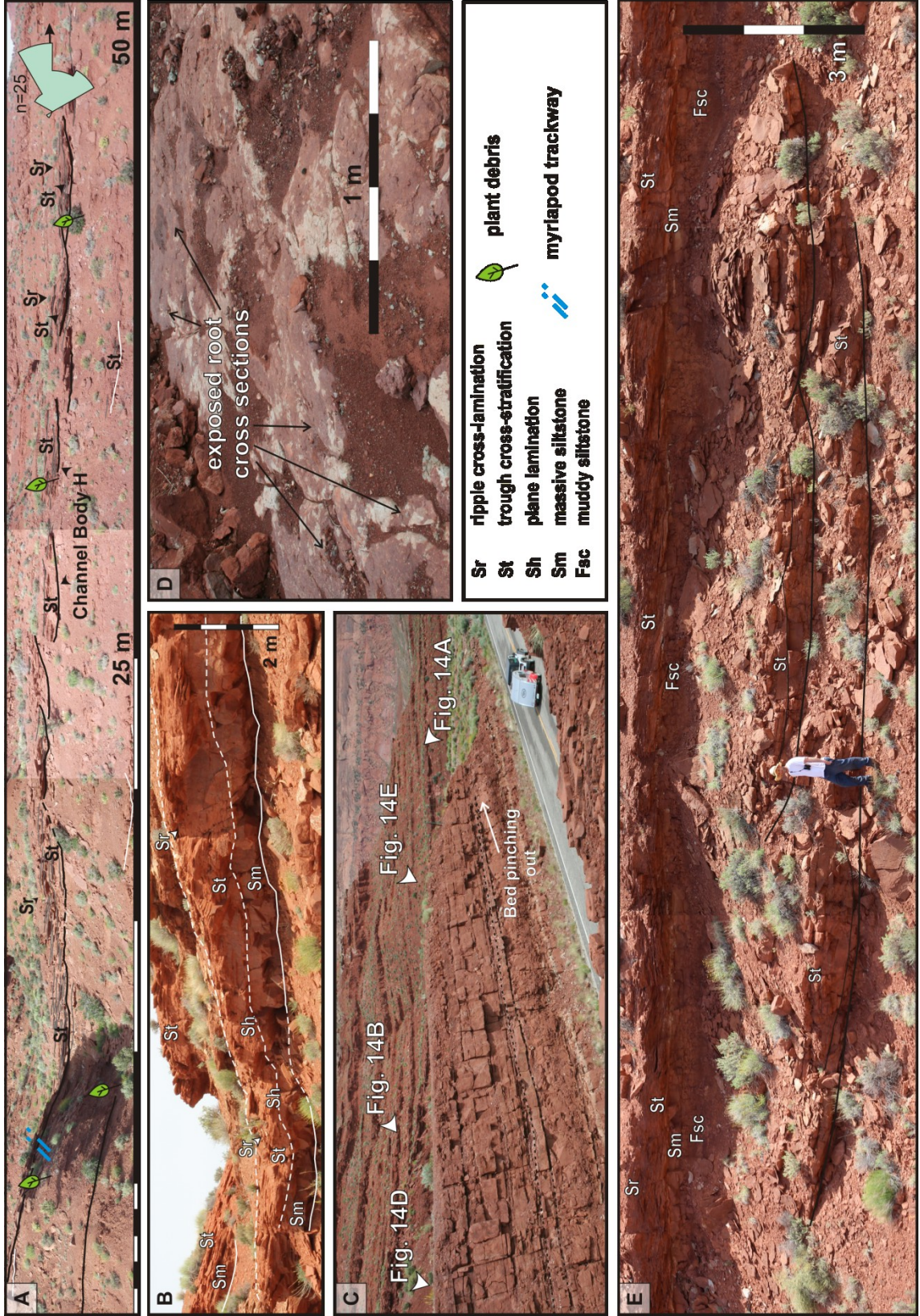




**Figure 15: Series of images of Lime Ridge to highlight the slight differences to sites found within the Valley of the Gods. A) Channel Body H with sub-planar base, facies St and Sr, and the location of plant fossils and myriapod trackway indicated. B) Sheet-like channel body 2 m thick at 29-30 m in the section, with upward succession from structureless siltstone (Sm) resting on the basal surface to laminated (Sh), trough cross-stratified (St) and ripple cross-laminated (Sr) siltstone. C) Wide scale photo of the Lime Ridge site, showing the road cut in the foreground, and the background shows the stepped back nature of the rest of the outcrop. There is no upper butte as with the sites in the Valley of the Gods. The scale for this image is variable (SUV in photo for reference). D) An exposed bedding surface of a paleosol bed found on the top of the road cut. Location of this figure is indicated on (C). E) Fluvial Ribbons found at Lime Ridge are similar in size and shape to those in the Valley of the Gods, but are scattered throughout the study area.**

Abundant root traces with depletion halos in the upper part penetrate up to 2 m and include root masses 1 m across (Fig. 7A). The topmost rooted layer of the roadcut is exposed in a bench (Fig. 15D) with cross-sections of root traces and abundant rhizoconcretions and rootlets that radiate from a central axis (Fig. 6G, 7B). The unit represents a standing-water body with a progradational fill (see below).

The 8 m of section above the road cut contains numerous small, isolated channel bodies 1-2 m thick and up to 10 m wide, with St and Sr (Fig. 15E). They are poorly exposed but resemble the narrow channel bodies at Rooster and Setting Hen. Desiccation cracks (Fig. 6J) and adhesion structures (Fig. 7G) are present on bedding surfaces at this level and in isolated surfaces throughout the section.

The top of the first major bench, 20.5 m above the formation base, marks the base of the middle division. The bench is underlain by Channel-Body H, a sheet-like unit that is typically ~1 m thick (0.5 to 2 m range) and extends for >300 m, cut into a 50 cm bed of silty mudstone (Figs. 2, 15A, 16).

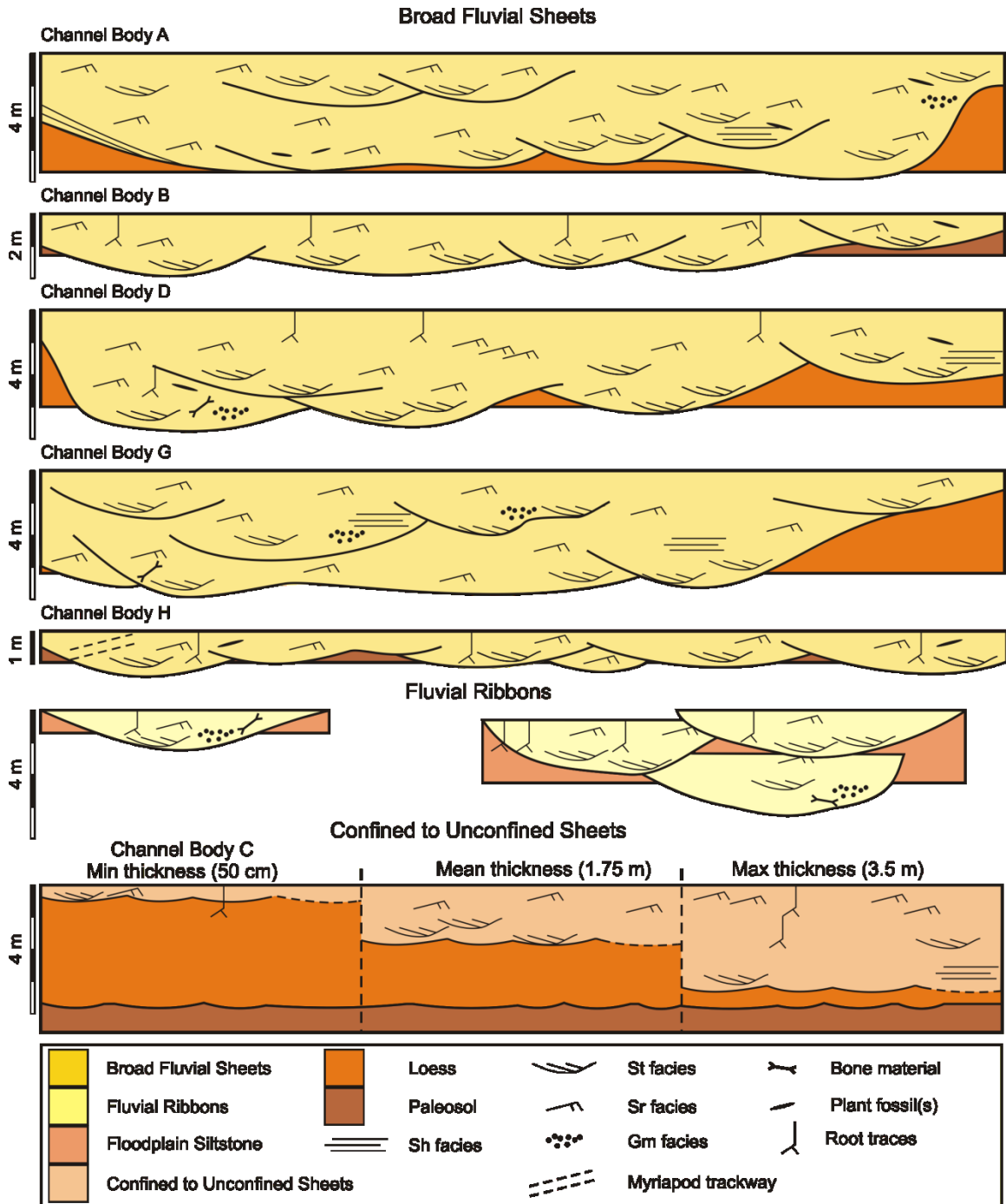


Figure 16: Channel geometries of the Halgaito Formation. Illustrations are vertically exaggerated. All five examples of Broad Fluvial Sheets (Channel Body A, B, C, D, G, and H) show a similar grain-size range. Fluvial Ribbons include single-storey and composite (multistorey) arrangements. Although loess is a major component of all channel bodies, Confined to Unconfined Sheets (CUS) are notable for reworking an underlying loess blanket. Shown here are the minimum thickness of a CUS (Channel Body C), mean thickness (1.75 m), and maximum thickness (3.5 m).

Abundant ripple cross-lamination yielded a mean paleoflow of 91°E, roughly along strike of the outcrop, which prevents an estimation of true width. The channel body comprises a single storey with small-scale, cross-cutting scours filled with facies St and Sr, with climbing ripples and adhesion structures prominent. Fallen blocks yielded abundant *Palaeophycus* traces (Fig. 7F), plant fossils of *Annularia* (Fig. 7D), and *Walchia* (Fig. 7E), and several *Diplichnites cuithensis* trackways about 25 cm wide with exposed portions up to 1 m long (Fig. 7J; Chaney et al. 2013).

Numerous sheet-like channel bodies are discontinuously exposed in the overlying strata. They are typically 0.5 to 3.5 m thick with sub-planar bases, and they comprise facies Sr and St, with minor Sh and Sm (Fig. 15E). In some of these bodies, conchoidally weathered lenses of facies Sm up to 2 m thick rest on the basal erosion surface (Fig. 15B).

Although less clearly developed than at Rooster and Setting Hen, the upper division has an increased proportion of loess (Sm), interbeds of silty mudstone (Fsc), and a decreased proportion of fluvial deposits (St and Sr). At the 43 m level, a small scour less than 2 m wide, cut into loess, is filled with Gm overlain by siltstone facies Sr, St and Sh (Fig. 7K), indicative of a short-lived cut-and-fill event under waning-flow conditions. Deeply penetrating root traces are especially prominent in the upper division.

## 2.7 Facies Associations

The Halgaito strata are divided into facies associations that represent fluvial channel, floodplain, eolian, and lacustrine settings (Table 4; Fig. 16).

### **2.7.1 Fluvial Ribbons (FR)**

Fluvial Ribbons are isolated single-storey to composite (multistorey) channel bodies that form the predominant fluvial style in the lower division. The channel bodies are up to 5 m thick and 17 m wide (Fig. 16), with a geometry of broad to narrow ribbons. The ribbons are incised into the Floodplain Siltstone association. Stacked bedsets of Sr and St, rarely Sh or Sm, fill the channels, and no Gm was found. Abundant root traces and depletion halos are present in some channel bodies, but bone and trace and plant fossils were not observed.

Channel-Bodies E and F at the Fossil Site (Huttenlocker et al. 2018) provide detailed information about coarser ribbon bodies. Channel-Body E is unusually large (7 m thick and up to 45 m wide), with the thickest basal conglomerate observed in the area, whereas Channel-Body F with the bonebed is less than 1 m thick but also has a prominent basal conglomerate.

Fluvial Ribbons represent narrow, fixed channels with up to 5 m instantaneous depth that aggraded vertically and probably were active for a relatively short period, cut into relatively unconsolidated silt and more cohesive paleosols that may have assisted in stabilizing the narrow channels. Multistorey bodies may reflect more prolonged occupation of some fluvial tracts, with local avulsion and coalescence of bodies in a small area. Flow was largely subcritical with aggradation of bedforms forming architectural element silty bedforms (SB). The two ribbon-channel bodies at the Fossil Site represent a much larger fixed channel and a small tributary, with evidence for strong erosional reworking of the landscape to yield thick intraformational clast accumulations.

### **2.7.2 Broad Fluvial Sheets (BFS)**

Broad Fluvial Sheets up to 5 m thick and in some cases >500 m wide are the predominant channel style in the middle division. Basal erosional surfaces are generally planar

but locally scoured, and their internal geometry is characterized by multiple cross-cutting scours, the fills of which are typically 1-2 m thick and tens of meters wide, locally as wide as 100 m. Thinner channel bodies (1-2 m) are single-storey, but thicker bodies (2-5 m) are multilateral, exhibiting systematic lateral cutting of new scours at about the same level, with local vertical stacking where erosion surfaces cut into underlying scour fills. The thinner bodies represent fewer channelized events or shorter periods of fluvial activation.

Channel-Body G at Fossil Site forms a broad sheet but is a composite of narrow scours with steep margins. Bedforms are mostly Sr, St and less commonly Sh, minor Gm on scoured surfaces, and local Sm beds and lenses. Desiccation cracks and adhesion structures are locally prominent. There is little indication of an upward succession of bedforms in the scour fills, and trough sets and ripple sets commonly grade up into each other, indicating both waning and waxing flow. Architectural elements are mainly flat-lying silty bedforms (SB) and laminated sheets of plane beds (LS) that indicate vertical aggradation, and an abundant silt load is indicated by the high frequency of ripple-drift cross-lamination. There is no evidence of downstream or laterally accreted elements (DA, LA). Plant fossils, where present, are associated with Sh and, less commonly, St. Other fossils include myriapod trackways, *Palaeophycus*, and bone fragments.

Broad Fluvial Sheets represent the deposits of channels up to 5 m deep that shifted laterally and commonly systematically through episodic channel-cutting events, probably avulsing a short distance within the river tract by cutting into the adjacent banks. The multilateral nature of many channel bodies may reflect a substrate of relatively unconsolidated loess, which allowed the channels to expand laterally during high-discharge events, incorporating a large silt load into the flow.

**Table 4: Facies associations in the Halgaito Formation, representing fluvial, eolian, lacustrine, and paleosol strata. Lacustrine Fines were identified only at Lime Ridge. See Table 1 for facies codes.**

<b>Facies Association</b>	<b>Grain size</b>	<b>Geometry</b>	<b>Facies</b>	<b>Interpretation</b>
<b>Broad Fluvial Sheets (BFS)</b>	Very coarse to fine silt, minor gravel	1-5 m thick, >500 m wide with sub-planar, erosive bases; internal cross-cutting scour fills up to 5 m thick and 100 m wide; little facies organization; single-storey to multilateral bodies	Sr, St, Sh, Sm, Gm; elements SB, LS	Broad ephemeral channels up to 5 m deep with varying flow strength and periodic scouring that generated smaller channels within the flow tract; channels cut laterally into loess blankets
<b>Fluvial Ribbons (FR)</b>	Very coarse to fine silt	1-5 m thick and 17 m wide; one case at Fossil Site 7 m thick and 45 m wide; broad to narrow ribbons, locally cross-cutting and grouped into a composite, multistorey ribbon	Sr, St, rare Sh, Sm; element SB	Narrow, fixed channels up to 5-7 m deep with an aggradational fill
<b>Confined to Unconfined Sheets (CUS)</b>	Very coarse to fine silt	1-5 m thick, planar base that is abrupt to gradational, traceable for up to 5 km, thicken locally into channel fills; typically, Sm passes upwards to Sh, St and Sr, with a rooted Fsc cap; single-storey bodies	St, Sr, Sh, capping bed of Fsc; element SB	Largely unconfined flood deposits that reworked loess into waning-flow deposits; locally capped by a soil horizon that indicates brief landscape stabilization

<b>Facies Association</b>	<b>Grain size</b>	<b>Geometry</b>	<b>Facies</b>	<b>Interpretation</b>
<b>Floodplain Siltstone (FS)</b>	Very coarse to fine silt	2-3 m planar bedsets of structureless siltstone (Sm), rooted paleosols (Fsc), and ripple cross-laminated and trough cross-stratified siltstone (Sr, St); ripple-drift cross-lamination prominent	Sm, Fsc, Sr, St	Floodplain deposits with eolian layers and paleosols; climbing ripples indicate periodic rapid silt accumulation
<b>Loess-Paleosol Blankets (LPB)</b>	Very coarse silt	Extensive beds up to 1 m thick with thin Fsc interbeds, forming stacked successions up to 4 m thick; contain deeply penetrating root traces	Sm, Fsc	Eolian silt (loess) with intervals of reduced silt accumulation that allowed pedogenesis and growth of vegetation; deep roots indicate low water table
<b>Lacustrine Fines (LF)</b>	Very coarse to fine silt	Interbedded Sm, Fsc, and rare Sr (ripple-drift); Sm forms scour-based lenses that wedge out within Fsc; Sm beds thicken upwards; locally high bioturbation index; prominent deep root traces from upper part	Sm, Sr, Fsc	Standing-water deposits with irregular pulses of coarser silt from eolian settling or small fluvial deltas

The planar bases of the channel bodies are in several cases cut into silty mudstone (Fsc), which may have been more cohesive and limited downcutting. One instance was noted of a channel base cutting steeply or vertically into loess, which also filled some channels. Bedsets are localized to individual scour fills, and flow seems rarely to have occupied the entire channel belt. Flow was largely subcritical with minor episodes of critical to supercritical flow, and the general lack of systematic bedform successions suggests variable flow strength, with periods of complete dryness. Thin, single-story channel bodies probably reflect a brief occupation of the fluvial tract.

### **2.7.3 Confined to Unconfined Sheets (CUS)**

These sediment bodies in the upper division are unusually extensive as very broad sheets: Channel-Body C extends for at least 5 km, with no channel margins observed. The deposits are typically 1-2 m thick, locally thickening to 3.5 m within channel forms that are present locally. The basal contact with structureless siltstone (Sm) is commonly abrupt but locally gradational and difficult to identify, and the overlying strata grade up from Sm to Sh, St and Sr, denoting a waning-flow succession with little grain-size change. Beds of silty mudstone (Fsc) locally top the successions, from which root traces bifurcate downwards, passing completely through the bedsets in places. The channel bodies represent widespread, largely unconfined flows that reworked loess blankets. The waning-flow successions suggest that they represent individual discharge events, probably generated by high-magnitude flood events that overtopped channels up to 3.5 m deep. The capping Fsc units with root systems indicate incipient pedogenesis and landscape stabilization following flood events.



#### **2.7.4 Floodplain Siltstone (FS)**

Floodplain Siltstone is poorly exposed but forms the background sediment in the lower and middle division in all sections. The strata comprise thin and extensive planar units of Sr, St and Sm, with Fsc locally prominent with root traces and depletion halos. This association is interpreted as a floodplain deposit with irregular deposition from eolian settling (Sm and possibly some Sr units), episodes of overbank flow (Sr, St) that may include crevasse splays from the associated channels, and pedogenesis associated with the establishment of vegetation (Fsc).

#### **2.7.5 Loess-Paleosol Blankets (LPB)**

This association predominates in the upper division, where it comprises decimeter- to meter-scale beds and packages that can be traced from butte to butte for at least 5 km. The predominant facies is structureless, conchoidally weathered siltstone (Sm), typically forming planar beds about 1 m thick, interbedded with thin Fsc beds. Bedsets 4-5 m thick comprise individual Sm beds that thicken upwards below an Fsc cap, from which roots with depletion halos and rhizoconcretions penetrate downwards. The Sm units are locally reworked into the CUS association.

In accord with previous research in western Pangea, Loess-Paleosol Blankets are interpreted as climatically related rhythms that were laid down over a large area of the southern Paradox Basin. Similar rhythms in the Halgaito Formation near Mexican Hat were attributed by Soreghan et al. (2002) to high-frequency glacial - interglacial climatic fluctuations, analogous to those documented in late Cenozoic strata in the Chinese Loess Plateau and other locations worldwide (Porter 2001; Pendea et al. 2009; Lehmkuhl et al. 2016; Schirmer 2016). Similar rhythms are prominent in other Late Paleozoic basins in the southwest US (Kessler et al. 2001;

Soreghan et al. 2008; Soreghan et al. 2014). Soreghan et al. (2002) noted that the paleosols contain windblown dust, implying that dust accession continued during paleosol formation but with a reduced volume.

### **2.7.6 Lacustrine Fines (LF)**

The facies association is restricted to one 7 m occurrence at the base of the Lime Ridge section. Beds of Sm, Fsc and rare Sr and St show a broadly thickening upward trend, *Palaeophycus*, desiccation cracks and adhesion structures are present, and root traces penetrate down from the topmost strata.

The facies association is attributed to standing-water deposits with periods of exposure, broadly shallowing upwards to a vegetated surface as a progradational fill. Lenses of Sm in the lower strata were probably laid down as loess accumulations in standing water, and the more planar Sm beds may represent eolian additions or pulses of silt from small fluvial deltas. The strata lie shortly above the “A” limestone, but the ichnofauna provides no clear indication of marine influence and a lacustrine freshwater setting is probable.

### **2.7.7 Fluvial Paleoflow Patterns**

Paleoflow data from the study area represent numerous channel bodies of varied scale (Figs. 5, 12, 15), principally Fluvial Ribbons and Broad Fluvial Sheets in the lower and middle divisions. Large suites of measurements were obtained for ripple cross-lamination on bed surfaces in the larger channel bodies, providing an especially reliable determination. At the Fossil Site in the western part of the Valley of the Gods, channel bodies through 10 m of section yielded consistently northeasterly to easterly paleoflow, and Huttenlocker et al. (2018) recorded

an 80° ENE trend for Channel Body E. At Rooster and Setting Hen, northerly to northeasterly paleoflow characterizes the basal 35 m of the section, with north-northeasterly paleoflow for Channel-Bodies A and B. At Lime Ridge in the eastern part of the study area, 45 m of section yielded an overall easterly paleoflow, varying from northeasterly to southeasterly and including easterly paleoflow for Channel-Body H. The implications of these measurements are discussed further in section 2.8.5.

## 2.8 Discussion

### 2.8.1 Fluvial-Eolian Interaction on the Halgaito Plains

The rivers which deposited the Halgaito Formation traversed a landscape that aggraded steadily through the buildup of loess, requiring frequent adjustment of their equilibrium level. The present study yielded several lines of evidence for fluvial / eolian interaction on the plains:

- 1) *Petrographic evidence for reworking of eolian silt into channels.* Both eolian and fluvial samples are predominantly coarse silt, an unusually fine grade for fluvial-channel deposits, with the fluvial samples slightly less well sorted and with a more extended coarse tail to very fine sand (Fig. 10). Along with similar composition of framework grains in the eolian and fluvial samples and a paucity of finer matrix, the grain-size analysis confirms that reworked loess provided the bulk of the fluvial sediment. Under the microscope, Gm samples (Fig. 9F) also show similarities to both the eolian and fluvial samples (within individual pebbles). Composition of grains, grain-size and a lack of a finer grained matrix support the interpretation of reworked loess being the main source for fluvial sediment.

2) *Channel incision into loess.* Broad Fluvial Sheets and Fluvial Ribbons are incised into loess below the channel bases and at cutbanks (Figs 12F and 13A & B). Several visible channel margins are low-angle, suggesting a relatively unconsolidated substrate since the underlying material was unable to form or support a higher angle of erosion. However, local consolidation of loess at shallow depth is indicated by a vertical to overhanging step 60 cm high below the base of Channel Body A, against which the fluvial deposits abut (Fig 13C). In this location the underlying substrate had sufficient cohesion to support the incision of the channel without eroding the banks to a more shallow angle. This location also had a mix of Sh, Sr, and Gm, which would indicate a high flow rate, and thus an increased erosive capacity, which still did not degrade the bank to a shallow angle. As mentioned previously, the pebbles within Gm share petrographic traits with regular fluvial and eolian deposits, and as it is found within the channel-fill of this overhanging cutbank, this supports the interpretation of channels incising into loess.

3) *Loess buildup in channels.* It was frequently difficult to discern whether channels contained loess or cut into loess as contacts are commonly poorly defined and gradational. However, loess forms structureless layers and lenses up to 1 m thick in some channels (Fig. 13B), indicating that eolian dust periodically choked the channels or laid down a thin sheet that was reworked by water. The numerous instances of well formed ripple-drift cross-lamination (Fig. 6G) give evidence to the high sediment load during deposition. The presence of St formed with silt and fine sand sized grains also supports the interpretation of a high sediment load (Sambrook Smith et al. 2016).

4) *Flows reworking Loess-Paleosol Blankets.* In the upper division, Confined to Unconfined Sheets of water-laid silt rest exclusively on loess. Their bases vary from abrupt to gradational, indicating active scouring or partial remobilization of the underlying loess (Figs.

13D, 15B, & 16). In some locales the transition is quite cryptic; as beds are traced laterally the boundary between the lower loess and upper CUS changes is not a horizontal surface but has irregularities (Fig. 15B). Quaternary loess yields examples of some of the same interactions. Features observed in European and Chinese loess exposures include gullied landscapes where loess was reworked into erosive channels, watershed valleys cut into loess, incision from slope wash, and reworking by sheet flows (Porter and An 2003; Pendea et al. 2009; Lehmkuhl et al. 2016).

Loess in modern settings is commonly cliff-forming and readily erodible (Pye 1984; Pecsli 1990). Consolidation is typically promoted by precipitation of secondary carbonate as grain coatings and meniscus cements, needle-fibre calcite, calcified root cells, nodules, and petrocalcic horizons, with the carbonate derived from groundwater, aerosols, weathering, and dissolution of carbonate grains to form oversized pores (Pye 1995; Cilek 2001; Antoine et al. 2003; Jeong et al. 2011; Smalley and Markovic 2014; Li et al. 2015; Li et al. 2018). Clay bridges between grains are locally impregnated with calcite and other minerals (Pye 1984; Cilek 2001), and cohesive forces between small particles (Pye 1984) and sticky extracellular polysaccharides from biological crusts (Svircev et al. 2013, 2019) may assist consolidation. Slaking on wetting may initiate structural collapse through the breakdown of clay bridges and calcite cement. In the Chinese Loess Plateau, loess cliffs tend to collapse and flow during rainfalls or where rivers have undercut loess banks, especially where agricultural irrigation has raised the water table (Pye 1984; Xu et al. 2012; Smalley and Markovic 2014; Li et al. 2015).

Thin sections of loess in the Halgaito Formation (Fig. 8) show the presence of detrital carbonate grains, initial loose packing with many point contacts, and poikilotopic calcite cements that in places fill oversized pores. No indication was observed of the early diagenetic

features noted above, and the pervasive calcite cement formed during deeper burial may have overprinted these subtle fabrics. Distinguishing early diagenesis of loess from deep-basin diagenesis is often problematic (Sprafke and Obreht 2016). Thus, it is not clear that the observed diagenetic features (shared also with the fluvial siltstones) were responsible for the near-surface consolidation of the eolian siltstone.

Interaction between rivers and loess in ancient examples may yield distinctive features in view of the unusual properties of loess. The infiltration of river water into porous loess is likely to build up groundwater lenses and promote framework collapse, possibly enhancing local accommodation space. Bank collapse might promote rapid bank retreat and generate distinctive features such as slurry flows or slump blocks. However, these were not identified in this study.

### **2.8.2 Comparison of Fluvial Architectural Styles with Facies Models**

Fluvial-sandstone sheets in the geological record commonly represent the channel belts of braided systems with in-channel bars (Bristow 1993), meandering systems with laterally accreted point bars (Kraus and Gwinn 1997), and combinations of both styles (Hampson et al. 2013). Some sandstone sheets in seasonal settings lack evidence for braided barforms but have been provisionally attributed to braided systems (Robinson and McCabe 1998).

In modern dryland settings, many seasonal rivers are swept by high-discharge floods in channelized to poorly channelized settings, followed by periods of exposure (Tooth 2000). The examples in Table 5 include rivers in Africa, Australia, and India and are perhaps best described as “sandbed rivers” that range from broad “washes” with well-defined banks to largely unconfined overbank flows and “floodouts” (Tooth 2000). These rivers show little systematic development of bank-attached or in-channel bars, have relatively flat-lying sediment surfaces,

and show a predominance of critical to supercritical bedforms, although subcritical bedforms are locally predominant (Williams 1971). Riverbed exposure may be enhanced by high transmission losses into porous substrates (Knighton and Nanson 1994).

A distinctive feature of these examples is scours that vary from small hollows to deep incisions that are rapidly filled. In an analysis of fluvial architecture and discharge variation, Fielding et al. (2018) characterized the Platte River of Nebraska as showing high variance in peak discharge. In geophysical traverses of the Platte River, numerous secondary-channel scours with up to 3 m of relief and 20 m width are accompanied by smaller scours up to 1 m deep and 4 m wide that represent bar-top channels (Horn et al. 2012). Horn et al. (2012) identified downstream- and lateral-accretion surfaces formed by macroform migration but noted the lack of accord between the abundance of scours and standard facies models for braided rivers. In geophysical traverses across the sandbed Burdekin River of Australia, Fielding et al. (1999) noted numerous scoured surfaces with up to 3 m of relief and 40 m width, overlain by cross-bedded fills; in places, high-discharge floods had mobilized and redeposited sediment down to 6 m depth. The authors considered such scour fills to be a distinguishing feature for variable-discharge, sandbed rivers in the rock record.

Numerous sheet sandstones from seasonal settings in the ancient record show features that accord with modern rivers subject to highly variable discharge (Table 5). As shown in table 5, these ancient deposits were attributed to broad, shallow channels with periods of high-intensity flow. Channels were commonly poorly confined with low-angle margins, systematic lateral migration, abundant scours with a range of scales, aggradational fills, critical to supercritical bedforms that include plane beds and antidunes, a paucity of macroform surfaces, and abrupt vertical and lateral facies changes. The examples in Table 5 include Devonian

examples where rooted vegetation was scarce and riverbanks poorly supported, as well as younger examples with vegetation cover.

The Halgaito Formation sheet bodies contain many features in accord with high discharge variation (Table 5), particularly the prominence of aggradationally filled scours, and the lack of macroform surfaces. Sheet Bodies of the Halgaito Fm differ from examples in Table 5 in their siltstone composition, due to reworking of loess, and largely subcritical flow conditions. A similar analogue is part of the Permian Beaufort Group of South Africa (Stear 1983), in which sheet sandstones were generated by channels with a fluctuating hydrograph that shifted laterally through sandy flood deposits.

Ribbon bodies in the Halgaito Formation form small channel fills up to a five metres thick as well as isolated narrow bodies up to 2 m thick (Figs. 11A and B, 15E, and 16). Their geometry and fills accord with many dryland ribbon bodies in the geological record (Eberth and Miall 1991; Kraus and Gwinn 1997), some of which may represent anastomosing rivers with suites of narrow fixed channels.

No clear evidence was noted in the Halgaito Formation for tiers of ribbons at the same stratigraphic level, a hallmark of multichannel systems (Rust et al. 1984; Kraus and Gwinn 1997). The distinction of sheets from ribbons is difficult at Lime Ridge. Although this is partly due to paleoflow being near-parallel to the outcrop face, there may also be a gradation between ribbon- and sheet-bodies as end members of an architectural spectrum, as noted by Eberth and Miall (1991) in the Cutler Formation of New Mexico.

Very broad sheets that thicken locally into channels have been attributed largely to unconfined flows. As in the case of Channel-Body C, the lateral extent of VBS is very large; their features resemble those of other modern and ancient examples (Table 5).



**Table 5: Architecture of some dryland-river deposits in the geological record. See Table 1 for facies codes. ST = silt; VF, FS, MS, CS, VC = very fine, fine, medium, coarse and very coarse sand; cgl = conglomerate. Elements (Miall 1996): SB = sandy bedforms; LS = laminated siltstone**

<b>Formation and Age</b>	<b>Grain Size</b>	<b>Geometry and Architecture</b>	<b>Internal Features</b>	<b>Interpretation</b>	<b>Reference</b>
<b>Modern Dryland Rivers</b>					
<b>R. Gash, Sudan</b>	FS to MS, minor gravel and fines	Channel 1-2 m deep, 100-800 m wide (average 200-300 m); sheets with prominent scour fills	Sh predominant, St, Sp, Ss, Sr, Fl with desiccation cracks; roots; scours up to 3.5 m deep	Ephemeral braided channel, laterally mobile, seasonal flow, upper-regime flow prominent; channelized and unchannelized flow	Abdullatif 1989
<b>Rivers west of Lake Eyre, Australia</b>	FS to VC, minor gravel and fines	Channels 2 to 6 m deep, flooded to several km width	St and Sp predominant, Sr (climbing ripples), local Sh, minor scours	1967 floods, extending beyond channels; subcritical flow prominent	Williams 1971
<b>R. Luni, India</b>	FS to MS, minor gravel and fines	Channel in study reach 850 m wide, mean flow depth 2 m, usually dry, floods to 14,000 m <sup>3</sup> s <sup>-1</sup>	Sh to 1 m thick predominant, St and Sp, rare Sr, Sm, scours commonly 3-7 m deep cause discontinuous facies	Critical to supercritical flow prominent, steep gradient; dry for most of year	Carling & Leclair 2019
<b>Ethiopian rivers, Kobo Basin</b>	MS-CS, pebbly	Channels 2-4 m deep, several hundred m wide; w/d 73-414 in study area	Sh predominant, minor St, Sp; small scour pockets	Critical to supercritical flow flow prominent, steep gradient; dry for most of year	Billi 2008
<b>Wadi El Arish, Egypt</b>	Sand and mud, minor gravel	Confined segments several hundred m wide and 3 m deep; unconfined shallow reaches several km wide	Sh, St, Sp, Sr (climbing ripples common), waning-flow units; desiccation cracks	Episodic floods; varied predominance of subcritical and critical to supercritical flow	Sneh 1983
<b>Formation and Age</b>	<b>Grain Size</b>	<b>Geometry and Architecture</b>	<b>Internal Features</b>	<b>Interpretation</b>	<b>Reference</b>

**Dryland Sheet Channel Bodies in the Geological Record**

<b>Formation and Age</b>	<b>Grain Size</b>	<b>Geometry and Architecture</b>	<b>Internal Features</b>	<b>Interpretation</b>	<b>Reference</b>
<b>Moor Cliffs Fm., Devonian, UK</b>	MS-CS, fining up to VF-ST, cgl	Sheet sandstones, up to 4.5 m thick, average 1.5 m, apparent w/t >250	St, Sp, Sr (climbing ripples common), desiccation cracks; scour surfaces prominent; some low-angle accretion surfaces (LA or DA)	Broad, shallow channels with flow over interfluves; low-angle banks; ephemeral in humid climate, high-intensity storms	Love & Williams 2000
<b>Trentishoe Fm., Devonian, UK</b>	FS, cgl, minor fines	Sheet sandstones, up to 200 m wide, 1.5 m thick; single storey	Sh prominent, waning-flow to siltstone, desiccation	Broad, shallow channels with aggradation and critical to supercritical flow; association with playa lakes	Tunbridge 1984 (Facies 2)
<b>Brownstones, Devonian, UK</b>	MS, minor cgl	Sheet sandstones, >2 km extent, 3-11 m thick; cross-cutting channel-fill networks; multistorey	Sh, Sp, Sp; concave-up scours (channel bases) up to 80 cm deep, 12-15 m wide	Small ephemeral channels with sandy bedload, repeated cut-and-fill events	Tunbridge 1981 (Facies 2)
<b>Clear Fork Fm., Permian, USA</b>	VF-CS, minor cgl	Sheet sandstone, hundreds of meters wide, 1.3 to >6.5 m thick	St, Sh, Sr (climbing ripples prominent), Sm; waning-flow bedset; scours to 1 m deep prominent	Brief floods in ephemeral systems, poorly confined to unconfined; subcritical and critical to supercritical flow	Simon & Gibling 2017
<b>Cutler Fm., Pennsylvanian – Permian, USA</b>	FS-VC, minor cgl	Sheet sandstones up to 1 km wide and 10 m thick; multistorey to multilateral	St, Sh locally prominent; scours up to 4 m deep; scarcity of LA and macroforms	Broad, shallow ephemeral channels, rapid flow; nature of storeys depends on degree of confinement; lack of bank-attached or mid-channel bars	Eberth & Miall 1991

<b>Beaufort Group, Permian- Triassic, S. Africa</b>	VF-MS, minor cgl and fines	Sheet sandstone, regionally extensive for several km; up to 32 m thick; multistorey	St, Sp, Sr, Sm; amalgamated wide, shallow scour fills with concave-up bases; lack of inclined surfaces	Ephemeral flow systems; scour forms interpreted as a downstream-accreted channel belts; low subsidence rate promoted lateral migration	Wilson et al. 2014 (Type 6); Gulliford et al. 2014 (Type 6)
<b>Beaufort Group, Permian- Triassic, S. Africa</b>	Sand, minor cgl and fines	Sheet sandstones, >1 km wide, up to 20 m thick, multilateral and multistorey; channels up to 100 m wide and 3-5 m deep	Sh prominent, St, Sr; waning-flow successions; LA present, low-angle accretionary units; scours prominent; desiccation evidence	Ephemeral rivers localized in an area, channels migrated laterally through sheet-flood deposits; critical to supercritical flow prominent, seasonal flash floods; braided – meandering transition	Stear 1983
<b>Chinle Fm., Triassic, USA</b>	MS-FS, cgl	Sheet sandstones; multistorey	Sh, St, Sm	Broad, shallow channels with ephemeral flow, critical to supercritical flow common	Deluca & Eriksson 1989
<b>Kayenta Fm., Jurassic, USA</b>	FS-MS, minor cgl	Sheet sandstones, locally ribbon geometry, up to 350 m wide, 6 m thick, planar bases and poorly defined margins; multistorey	Variably Sh, St, and interbedded facies predominant; rare fining- up and desiccation cracks; scour fills up to 20 m wide and 2 m thick	Broad, shallow ephemeral rivers, channelized to poorly channelized; subcritical and critical to supercritical flow indicated	North & Taylor 1996
<b>Morrison Fm., Jurassic, USA</b>	VF-CS, minor cgl	Sheet sandstones, up to 1200 m wide (ave. 390 m) and 18 m thick (ave. 7 m); single storey and multistorey	St, Sp, Sh, Sm, minor Sr; scours present, disorganized structure; lack of accretion bedding but small unit bars	Braided channels under warm and dry climate	Robinson & McCabe 1998
<b>Formation and Age</b>	<b>Grain Size</b>	<b>Geometry and Architecture</b>	<b>Internal Features</b>	<b>Interpretation</b>	<b>Reference</b>

<b>Willwood Fm., Paleogene, USA</b>	VF-CS	Sheet sandstones, >1.5 km wide, 10-25 m thick, w/t >50, storeys up to 4.5 m thick; multistorey	St, Sh; LA prominent	Meandering rivers up to ~5 m deep with point bars	Kraus & Gwinn 1997
<b>Halgaito Fm., Pennsylvanian – Permian, USA</b>	ST, minor VF	Sheet bodies up to 5 m thick and >500 m wide, w/t >75, cut into loess; low-angle cutbanks	Sr, St, Sm, local Sh; scours prominent with a range of scales	Ephemeral channels up to 5 m deep, locally with systematic migration direction; episodic cut and fill; mainly subcritical flow	This study

#### Dryland Unconfined Sheet Bodies in the Geological Record

<b>Trentishoe Fm., Devonian, UK</b>	FS-MS	Sheet sandstones, thick to thin bedded, >100 m wide, 1 m beds, planar base, no channel forms	Sh passing up into Sr and siltstone; waning-flow units	Unconfined flood deposits with shallow, fast flows; degeneration of channel flow into flood sheets	Tunbridge 1984 (Facies 4)
<b>Brownstones, Devonian, UK</b>	FS-MS, minor cgl	Sheet sandstones, >300 m wide, up to 1.5 m thick	Sh passing up into Sr and siltstone; waning-flow units	Unconfined flood deposits over desiccated surface, rapid energy decline	Tunbridge 1981 (Facies 1)
<b>Halgaito Fm., Pennsylvanian – Permian, USA</b>	ST, minor VF	Sheet bodies 1-5 m thick, >5 km extent, thicken locally into channel fills	Abrupt to gradational base on Sm, St passes up into Sr and Fsc	Confined to unconfined flood deposits, reworking a loess substrate	This study

Many dryland river floods extend beyond channels across unconfined plains (Williams 1971; Sneh 1983), and many of the formations in Table 5 were laid down by variably confined and unconfined flows (Tunbridge 1981, 1984; North and Taylor 1996; see also Hirst 1991). The prominence of VBS in the upper division suggests a setting characterized by extreme discharge variability, with channels generally able to contain the flows but periodically swept by exceptionally high-magnitude floods that generated sheet flows in overbank areas.

### **2.8.3 Contribution of Vegetation to the Halgaito Landscape**

Plant macrofossils were identified in several channel bodies in the lower and middle divisions (DiMichele et al. 2014; our observations) but are generally uncommon. Plants are especially prominent in Channel-Body A at Setting Hen, where large calamitalean fragments and comminuted debris are concentrated low in the channel body in laminated siltstone, formed by critical to supercritical flow, and on the scoured bases of trough cross-sets. In Channel-Body H at Lime Ridge, plant fragments are present in mudstone drapes within sandstone packages (Chaney et al. 2013). These occurrences represent situations of rapid burial. In situ stems were not identified in the present study, either in floodplain deposits or rooted in the channel sediment, but DiMichele et al. (2014) noted putative examples above a paleosol at Setting Hen. Plant detritus was probably a food source for the arthropleurid that made the *Diplichnites* trackway in the channel at Lime Ridge (see Prescott et al. 2014).

DiMichele et al. (2014) identified a range of plant taxa (see above) that variously were adapted to wet substrates or seasonally dry conditions. Calamitaleans were associated with high soil moisture and were adept at colonizing disturbed habitats with rapidly shifting substrates (Gastaldo 1992). Walchians were capable of tolerating seasonal aridity and may have grown on

interfluves, and cordaitaleans tolerated a wide range of conditions (Bashforth et al. 2014). *Sigillaria brardii* was a wetland lycopsid with deeper roots, more tolerant of droughts.

In view of the cryptic plant record of the Halgaito Formation, it is difficult to use fossil evidence to assess the original abundance of vegetation, its geomorphic importance, and the paleoclimate. Vegetation was probably more abundant than the macrofossil record suggests because root traces descend from paleosols at many levels in the formation. Some of the best examples are in the upper division where closely spaced roots penetrate up to 3 m through Loess-Paleosol Blankets. However, channel margins are not noticeably rooted, and no definite indication was obtained during the present study that vegetation influenced the channel morphology. As suggested by Scott (2005), a key factor for loess accumulation in the Halgaito Formation would have been the stabilizing presence of vegetation (Tsoar and Pye 1987), possibly assisted by the presence of biological crusts (Svircev et al. 2019).

In terms of paleoclimate, the presence of wetland taxa may correspond to a wetter episode identified by Soreghan et al. (2002) near the Pennsylvanian-Permian boundary, and the rooted levels associated with paleosols, especially in the Loess-Paleosol Blankets of the upper division, may reflect relatively humid periods as the water table rose slightly (Golab et al. 2018). However, under the conditions of intermittent flow inferred for the Halgaito channels, wetland taxa would have been confined to parts of the landscape with high water tables, including areas of standing water within channels, the riparian zone, and floodplain swamps. Furthermore, groundwater lenses formed by infiltration below the channels would have promoted the growth of vegetation in the riparian zone, as in Australian dryland systems (Cendón et al. 2010). Thus, the presence of wetland plants may be a measure of local water availability in the landscape rather than a humid paleoclimate (DiMichele et al. 2006; Simon and Gibling 2017; Simon et al.

2018). An additional consideration is the rapid burial of plant fossils in channels which, in comparison with their exposure to oxidation on floodplains, may have favored the preservation of wetland taxa (DiMichele et al. 2014).

DiMichele et al. (2014) suggested that plant dispersal across the Paradox Basin took advantage of riverine corridors descending from the Uncompahgre Uplift. However, northerly and easterly paleoflow for the Halgaito Formation in this area indicates a separate catchment area, as discussed below, possibly unconnected to the northern drainage system.

#### **2.8.4 Evolution of Fluvial and Eolian Processes during Halgaito Deposition**

The Halgaito divisions exhibit an upward change in depositional style and in the balance of fluvial and eolian processes (Figs. 17 and 18). Although no precise assessment of climatic conditions is possible from our dataset, the landscape changes were probably mediated by long-term climatic trends associated with changes in moisture availability and discharge (Soreghan et al. 2002), although autogenic changes in channel networks cannot be ruled out.

The lower division is characterized by Fluvial Ribbons, laid down by short-lived channels up to 5 m deep that reworked Floodplain Fines including loess and paleosols (Fig. 17 and 18). Some channels, as well as the Lacustrine Fines facies association, yield evidence for desiccation (adhesion structures, desiccation cracks) and loess build up (climbing ripples, St formed in silt rich environment). Trace fossils that include myriapod trackways are present in some channel bodies, along with fronds of *Walchia*. We infer seasonal flow conditions and periods of eolian activity, but sufficient water was present at times to support riparian vegetation. A slightly different scenario is suggested for the western area near Fossil Site where thick intraformational conglomerates, some fine-grained sandstone, and large, deeply incised channels were present.

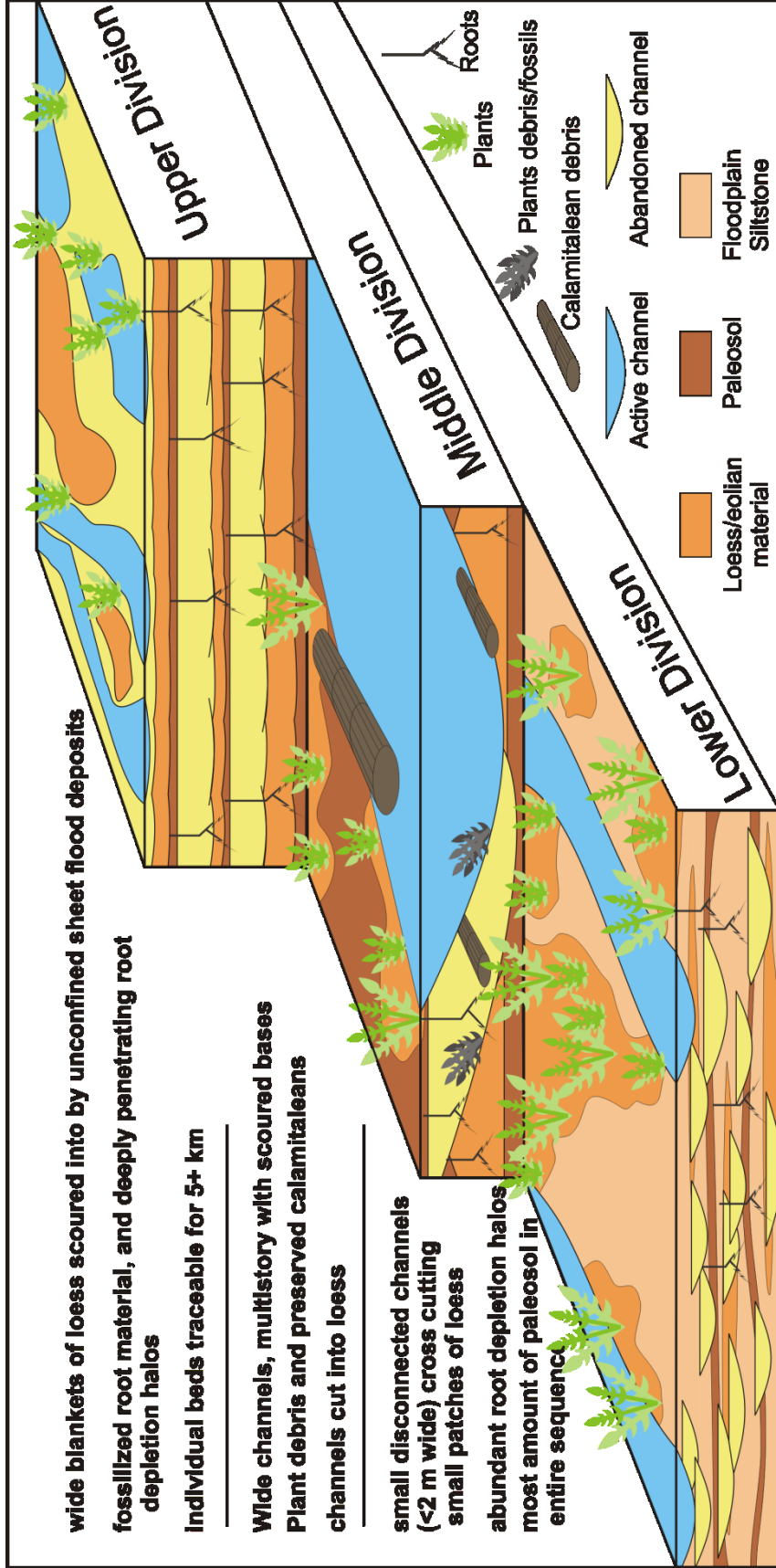
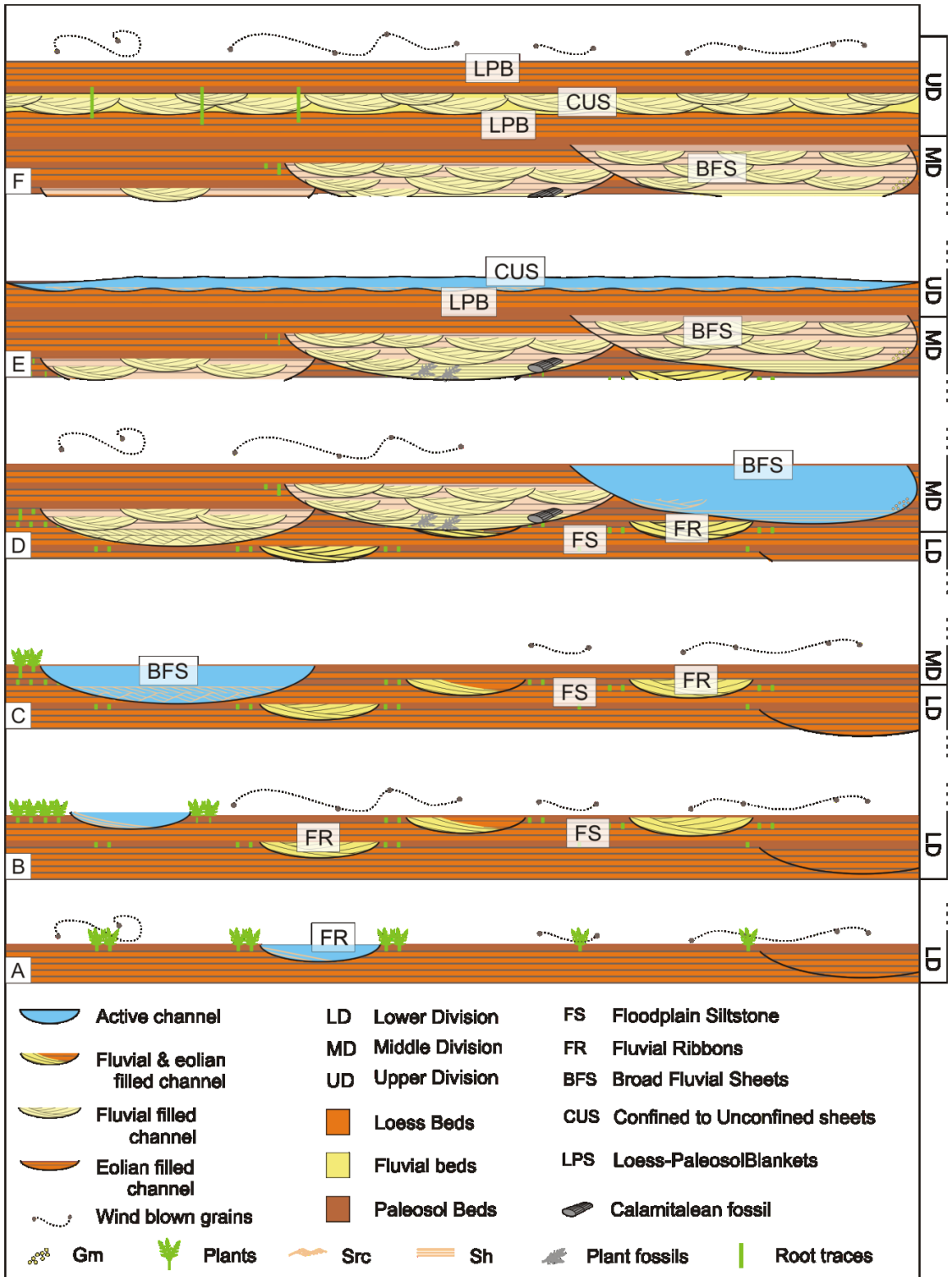


Figure 17: An idealized view of the Upper, Middle, and Lower Halgaito showing channel geometry, channel relationships, and vegetation combined.





**Figure 18: Evolution of the three main environments within the study area. These different environments are the result of interacting fluvial and eolian systems. (A) Initial landscape of loess with abandoned channel filled with eolian material and active channel forming Fluvial Ribbons (FR). (B) Landscape is incised by sequences of fluvial channels. Eolian material is still being deposited where channel is not incising. (C) Lower Hala Bala is incised by Broad Fluvial Sheets (BFS). These channels have climbing ripples and dunes formed in the bottom of the channel. (D) The channel has shifted several times and has truncated the previous channel(s); continued deposition of windblown material on the landscape has caused aggradation but less than during A – B. While the abandoned channel was being filled small internal scours are formed possibly by partial reactivation. Plant fossils and upper flow regime deposits are also found within these BFS. The active channel scoured into the loess to cause an overhanging edge. Eroded portions of the loess material are redeposited in the channel as Gm. (E) Confined to Unconfined Sheets (CUS) of floodwaters rework the upper portions of the loess of the Loess-Paleosol Blankets (LPB). This material is also being deposited in situ as dune and ripples as the flow wanes. (F) The water has evaporated and plants have grown with deeply penetrating tap roots. Loess buried the plants and again blankets the landscape before another flood event occurs.**

The overall interpretation of seasonal flow conditions, and eolian activity are the same, however the steepness of the cut banks and abundance of Gm with Sh (Figs. 13B & C, 14D & E), is interpreted herein to have been laid down by more turbulent channels and higher flow velocities capable of carrying the increased grain size of Gm, and the force required to scour the fragments from the underlying loess material.

The middle division has much larger channel bodies of the Broad Fluvial Sheet association (Figs. 17 and 18), observed at all studied sites in the Valley of the Gods. Instantaneous channel depth, as indicated from the relief of erosion surfaces, was up to 5 m, similar to that of channels in the lower division, but channel widths were much greater and the channel bodies show a more complex multilateral architecture and systematic migration of the channel in places. Critical to supercritical bedforms are present locally, periods of dryness are shown by adhesion structures, and preserved vegetation in some channels. The presence of an oncolite in one conglomerate suggests local ponding in the channel or on the adjacent landscape.

These observations suggest a more prolonged occupation of channel belts that experienced high-intensity floods and no-flow periods. The channels reworked and incised loess blankets, as indicated by an abundant silt load and climbing ripples. Although active eolian contributions cannot be ruled out, there is less indication that loess filled the channels. We infer more water on the landscape and higher fluvial discharge, in accord with evidence for relatively humid conditions in the Halgaito Formation (Soreghan et al. 2002). It is possible, however, that a trunk river network with larger channels shifted into the area.

The upper division is characterized by a marked shift across the region to Loess-Paleosol Blankets with Confined to Unconfined Sheets (Figs. 17 and 18). This suggests a more arid setting in which eolian processes dominated the landscape, accompanied by climatic rhythms with varying but at times intense dust flux (Soreghan et al. 2002). The water table was relatively low (Golab et al. 2018) and root systems penetrated more deeply. Although water was available periodically on the landscape, organized channel systems were not prominent, with shallower channels and periods of unconfined flow in response to high-magnitude floods. The strata are overlain by eolian dune sands of the Cedar Mesa Sandstone, and the upper division may in part reflect increasing proximity to an erg with windblown dust.

The fluvial sediments are largely calcite-cemented but include small patches of early-formed barite and celestite cement. The presence of barite and celestite suggest that shallow groundwater had elevated salinity in places, linked to strong surface evaporation and relatively arid conditions (García-Veigas et al. 2011; Bodzioch and Kowal-Linka 2012).

### 2.8.5 Rivers Flowing North into the Paradox Basin

As previously described in this study, the paleoflow analysis for Halgaito Formation rivers in the Valley of the Gods and Lime Ridge indicates a predominant flow direction to the north and east (Figs. 5, 12, and 15). This observation adds a previously unrecognized drainage component with a source to the south and west and suggests that the Paradox Basin had a more complex drainage system than formerly assumed (Fig. 19).

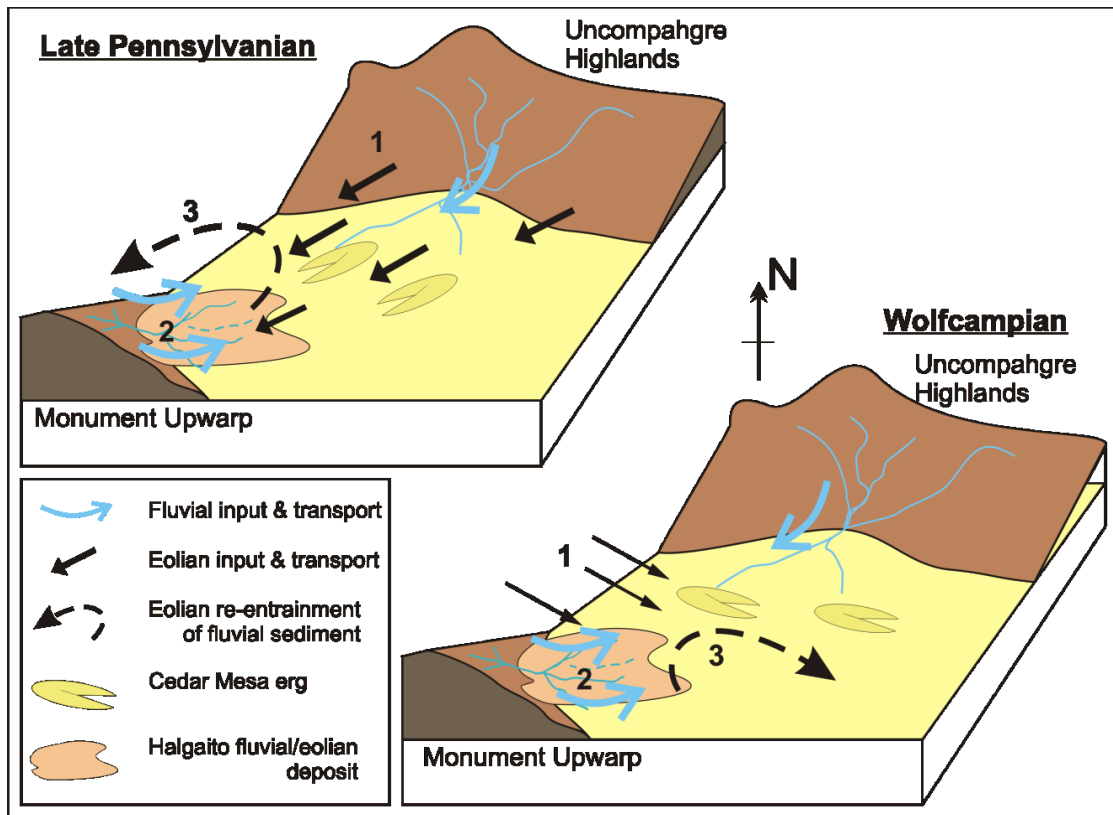


Figure 19: The paleogeographic positions of the Uncompahgre Highlands and Monument Upwarp with the transition from the proximal alluvial fan, middle erg deposit and the distal loess field. During the Late Pennsylvanian the wind direction from the Uncompahgre Highlands (1) brought silt from the north towards the Monument Upwarp, while the paleo flow direction (2) off the Monument Upwarp transported sediment downstream into the same catchment area, which possibly created a recycling of sediment (3). Through the Wolfcampian the wind direction shifted to be from the northwest (1) which reduced the amount of sediment recycling in the area.

Numerous previous studies documented southward sediment transport from the Uncompahgre Uplift into the proximal Paradox Basin, where some 5 km of Cutler redbeds were laid down in alluvial fans and fluvial megafans (see summaries of earlier work in Condon 1997). Barbeau (2003) noted that waning subsidence in the foreland basin would have allowed proximal accommodation to be filled, promoting sedimentation in the distal basin in the Early Permian and implying a southward extension of Uncompahgre drainage. However, sediment may have continued to be trapped in proximal areas where the topmost Cutler beds onlap the uplift, indicating that both uplift and basin subsided during the Early Permian (Moore et al. 2008; Soreghan et al. 2012).

The rise of salt walls in the proximal basin confined much of the Uncompahgre sediment to minibasins where rivers flowed west and northwest to the ocean (Lawton et al. 2015; Venus et al. 2015). This may have limited the ability of the rivers to reach the distal basin and encouraged a greater northward extension of drainage from the south, although the northern rivers may have overtopped the salt walls or followed bypass zones along transfer faults (Lawton et al. 2015). Additionally, continental-scale rivers brought Appalachian sediment to the west coast during the Pennsylvanian and Permian (Dickinson and Gehrels 2003; Gehrels et al. 2011), although it is unclear whether they formed axial flow systems in the Paradox Basin. Venus et al. (2015) noted that the Cutler strata may be too thick to have been sourced entirely from the Uncompahgre Uplift, suggesting drainage contributions from other uplifts and possibly from distant mountains via large axial rivers.

Little attention has been paid to sediment sources on the southern margin of the Paradox Basin, where the Defiance-Zuni Uplift lay to the south and the Emery-Piute Uplift to the west. In the Arizona/Utah border area, the Monument Upwarp is a prominent tectonic feature

(Gregory 1938), largely a Laramide structure in its present form but with Permian and Triassic antecedents (O'Sullivan 1965; Dubiel et al. 1996; Barbeau 2003). The uplifts may have originated as cratonic basement structures and may have been forebulge locations during Uncompahgre thrust activity, as suggested for uplifts elsewhere in the region (Hoy and Ridgway 2002).

Evidence from latest Pennsylvanian and Early Permian strata testifies to syndepositional tectonism of the Monument Upwarp. Wengerd and Matheny (1958) noted that the upwarp rose slowly during deposition of the Paradox Formation salt, and the Halgaito Formation and Cedar Mesa Sandstone thin over the upwarp, with the maximum thickness of the Cedar Mesa Sandstone on the eastern side (Gregory 1938; Baars 1962; Stanesco and Campbell 1989; Condon 1997). Vaughn (1962) suggested northward drainage for the Halgaito Formation based on the general disposition of conglomerates, and Stanesco and Campbell (1989) inferred a northwestern paleoflow for fluvial deposits in the Cedar Mesa Sandstone, which they attributed to deflection of Uncompahgre streams around the nose of the upwarp.

The present study yielded no evidence for a substantial contribution to the Halgaito Formation from bedrock in the Monument Upwarp area. The conglomerates are intraformational and the fluvial deposits are largely silt-sized, with little sand and a relatively constant grain size through the formation, with no sign that the larger river channels tapped coarser sources. An exception may be in the western part of the study area where the Fossil Site has slightly coarser sediments, thicker intraformational conglomerates, and deeper channels. More significantly, our grain-size analysis indicates that the fluvial sediments reworked an aggrading blanket of loess, transported from the Ancestral Rocky Mountains by northeasterly winds during the Pennsylvanian but from the Pangean coast by northwesterly winds early in the Permian (Soreghan et al. 2002). During glacial lowstands when the continental shelf was

exposed, the northwesterly winds remobilized authigenic carbonate and river sediment, generating the Cedar Mesa erg and suspension clouds of dust that were transported for distances of tens to perhaps 100 km to form the Halgaito loess (Murphy 1987; Johansen 1988; Dickinson and Gehrels 2003; Scott 2005). In turn, dry periods would have exposed the ephemeral river sediment to the wind for renewed eolian transport, as noted for Quaternary systems in central Asia where such feedback processes tend to homogenize the loess sources (Stevens et al. 2013; Licht et al. 2016).

In summary, the Monument Upwarp had sufficient relief to generate north- and east-flowing river systems capable of reworking the aggrading loess, although there is no evidence that erosion cut down to older bedrock. It is not clear how far into the basin the rivers extended, nor whether they terminated in the basin or became tributaries to Uncompahgre or axial drainage systems.

## **2.9 Conclusions**

The Pennsylvanian to Permian Halgaito Formation is an example of rivers reworking loess to yield unusually fine-grained fluvial fills, largely in the coarse silt range. The fluvial channel deposits include ribbon bodies, sheet-like bodies with many scour fills, and largely unconfined sheets from channel overspill, with common evidence for desiccation. The river systems were ephemeral with a fluctuating hydrograph but largely subcritical flow, and they were probably too shallow and episodic to generate macroforms. Riverbank vegetation was present in places but may not have contributed much to channel stability as channel and scour

margins are largely low-angled, cut into loess. Deeply rooted vegetation in overbank areas would have assisted in stabilizing the accumulating loess.

Traversing an aggrading landscape of loess derived from westerly winds over exposed coastal flats, the rivers would constantly have adjusted their equilibrium profiles, cutting into loess below and along the banks and locally choked with newly deposited loess. The loess was probably weakly consolidated but locally consolidated at shallow depth. As in Quaternary loess tracts, collapse of saturated loess may have contributed to channel dynamics, although no firm evidence for this was observed. Other aggrading landscapes where adjustment of river equilibrium profiles would be forced in a similar manner include volcanic terrains and megafans with rapid floodplain buildup.

The study suggests that Paradox Basin drainage systems were more complex than previously considered. Rivers flowed north and east from the southern basin margin, possibly joining northern rivers with headwaters in the Uncompahgre Uplift, forming tributaries to axial fluvial systems, or dying out in the basin. Feedbacks between fluvial and eolian systems would have been important, as in Quaternary loess terrains, with ephemeral rivers reworking loess derived from westerly winds and in turn providing exposed sediment for renewed eolian transport.



# Chapter 3: Discussion

## 3.1 Synthesis

### 3.1.1 Purpose of the Research

Stratigraphic changes over relatively short distances characterize the Halgaito Formation and are the reason that so many regional names were attributed to the Late Pennsylvanian and Early Permian deposits within the Paradox Basin. The Valley of the Gods is cut into the Colorado Plateau and exposes an approximately 30 km wide expanse of the Halgaito and Rico formations. Many regional studies of the area have focused on specific details of the landscape: for example, Soreghan et al. (2002b) focused on paleowind fluctuations, Soreghan and Soreghan (2007) analyzed whole rock geochemistry of loessites, Jordan and Mountney (2012) detailed the Lower Cutler bed sequence stratigraphy, and DiMichele et al. (2014) categorized fossilized plant remains from several sites within the southern Paradox Basin. Soreghan et al. (2002a) conducted a comprehensive field study of a 230 m section near Mexican Hat, Utah focusing on paleosol characterization and inferred climate trends. Focused and topical studies of the region have yielded a wealth of information regarding the landscape and climate of western Pangea during the early Permian; however, the overall sedimentological understanding of the region was left with significant gaps.

The first main gap in data which this study has attempted to cover is the relation of the fluvial and eolian depositional systems within the Halgaito Formation. The presence of loess within the Halgaito Formation has been well documented; however, the relation to any channel bodies within the region was largely unknown. This study has described the channel size and

morphology, and the upward changes within the formation, as well as the stratigraphic relationship to loess within the Halgaito Formation.

Secondly the link between fluvial morphology and vegetation is broadly understood from the Cambrian through to the Pennsylvanian (Gibling and Davies 2012) but the link has received less attention for the Permian. The identification of fossil plant remains within the Valley of the Gods (DiMichele et al. 2014), as well as the presence of abundant rooted horizons afforded the opportunity to examine the interaction of a fluvio-eolian system in a vegetated arid landscape.

The research presented here is significant for three main reasons:

- (a) This particular location offered the opportunity to study an unusual fine-grained fluvial system interacting with increasing loess and eolian sediment input from the highlands to the northeast.
- (b) The Valley of the Gods offered an unparalleled opportunity to observe fluvial deposits in an eroded valley with towering mesas and buttes, providing a three-dimensional view of channel bodies of varying size and scale across distances not often afforded to fluvial sedimentologists.
- (c) Studying recorded climate change evident in the stratigraphy, sedimentology and paleobotany of the late Pennsylvanian and early Permian gives perception into current climate dynamics.

### 3.1.2 Modern implications

The upward trend recorded in the Halgaito Formation of decreased amounts of vegetation, changing fluvial morphology, lowering of the water table, and eventually a reduction of channels in favour of overland sheet floods is reasonably attributed to extreme climate change as the humid Pennsylvanian transitioned into the more arid Permian and Triassic. These landscape changes are broadly interconnected, and it is unknown if particular aspects of climate change (for example, precipitation, temperature, seasonality, storminess, and/or wind patterns) led to particular landscape changes, or whether a “perfect storm” of climate aspects collectively caused the landscape effects. However, some positive feedbacks can reasonably be inferred from general principles. Reduced vegetation decreases riverbank stability and increases erosion into overbank sediments (Ielpi and Lapôtre 2019). Decreased vegetation also reduces the ability of a landscape to capture eolian material (Tsoar and Pye 1987), increasing the flux of windblown silt to rivers. Increased silt flux to rivers helps to fill channels, and in-channel aggradation can worsen flooding during storm events, promoting overbank flow and further decreasing channel stability (James 1994). The balance of vegetation, precipitation, and deflation of sediments is therefore highly susceptible to climate fluctuations, of significant importance in the climate discussions in the world today. This balance was upset during the 1930s in the Midwest United States. Increased plowing of stabilizing prairie grasses in favor of wheat and corn, decreased precipitation, and the crash of the stock market caused fields to be left fallow and resulted in a feedback cycle that amplified the drought and increased sediment available for entrainment by the wind, causing the “Dust Bowl” (Schubert et al. 2004; Cook et al. 2009).

The global climate is ever changing, and human activity has to be factored into climate cycles as the Anthropocene intensifies. Using the knowledge gained from studying deposits like

the Halgaito Formation, coupled with an example of how human activity can increase these effects, we as a global community can develop ways to mitigate these effects. One such example would be to implement agricultural practices to preserve vegetation during fallow seasons, which in turn can reduce deflation, decreasing dust flux into rivers. It is hoped that by studying the past, both recent and ancient, human society can learn and grow.

## **3.2 Analogues**

### **3.2.1 Namibia.**

The Atlantic coast of Namibia, known as the Skeleton Coast, is a modern example of fluvio-eolian interaction but the sediments are much coarser grained, as evidenced by the formation of an extensive set of sand dunes (Krapf et al. 2003). These dunes, formed transverse to the ephemeral rivers which flow from the northeast catchment areas, will often block the path of a river which then forces the next flooding event to carve a path through the dune field and in some cases causing debris flows (Krapf et al. 2004). This location is not an exact analogue for the Halgaito Formation; however the Lower Halgaito displays a similar pattern, with the channels having carved new, narrow paths through the inter-fluvial material during flood events.

### **3.2.2 Loess Plateau.**

The Loess Plateau in northern China is a large expanse of loess that accumulated through the late Cenozoic, through which runs the Yellow River (Sun and Huang 2006). The proximity of loess and large rivers with a major loess load in northern China and elsewhere (Smalley et al., 2009) suggests comparison with the channel bodies and loessic terrain of the

Middle Halgaito. These are large channel deposits, underlain by loess deposits, with evidence for rapid aggradation in the form of climbing ripples and dunes.

### **3.2.3 Volcanic ash.**

Any significant volcanic ash fall could result in a similar scenario to the Halgaito Formation. Regions with frequent ash fall commonly contain small channels carved through the landscape (Fisher 1977; Rodolfo 1989), like those of the Lower Halgaito. If there was a significantly thick ash fall followed by a period of fluvial activation, the channels could incise into and rework the ash to form deposits similar to those of the Middle Halgaito. Finally an ash deposit which is given time to partially solidify, but not yet have regrowth of vegetation, with intense rainfall and flooding could produce a deposit like that found within the Upper Halgaito, with thick undisturbed ash (loess) with reworked sediments deposited over the top as ripples and dunes.

## **3.3 Further Work**

### **3.3.1 Paleoflow.**

One question which arises from the results of this research pertains to the location and regional scale of the Monument Upwarp, which impacted the formation of the Halgaito Formation. With further exploration of the surrounding buttes and mesas in the Valley of the Gods, paleoflow azimuths might yield significant insight into the general shape and extent of this lesser known topographical highland.

### **3.3.2 Grain Size.**

The precise relationship of the reworked grains to the original loess deposits are another area which would benefit from further study. The comparisons provided here are preliminary and with extensive sampling and point counting a more complete set of data would provide potential information into the grain-size reduction due to reworking. The samples being cemented primarily by calcite afford an opportunity to dissolve the cements and perform more precise measurements of grain size. This would then give an opportunity to test the correction factor proposed by Johnson (1994) and perhaps create a correction factor for the study region specifically.

### **3.3.3 Biostratigraphy.**

As the timeframe represented by the Halgaito Formation is unknown, increased biostratigraphic constraints for the area would help interpretations into the timescale of the fluvial events. Were these channels active for hundreds or thousands of years, or were they the product of intense and sudden flood events? To the same end, were the loess deposits the result of steady yet slow sediment deposition, or were the 1 – 2 m thick loess beds deposited rapidly like those seen in the Dust Bowl of the 1930s? It is improbable that an improved biostratigraphic framework could resolve such fine-scale questions, but a better bracketing of intervals would help to constrain the events documented here.

### **3.3.4 Diagenesis.**

As established in this research, the loess deposits of the Halgaito were in places semi- to fully cemented with calcite at an early stage, and with little to no burial. Some questions that could be answered by further work are: over what range of time did diagenesis occur, and how

much took place during early and late stages of burial and exhumation; from where does the calcite originate; and where are the minor amounts of dolomite, barite, and celestine concentrated? The answers to these questions can increase the confidence in the environmental conditions at the time of deposition, and therefore improve the entire depositional framework which this study hopes to create.

## References

- Abdullatif, O.M., 1989, Channel-fill and sheet-flood facies sequences in the ephemeral terminal River Gash, Kassala, Sudan: *Sedimentary Geology*, v. 63, p. 171-184.
- Allen, J.P., Fielding, C.R., Gibling, M.R., and Rygel, M.C., 2014, Recognizing products of palaeoclimate fluctuation in the fluvial stratigraphic record: An example from the Pennsylvanian to Lower Permian of Cape Breton Island, Nova Scotia: *Sedimentology*, v. 61, p. 1332-1381.
- Barbeau, D.L., 2003, A Flexural Model for the Paradox Basin: Implications for the tectonics of the Ancestral Rocky Mountains: *Basin Research*, v. 15, p. 97-115.
- Bashforth, A.R., Cleal, C.J., Gibling, M.R., Falcon-Lang, H.J., and Miller, R.F., 2014, Paleoeecology of Early Pennsylvanian vegetation on a seasonally dry tropical landscape (Tynemouth Creek Formation, New Brunswick, Canada: *Review of Palaeobotany and Palynology*, v. 200, p. 229-263.
- Bhattacharya, J.P., 2006, Deltas, in Posamentier, H.W., and Walker, R.G., eds., *Facies Models Revisited: SEPM, Special Publication 84*, p. 237–292.
- Bhiry, N., and Occhietti, S., 2004, Fluvial Sedimentation in a Semi-Arid Region: The Fan and Interfan System of the Middle Souss Valley, Morocco: *Proceedings of the Geologists' Association*, v. 115, p. 313-324.
- Brezinski, D.K., Cecil, C.B., and Skema, V.W., 2010, Late Devonian glacial and associated facies from the central Appalachian Basin, eastern United States: *Geological Society of America Bulletin*, v. 122, p. 265-281.
- Bristow, C.S., 1993, Sedimentology of the Rough Rock: a Carboniferous braided river sheet sandstone in northern England, in Best, J.L., and Bristow, C.S., eds., *Braided Rivers, Geological Society Special Publication 75*, p. 291-304.
- Bullard, J.E., and McTainsh, G.H., 2003, Aeolian–fluvial interactions in dryland environments: examples, concepts and Australia case study: *Progress in Physical Geography*, v. 27, p. 471-501.
- Burke, M., 2001, Stratigraphy of the Wasatch Formation, Washakie Basin, south-central Wyoming: implications for the evolution of the genus *Microsyops* [MS Thesis]: University of Colorado, Boulder, Colorado, 233 p.
- Cain, S.A., and Mountney, N.P., 2009, Spatial and temporal evolution of a terminal fluvial fan system: the Permian Organ Rock Formation, south-east Utah, USA: *Sedimentology*, v. 56, p. 1774-1800.



- Chaney, D.S., Lucas, S.G., and Elrick, S., 2013, New occurrence of an arthropleurid trackway from the Lower Permian of Utah, in Lucas, S.G.e.a., ed., *The Carboniferous-Permian Transition: Albuquerque, New Mexico*, New Mexico Museum of Natural History and Science, Bulletin 60, p. 64-65.
- Condon, S.M., 1997, *Geology of the Pennsylvanian and Permian Cutler Group and Permian Kaibab Limestone in the Paradox Basin, Southeastern Utah and Southwestern Colorado*: US Geological Survey Bulletin 2000-P, p. 46.
- DiMichele, W.A., Cecil, C.B., Chaney, D.S., Elrick, S.D., and Nelson, W.J., 2014, Fossil floras from the Pennsylvanian-Permian Cutler Group of southeastern Utah, in MacLean, J.S., Biek, R.F., and Huntoon, J.E., eds., *Geology of Utah's Far South*, Utah Geological Association Publication 43, p. 491-504.
- Deluca, J.L., and Eriksson, K.A., 1989, Controls on synchronous ephemeral- and perennial-river sedimentation in the middle sandstone member of the Triassic Chinle Formation, northeastern New Mexico, U.S.A.: *Sedimentary Geology*, v. 61, p. 155-175.
- Dubiel, R.F., Huntoon, J.E., Stanesco, J.D., Condon, S.M., and Mickelson, D., 1996, Permian-Triassic depositional systems, paleogeography, paleoclimate, and hydrocarbon resources in Canyonlands, Utah: Colorado Geological Survey, Department of Natural Resources, Open-File Report 96-4, Field Trip No. 5, p. 24.
- Fielding, C.R., Alexander, J., and McDonald, R., 1999, Sedimentary facies from ground-penetrating radar surveys of the modern, upper Burdekin River of north Queensland, Australia: consequences of extreme discharge fluctuations, in Smith, N.D., and Rogers, J., eds., *Fluvial Sedimentology VI*, International Association of Sedimentologists Special Publication 28, p. 347-362.
- Fielding, C.R., Trueman, J.D., and Alexander, J., 2005, Sharp-based, flood-dominated mouth bars sands from the Burdekin River Delta of northeastern Australia: extending the Spectrum of mouth-bar facies, geometry, and stacking patterns: *Journal of Sedimentary Research*, v. 75, p. 55-66.
- Fielding, C.R. 2006. Upper flow regime sheets, lenses and scour fills: Extending the range of architectural elements for fluvial sediment bodies: *Sedimentary Geology*, v. 190, p. 227-240.
- Fielding, C.R., Allen, J.P., Alexander, J., and Gibling, M.R., 2009, A facies model for fluvial systems in the seasonal tropics and subtropics: *Geology*, v. 37, p. 623-626.
- Gastaldo, R.A., 1992, Regenerative growth in fossil horsetails following burial by alluvium: *Historical Biology*, v. 6, p. 203-219.
- Ghosh, P., Sarkar, S., and Maulik, P., 2006, Sedimentology of a muddy alluvial deposit: Triassic Denwa Formation, India: *Sedimentary Geology*, v. 191, p. 3-36.

- Gibling, M.R. 2006. Width and thickness of fluvial channel bodies and valley fills in the geological record: A literature compilation and classification: *Journal of Sedimentary Research*, v. 76, p. 731-770.
- Gibling, M.R., and Davies, N.S., 2012. Paleozoic landscapes shaped by plant evolution: *Nature Geoscience*, v. 5, p99-105.
- Gibling, M.R., Nanson, G.G., and Maroulis, J.C. 1998. Anastomosing river sedimentation in the Channel Country of central Australia: *Sedimentology*, v. 45, 595-619.
- Golab, J.A., Smight, J.J., Hasiotis, T., 2018 Paleoenvironmental and Paleogeographic Implications of Paleosols and Ichnofossils in the Upper Pennsylvanian Halgaito Formation, Southeastern Utah: *Palaios*, v. 33, p. 296-311.
- Goldhammer, R.K., Oswald, E.J., and Dunn, P.A., 1991. Hierarchy of stratigraphic forcing: Example from Middle Pennsylvanian shelf carbonates of the Paradox basin: *Kansas Geological Survey Bulletin* v. 233, p. 361-413.
- Hampson, G.J., Jewell, T.O., Irfan, N., Gani, M.R., and Bracken, B., 2013, Modest change in fluvial style with varying accommodation in regressive alluvial-to-coastal-plain wedge: Upper Cretaceous Blackhawk Formation, Wasatch Plateau, Central Utah, U.S.A.: *Journal of Sedimentary Research*, v. 83, p. 145-169.
- Hattori, M., Suzuki, T., and Sato, T., 1974, Beach processes and littoral drifts on the middle region of Enshu Coast: *Conference on Coastal Engineering, Proceedings*, v. 21, p. 127-133.
- Herries, R.D., 1993 Contrasting styles of fluvial-aeolian interaction at a downwind erg margin: Jurassic Kayenta-Navajo transition, northeast Arizona, USA: From North, C. P. & Prosser, D. J. (eds), *Characterization of Fluvial and Aeolian Reservoirs*, Geological Society Special Publication No 73, pp 199-218.
- Hirst, J.P.P., 1991, Variations in alluvial architecture across the Oligo-Miocene Huesca fluvial system, Ebro Basin, Spain, in Miall, A.D., and Tyler, N., eds., *The Three-Dimensional Facies Architecture of Terrigenous Clastic Sediments and Its Implications for Hydrocarbon Discovery and Recovery: Concepts in Sedimentology and Paleontology*, SEPM, p. 111-121.
- Horn, J.D., Fielding, C.R., and Joeckel, R.M., 2012, Revision of Platte River alluvial facies model through observations of extant channels and barforms, and subsurface alluvial valley fills: *Journal of Sedimentary Research*, v. 82, p. 72-91.
- Huttenlocker, A.K., Henrici, A., Nelson, W.J., Elrick, S., Berman, D., Schlotterbeck, T., Sumida, S.S., 2018, A multitaxic bonebed near the Carboniferous–Permian boundary (Halgaito Formation, Cutler Group) in Valley of the Gods, Utah, USA: *Vertebrate paleontology and taphonomy: Palaeogeography, Palaeoclimatology, Palaeoecology*, v. 499, p. 72-92.

- Jansen, J.D., and Nanson, G.C., 2010, Functional relationships between vegetation, channel morphology, and flow efficiency in an alluvial (anabranching) river: *Journal of Geophysical Research*, v. 115, F04030, doi: 10.1029/2010JF001657.
- Johnson, M.R., 1994, Thin Section Grain Size Analysis Revisited: *Sedimentology*, v. 41, p. 985-999.
- Jones, L.S., and Blakey, R.C., 1997, Eolian-Fluvial Interaction in the Page Sandstone (Middle Jurassic) in south-central Utah, USA – A Case Study of Erg-Margin Processes: *Sedimentary Geology*, v. 109, p. 181-198.
- Knighton, A.D., and Nanson, G.C., 1994, Flow transmission along an arid zone anastomosing river, Cooper Creek, Australia: *Hydrological Processes*, v. 8, p. 137-154.
- Krapf, C.B.E, Stollhofen, H., Stanistreet, I.G., 2003, Contrasting styles of ephemeral river systems and their interaction with dunes of the Skeleton Coast erg (Namibia): *Quaternary International*, v. 104, p. 41-52.
- Langford, R.P., 1989, Fluvial-aeolian interactions: Part I, modern systems: *Sedimentology*, v. 36, p. 1023-1035.
- Langford, R.P., and Chan, M.A., 1989, Fluvial-aeolian interactions: Part II, ancient systems: *Sedimentology*, v. 36, p. 1037-1051.
- Love, S.E., and Williams, B.P.J., 2000, Sedimentology, cyclicity and floodplain architecture in the Lower Old Red Sandstone of SW Wales, *Geological Society of London*, 371-388 p.
- Mack, G.H., James, W.C., and Monger, H.C., 1993, Classification of paleosols: *Geological Society of America Bulletin*, v. 105, p. 129-136.
- Mack, G.H., Leeder, M.R., Perez-Arlucea, M., and Bailey, B.D.J., 2003, Early Permian silt-bed fluvial sedimentation in the Orogrande basin of the Ancestral Rocky Mountains, New Mexico, USA: *Sedimentary Geology*, v. 160, p. 159-178.
- McKee, E.D., Crosby, E.j., Berryhill, H.L.Jr, 1967, Flood Deposits, Bijou Creek, Colorado, June 1965: *Journal of Sedimentary Petrology*, v. 37, p. 829-851.
- Miall, A.D. 1974, Paleocurrent analysis of alluvial sediments: a discussion of directional variance and vector magnitude: *Journal of Sedimentary Petrology*, 44, 1174-1185.
- Miall, A.D., 1996, *The Geology of Fluvial Deposits*, Springer-Verlag Berlin Heidelberg, ISBN 978-3-540-59186-3.
- Mountney, Nigel P., 2006, Periodic accumulation and destruction of aeolian erg sequences in the Permian Cedar Mesa Sandstone, White Canyon, southern Utah, USA: *Sedimentology* 53, p789-823.

- Nanson, G.C., and Knighton, A.D., 1996, Anabranching rivers: their cause, character and classification: *Earth Surface Processes and Landforms*, v. 21, p. 217-239.
- Olsen, H., 1989, Sandstone-body structures and ephemeral stream processes in the Dinosaur Canyon Member, Moenave Formation (Lower Jurassic), Utah, U.S.A.: *Sedimentary Geology*, v. 61, p. 207-221.
- Parrish, J.T., and Peterson, F., 1988, Wind Directions Predicted from Global Circulation Models and Wind Directions Determined from Eolian Sandstones of the Western United States – A Comparison: *Sedimentary Geology*, v. 56, p. 261-282.
- Pécsi, M., 1995, The Role of Principles and Methods in Loess-Paleosol Investigations: *GeoJournal* 36.2/3, p. 117-131.
- Peterson, F., 1988, Pennsylvanian to Jurassic Eolian Transportation systems in the Western United States: *Sedimentary Geology*, v. 56, p. 207-260.
- Porter, S.C., 2001, Chinese loess record of monsoon climate during the last glacial - interglacial cycle: *Earth-Science Reviews*, v. 54, p. 115-128.
- Porter, S.C., and An, Z., 2003, Stratigraphic evidence of episodic gullying on the Chinese Loess Plateau, XV1 INQUA Congress, Programs with Abstracts: Reno, Nevada, p. 176.
- Prescott, Z.M., Stimson, M.R., Dafoe, L.T., Gibling, M.R., MacRae, R.A., Calder, J.H., and Hebert, B.L., 2014, Microbial mats and ichnofauna of a fluvial-tidal channel in the Lower Pennsylvanian Joggins Formation, Canada: *Palaios*, v. 29, p. 624-645.
- Pye, K., 1995, The nature, origin and accumulation of loess: *Quaternary Science Reviews*, v. 14, p. 653-667.
- Rankey, E., 1997, Relations Between Relative Changes in Seall Level and Climate Shifts: Pennsylvanian-Permian Mixed Carbonate-Silliclastic Strata, Western United States: *GSA Bulletin*, v. 109, p. 1089-1100.
- Ritter, S.M., Barrick, J.E., Skinner, W.R., 2002, Conodont Sequence Biostratigraphy of the Hermosa Group (Pennsylvanian) at Honaker Trail, Paradox Basin Utah: *Journal of Paleontology*, v. 76, p. 495-517.
- Rust, B.R., Gibling, M.R., and Legun, A.S., 1984, Coal depositional in an anastomosing-fluvial system: the Pennsylvanian Cumberland Group south of Joggins, Nova Scotia, Canada, in Rahmani, R.A., and Flores, R.A., eds., *Sedimentology of Coal and Coal-bearing Sequences*, International Association of Sedimentologists Special Publication 7, p. 105-120.

- Scott, K.M., 2005, Cohesion, water vapor, and floral topography: Significance for the interpretation of the depositional mechanisms of the Late Paleozoic Halgaito Formation, Cutler Group, Southeastern Utah, in Lucas, S.G., and Zeigler, K.E., eds., *The Nonmarine Permian: Albuquerque, N.M.*, New Mexico Museum of Natural History and Science Bulletin 30, p. 296-301.
- Scott, K.M., 2013, Carboniferous-Permian boundary in the Halgaito Formation, Cutler Group, Valley of the Gods and surrounding area, southeastern Utah, in Lucas, S.G., DiMichele, W.A., Barrick, J.E., Schneider, J.W., and Spielmann, J.A., eds., *The Carboniferous-Permian Transition: Albuquerque, N.M.*, New Mexico Museum of Natural History and Science Bulletin 60, p. 398-409.
- Simon, S.S.T., and Gibling, M.R., 2017, Fine-grained meandering systems of the Lower Permian Clear Fork Formation of north-central Texas, USA: Lateral and oblique accretion on an arid plain: *Sedimentology*, v. 64, p. 714-746.
- Simon, S.S.T., Gibling, M.R., DiMichele, W.A., Chaney, D.S., Looy, C.V., and Tabor, N.J., 2016, An abandoned-channel fill with exquisitely preserved plants in redbeds of the Clear Fork Formation, Texas, USA: An Early Permian water-dependent habitat on the arid plains of Pangea: *Journal of Sedimentary Research*, v. 86, p. 944-964.
- Smalley, I., O'Hara-Dhand, K., Wint, J., Machalet, B., Jary, Z., and Jefferson, I., 2009, Rivers and loess: The significance of long river transportation in the complex event-sequence approach to loess deposit formation: *Quaternary International*, v. 198, p. 7-18.
- Smalley, I., Markovic, S.B., and Svircev, Z., 2011, Loess is [almost totally formed by] the accumulation of dust: *Quaternary International*, v. 240, p. 4-11.
- Soreghan, G.S., Elmore, R.D., and Lewchuk, M.T., 2002a, Sedimentologic-magnetic record of western Pangean climate in upper Paleozoic loessite (lower Cutler beds, Utah): *Geological Society of America Bulletin*, v. 114, p. 1019-1035.
- Soreghan, M.J., Soreghan, G.S., and Hamilton, M.A., 2002b, Paleowinds inferred from detrital-zircon geochronology of upper Paleozoic loessite, western equatorial Pangea: *Geology*, v. 30, p. 695-698.
- Soreghan, G.S., Soreghan, M.J., Sweet, D.E., and Moore, K.D., 2009, Hot fan or cold outwash? Hypothesized proglacial deposition in the Upper Paleozoic Cutler Formation, western tropical Pangea: *Journal of Sedimentary Research*, v. 79, p. 495-522.
- Stanescio, J.D., and Campbell, J.A., 1989, Eolian and noneolian facies of the Lower Permian Cedar Mesa Sandstone Member of the Cutler Formation, southeastern Utah: *U.S. Geological Survey Bulletin 1808F*, p. F1-F13.

- Stear, W. M., 1985, Comparison of the bedform distribution and dynamics of modern and ancient sandy ephemeral flood deposits in the southwestern Karoo region, South Africa: *Sedimentary Geology*, V. 45, P. 209-230.
- Stevens, T., Carter, A., Watson, T.P., Vermeesch, P., Ando, S., Bird, A.F., Lu, H., Garzanti, E., Cottam, M.A., and Sevastjanova, I., 2013, Genetic linkage between the Yellow River, the Mu Us desert and the Chinese Loess Plateau: *Quaternary Science Reviews*, v. 78, p. 355-368.
- Tooth, S., 2000, Process, Form and Change in Dryland Rivers: a Review of recent Research: *Earth-Science Reviews*, v. 51, p. 67-107.
- Tooth, S., 2005, Splay Formation Along the Lower Reaches of Ephemeral Rivers on the Northern Plains of Arid Central Australia: *Journal of Sedimentary Research*, V75, p. 636-649.
- Torsvik, T.H., and Cocks, L.R.M., 2004, Earth geography from 400 to 250 Ma years: a palaeomagnetic, faunal and facies review: *Journal of Geological Society of London*, v. 161, p. 555-572.
- Tunbridge, I.P., 1981, Old Red Sandstone sedimentation - An example from the Brownstones (highest Lower Old Red Sandstone) of south central Wales: *Geological Journal*, v. 16, p. 111-124.
- Tunbridge, I.P., 1984, Facies model for a sandy ephemeral stream and clay playa complex; the Middle Devonian Trentishoe Formation of North Devon, U.K. : *Sedimentology*, v. 31, p. 697-715.
- Tweto, O., 1976, Preliminary geologic map of Colorado: U.S. Geological Survey, Miscellaneous Field Studies Map, no. 788, scale 1:5000.000.
- Vandenberghe, J., 2013, Grain Size of Fine-grained Windblown Sediment: A Powerful Proxy for Process Identification, *Earth-Science Reviews*, v. 121, p. 18-30.
- Vandenberghe, J., Sun, Y., Wang, X., Abels, H.A., liu, X., 2018, Grain Size Characterization of Reworked Fine-Grained Aeolian Deposits: *Earth-Science Reviews* v. 177, p. 43-52.
- Venus, J.H., Mountney, N.P., and McCaffrey, W.D., 2015. Syn-sedimentary salt diapirism as a control on fluvial-system evolution: an example from the proximal Permian Cutler Group, SE Utah, USA: *Basin Research*, v. 27, 152-182.
- Wakelin-King, G.A., and Webb, J.A. 2007. Upper-flow-regime mud floodplains, lower-flow-regime sand channels: sediment transport and deposition in a drylands mud-aggregate river: *Journal of Sedimentary Research*, v. 77, 702-712.
- Weissmann, G.S., Hartley, A.J., Nichols, G.J., Scuderi, L.A., Olson, M., Buehler, H., and Banteah, R. 2010. Fluvial form in modern continental sedimentary basins: Distributive fluvial systems: *Geology*, 38, 39-42.

Williams, G.E., 1971, Flood deposits of the sand-bed ephemeral streams of central Australia: *Sedimentology*, v. 17, p. 1-40.

Williams, M., 2015, Interactions Between Fluvial and Eolian Geomorphic Systems and Processes: Examples from the Sahara and Australia: *Catena*, v. 1, p.4-13.

Wright, V.P., and Marriott, S.B., 2007, The dangers of taking mud for granted: Lessons from Lower Old Red Sandstone dryland river systems of South Wales: *Sedimentary Geology*, v. 195, p. 91-100.